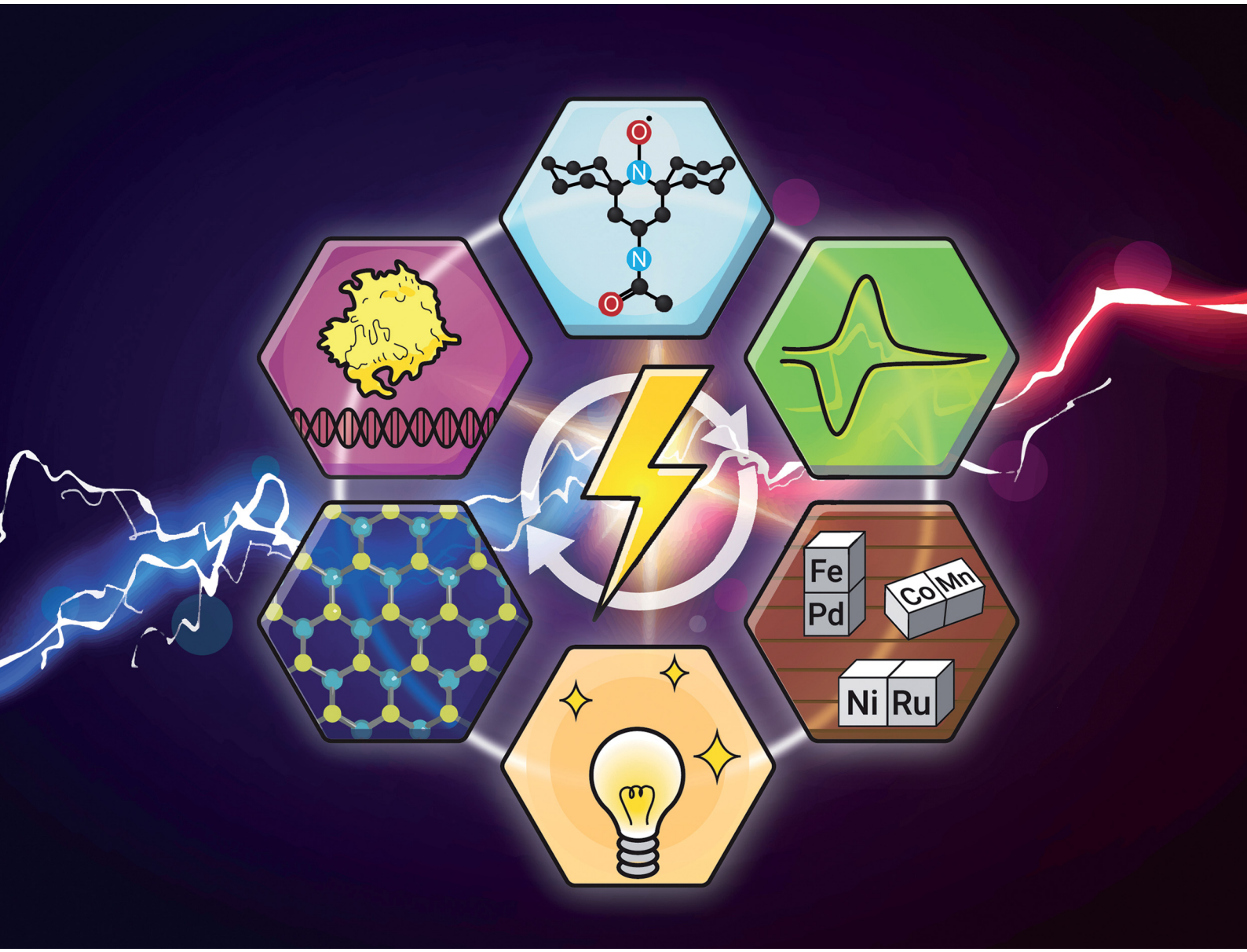
Volume 50
Number 14
21 July 2021
Pages 7883–8346

Chem Soc Rev

Chemical Society Reviews

rsc.li/chem-soc-rev



ISSN 0306-0012

ROYAL SOCIETY OF CHEMISTRY

REVIEW ARTICLE

Song Lin *et al.*

Electrocatalysis as an enabling technology for organic synthesis

Chem Soc Rev

REVIEW ARTICLE

View Article Online
View Journal | View Issue

Check for updates

Cite this: *Chem. Soc. Rev.*, 2021, **50**, 7941

Electrocatalysis as an enabling technology for organic synthesis

Luiz F. T. Novaes,† Jinjian Liu,† Yifan Shen,† Lingxiang Lu,† Jonathan M. Meinhardt and Song Lin*

Electrochemistry has recently gained increased attention as a versatile strategy for achieving challenging transformations at the forefront of synthetic organic chemistry. Electrochemistry's unique ability to generate highly reactive radical and radical ion intermediates in a controlled fashion under mild conditions has inspired the development of a number of new electrochemical methodologies for the preparation of valuable chemical motifs. Particularly, recent developments in electrosynthesis have featured an increased use of redox-active electrocatalysts to further enhance control over the selective formation and downstream reactivity of these reactive intermediates. Furthermore, electrocatalytic mediators enable synthetic transformations to proceed in a manner that is mechanistically distinct from purely chemical methods, allowing for the subversion of kinetic and thermodynamic obstacles encountered in conventional organic synthesis. This review highlights key innovations within the past decade in the area of synthetic electrocatalysis, with emphasis on the mechanisms and catalyst design principles underpinning these advancements. A host of oxidative and reductive electrocatalytic methodologies are discussed and are grouped according to the classification of the synthetic transformation and the nature of the electrocatalyst.

Received 2nd March 2021

DOI: 10.1039/d1cs00223f

rsc.li/chem-soc-rev

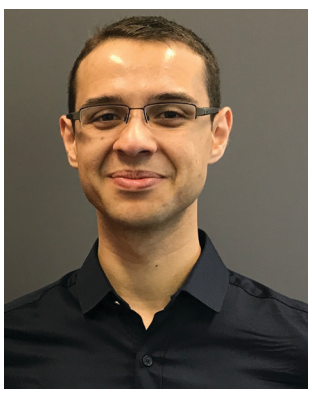
Published on 01 June 2021. Downloaded by University of Cambridge on 12/3/2022 1:39:05 PM.

1. Introduction

Since its inception in the 19th century, electrochemistry has matured to serve a variety of applications ranging from energy storage to metallurgy to chemical synthesis.[1] The success of electrochemistry in these diverse contexts can be credited to the unique capabilities afforded by electrochemical systems.

Department of Chemistry and Chemical Biology, Cornell University, Ithaca, NY 14853, USA. E-mail: songlin@cornell.edu

† These authors contributed equally to the article.



Luiz F. T. Novaes

Luiz Novaes received his BS (2013) and MS (2015) degrees in Chemistry from University of Campinas under the supervision of Prof. Ronaldo Pilli, working on total synthesis of natural polyketides. During his PhD studies (2015–2019), Luiz worked on total synthesis of the natural meroterpene actinoranone and the sesquiterpene pleocarpanone under the guidance of Prof. Julio Pastre (University of Campinas). In September of 2019, he joined the Lin group at Cornell University as a postdoctoral scholar, and has focused on developing electrochemical methodologies to enable the late stage functionalization of complex molecules.



Jinjian Liu

Jinjian Liu received her BS (2017) degree in Chemistry from The College of William and Mary under the supervision of Prof. William. R. McNamara, working on transition-metal catalyzed hydrogenation reactions. She joined Prof. Song Lin's research group at Cornell in 2018, since then, she has worked on electrophotochemical C–H functionalization of inert substrates. Her current research focuses on the development of electrochemical methodologies for enantioselective functionalization of complex molecules.

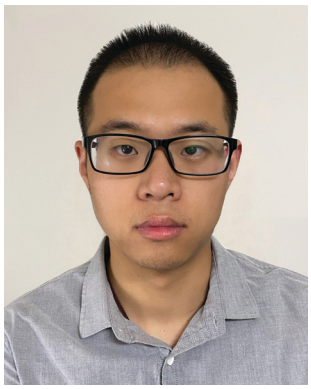
Published on 01 June 2021. Downloaded by University of Cambridge on 12/3/2022 1:39:05 PM.

Principally, the use of an external applied potential provides a means to drive reactions far from thermodynamic equilibria, enabling access to reaction pathways and chemical intermediates that would otherwise be difficult to employ. Additionally, electrochemical systems often afford mild conditions and the potential for scalability, supporting their use in the industrial synthesis of bulk and fine chemicals. The use of electricity in place of environmentally deleterious chemical reagents such as stoichiometric oxidants and reductants also renders electrochemistry an attractive approach for improving the efficiency and sustainability of synthetic chemistry.

In recent years, electrochemistry has experienced an exciting and ongoing renaissance in the context of organic synthesis. Driven in part by the characteristic advantages of electrochemistry described above, this surge of interest has led to the development of an increasing number of electrochemical synthetic methodologies, including reactivities not directly attainable through traditional chemical methods alone.[2,3] Specifically, single-electron oxidation and reduction events facilitated by electrochemistry are well-suited[4] towards the creative use of radical intermediates in achieving synthetic transformations. When the formation and downstream reactivity of these intermediates are placed under the control of catalytic redox mediators, electrochemistry emerges as a powerful strategy for addressing prevailing trends in organic synthesis.

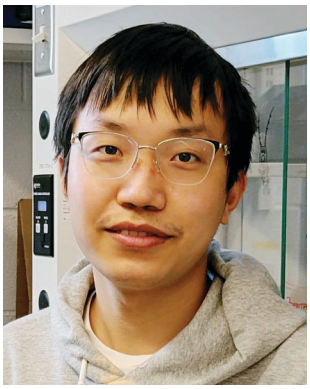
A conceptual analysis of an electrochemical reaction quickly reveals the enhanced capabilities offered by redox mediators in electrosynthesis. While electrochemistry can enable activation of substrates at the electrode surface (*i.e.*, direct electrolysis), this mode of activation often requires substrate engineering to regulate reactivity and can forgo control over the selectivity of chemical steps following electron transfer.[5] When electrochemistry is applied towards the construction and modification of complex organic molecules, the limitations of direct electrolysis can become more pronounced. However, such constraints can be addressed through the implementation of redox-active catalysts which facilitate efficient electron transfer events and offer increased selectivity relative to non-mediated processes.[6]

Electrocatalysis can either utilize molecular mediators as catalytic species (such as transition metal complexes or redox-active organic compounds; commonly referred to as homogenous or molecular electrocatalysis)[7] or an electrode surface



Yifan Shen

Yifan Shen is currently a doctoral candidate of Organic Chemistry at Cornell University, under the supervision of Prof. Song Lin. He received his BS degree in Chemistry from Shanghai Jiao Tong University in 2017, working on transition metal catalyzed oxidation reaction. His research interests include electrocatalysis and radical relay chemistry.



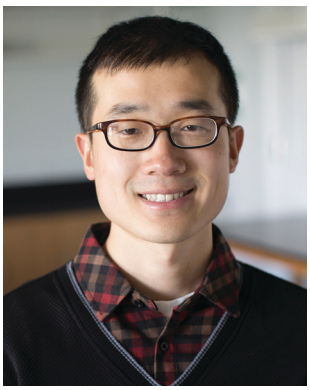
Lingxiang Lu

Lingxiang Lu received his BS degree (Hons) in Chemistry from Wuhan University under the supervision of Prof. Hexiang Deng and Fusheng Ke, working on metal–organic frameworks and lithium sulphur batteries. In 2017, he joined Prof. Song Lin's research group at Cornell for PhD studies on electrosynthesis. He is currently working on electroreductive transformations to construct value-added compounds.



Jonathan M. Meinhardt

Jonathan Meinhardt is an undergraduate student at Cornell University working in the research group of Professor Song Lin. Since joining the Lin group in 2019, Jon has worked on projects which developed and utilized structure–property relationships in the contexts of asymmetric catalysis and the design of energetic materials. In March of 2021, he received a Barry M. Goldwater Scholarship based on his efforts in these research areas. His current research interests involve the development of new strategies for site-selective C–H activation.



Song Lin

Song Lin is an Assistant Professor of Chemistry and Howard Milstein Faculty Fellow at Cornell University. He obtained BS at Peking University in 2008 and PhD at Harvard University, working under the guidance of Prof. Eric Jacobsen. After postdoctoral training with Prof. Christopher Chang at UC Berkeley, he joined Cornell University as a faculty member in 2016. Prof. Lin has served on the Early Career Advisory Board of ACS Catalysis and Chemistry – A European Journal. The Lin Laboratory is interested in developing new catalytic strategies for organic reaction discovery with a particular emphasis on electrochemistry and radical catalysis.

 This journal is © The Royal Society of Chemistry 2021

Published on 01 June 2021. Downloaded by University of Cambridge on 12/3/2022 1:39:05 PM.

itself (referred to as heterogenous electrocatalysis[8] herein). Traditionally, the term "electrocatalysis" is used to define the latter case involving an catalytic electrode, whereas systems featuring molecular mediators have been referred to as "molecular catalysis for electrochemical reactions."[9] In this review, electrocatalysis is described to encompass both homogeneous and heterogeneous cases, given that the defining feature of an electrocatalytic system is the use of a redox-active species which can facilitate a catalytic cycle and accelerate a specific reaction pathway.[10,11] In many of the examples presented herein, electrocatalysis gives rise to new reactivities that are not accessible through non-electrocatalytic means.

The scope of electrocatalysis in chemical literature is extensive, with major areas of growth including the development of electrocatalytic systems for energy-related applications (such as water splitting[12,13] and CO_2 reduction[14]) and, more recently, synthetic chemistry.[15,16] In the area of organic synthesis, continuing pressure to develop efficient and sustainable synthetic strategies has driven a tremendous surge of interest in electrocatalytic methodologies from within the broader organic chemistry community (Fig. 1).

This review highlights key innovations in the past decade (since *ca.* 2010) within the growing discipline of synthetic electrocatalysis. We aim to showcase the versatility of these electrocatalytic systems as well as illustrate the design principles used to develop the electrocatalytic mediators needed to power these systems. The electrocatalysts discussed herein can be subdivided into two general classes base on their role in mediating electrochemical transformations.[13] The first category of electrocatalysts encompasses redox mediators which serve the sole purpose of facilitating electron transfer events between electrodes and substrates, accelerating redox reactions relative to a non-mediated system. The second category of electrocatalysts we discuss are electrocatalysts that shuttle both electrons and chemical information to substrates, placing reactivity and selectivity directly under the control of the catalyst itself. Consistent with the general definition of a catalyst, we primarily focus on reactions that utilize electrocatalysts in sub-stoichiometric amounts. However, to fully describe the reactivities enabled by electrochemical systems, we include some examples where an electrochemical mediator is used in higher loadings.

Emphasis is placed on the mechanistic details of a host of oxidative and reductive electrocatalytic transformations at the cutting edge of the discipline. We first discuss advancements occurring within the well-established realm of oxidative electrocatalysis, and then proceed to discuss emerging discoveries in the less explored areas of electroreductive transformations, paired electrolysis, and heterogenous electrocatalysis. Finally, we explore bioelectrocatalysis electrophotocatalysis to demonstrate the extension of electrocatalytic strategies into interdisciplinary applications. These recent developments illustrate many of the design principles used to realize a range of electrocatalytic methodologies and showcase the capabilities of electrochemistry in facilitating increasingly complex transformations.

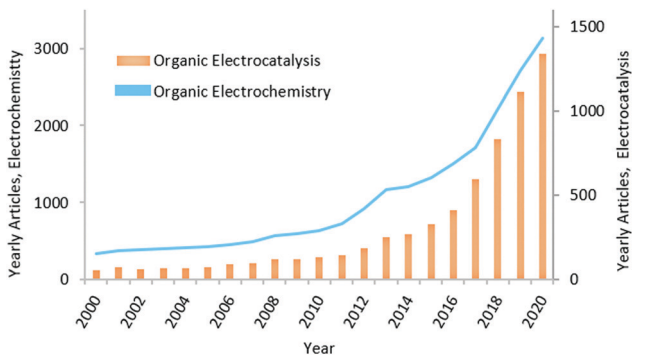


Fig. 1 Number of publications per year (indexed in SciFinder since 2000) in the research areas of organic electrochemistry and organic electrocatalysis.

Electrochemical glossary

Readers who are unfamiliar with electrochemical reactions can find valuable information on the basics of electrochemistry, including how to set up electrochemical reactions, in recent reviews by Hilt,[17] Schotten and Willans,[18] and in a recent account by Baran.[19]

In the present review, the following notation is used: a (+) sign denotes the anode; a (−) sign denotes the cathode; "|" denotes an undivided cell setup; "‖" denotes a divided cell setup. For example, "C(+)|Pt(−)" indicates that the electrolysis uses an C anode and a Pt cathode in an undivided cell. Current (i) or current density (j), electrode potential (E_c or E_a), cell voltage (U_{cell}) values are given when the electrolysis is conducted under constant current, constant potential, or constant cell voltage conditions, respectively. Potential values are listed with respect to a reference electrode such as ferrocene/ferrocenium (Fc/Fc^+) or saturated calomel electrode (SCE). The conversion between Fc/Fc^+ and SCE is $E_{1/2}(Fc/Fc^+)$ = 0.40 V *vs.* SCE.

Additionally, throughout the text, mechanistic schemes are color-coded by the nature of the electrochemical transformation discussed: oxidative reactions are identified by a beige background, reductive reactions are shown with a blue background, and paired electrolysis reactions are presented with a grey background.

2. Anodic oxidation

Oxidative reactions are important tools for the synthesis of complex molecules, enabling the efficient construction of C–C bonds and the incorporation of heteroatoms into molecular architectures. Common chemical methods for oxidative reactions typically rely on the use of stoichiometric amounts of oxidizing agents, such as high-valent chromium and manganese complexes as well as hypervalent iodine species, which can often be hazardous and generate substantial amounts of waste. Recent methodological advances have led to milder reaction systems using more desirable oxidants such as O_2 and H_2O_2.[20,21] Nevertheless, finding "alternatives for oxidations" remains one of the key green chemistry research areas identified by the ACS Green Chemistry

Published on 01 June 2021. Downloaded by University of Cambridge on 12/3/2022 1:39:05 PM.

Institute Pharmaceutical Roundtable in their 2018 report.[22] In this regard, the adoption of a catalyst that can be regenerated upon anodic oxidation is highly desirable from a green chemistry perspective, since waste generation is considerably reduced. Indeed, electrochemical oxidations are usually coupled with hydrogen evolution reaction to generate H_2 gas as the major by-product.

Beyond its utility in recycling traditional chemical oxidants, anodic oxidation has been exploited towards the design of electrocatalytic systems to accomplish a wide range of chemical transformations. The scope of chemical mediators for these oxidative systems is extensive. For instance, the radical cations of triarylamines and ferrocenium ion (Fc^+) have been employed for electron transfer. The phthalimide *N*-oxyl (PINO) radical, the radical cation from quinuclidine, chlorine radicals, and nitrate radicals have been used as hydrogen atom transfer (HAT) agents. Oxoammonium cations derived from nitroxyl radicals have been employed for formal hydride transfer. Further, anodic oxidation of metallic species to high valent states is often used to promote reductive elimination, which is commonly seen in C–H activation reactions. Recently, Earth-abundant 3d metals have been explored in a myriad of radical transformations. This diversity of electrooxidative reactions is discussed in the following subsections and is grouped based on the nature of the redox mediator.

Main group compounds as mediators

2.1. Halogen-based mediators (halides, hypervalent iodine)

Halide salts are among the simplest and most commonly used halogen-based mediators, which are non-toxic and inexpensive. Other less explored halogen-based mediators include iodate/periodate and hypervalent iodine compounds. Upon anodic oxidation, halides generate reactive halogen compounds (*e.g.*, Cl_2, Br_2, I_2), and when electrolysis is carried out in water, hypohalites can also form.

Well-established reactivities have been explored with oxidized halides, such as nucleophilic substitution and base-promoted elimination.[23,24] Generation of radicals from the homolytic cleavage of weak heteroatom–halogen bonds is a less explored yet powerful approach for forging carbon–heteroatom bonds. Although halogen-based mediators can in theory be regenerated in electrochemical systems, in some cases they are used in stoichiometric amounts to ensure high reaction yields.

2.1.1. Activation of alkenes with halogens. In 2016, Zeng, Sun, and co-workers generated 3-methoxyindolines *via* an electrochemical aminooxygenation reaction, mediated by iodide (Fig. 2).[25] This reaction uses anodically generated iodine to produce an iodonium ion **2–3**, which is subjected to an intramolecular S_N2 reaction, followed by a second substitution with cathodically generated methoxide. $LiClO_4$ can be removed from the system without affecting the yield, since the iodide source also functions as an electrolyte.

In 2020, the formation of iodonium intermediates was explored by Lennox and co-workers for vicinal difluorination

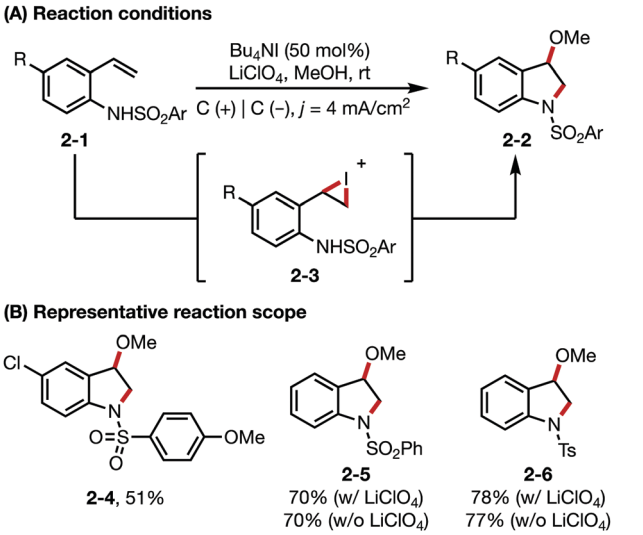


Fig. 2 (A and B) Iodide-mediated aminooxygenation of alkenes.

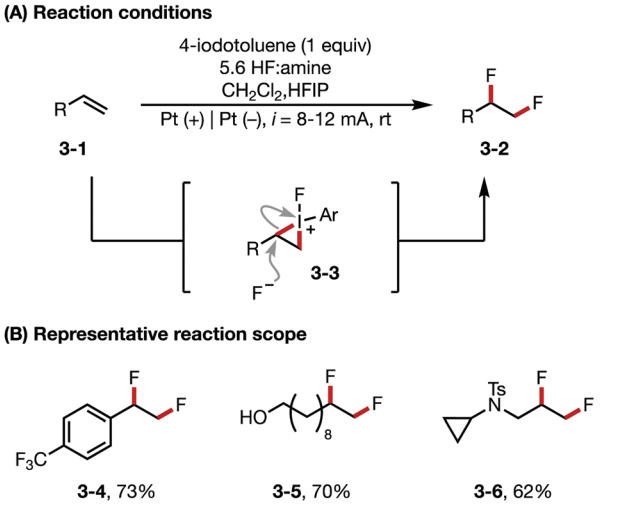


Fig. 3 (A and B) Hypervalent iodine-mediated difluorination of alkenes.

of alkenes (Fig. 3).[26] The fluorine source arises from a mixture of commercially available $Et_3N{\cdot}3HF$ and pyridine·9HF, to generate a ratio of 5.6 equivalents of HF per amine. The mechanism is proposed to start with formation of iodonium ion **3-3**, followed by ring opening with fluoride and displacement of aryl iodide with a second fluoride ion. For alkenes that are more easily oxidized than the iodoarene, the authors first generated a pool of hypervalent iodine reagent and later added the alkene, demonstrating a broad functional group compatibility for this methodology.

2.1.2. α-Functionalization of nitriles and carbonyls. Recently, the use of halides as electrochemical mediators for the α-functionalization of nitriles and carbonyls has been extensively explored. This reactivity relies on the α-deprotonation of these functional groups, generating stabilized anions, which can react with Br_2 or I_2 (see intermediate **4-3**, Fig. 4). This newly installed halogen group can be easily displaced by a wide range

 This journal is © The Royal Society of Chemistry 2021

Published on 01 June 2021. Downloaded by University of Cambridge on 12/3/2022 1:39:05 PM.

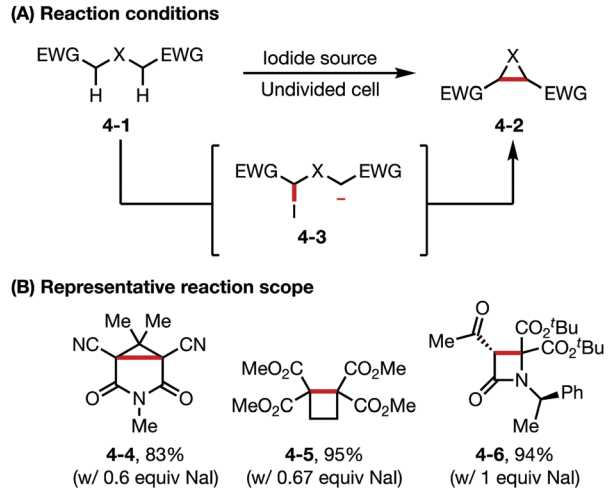


Fig. 4 (A and B) Iodide-mediated cyclization.

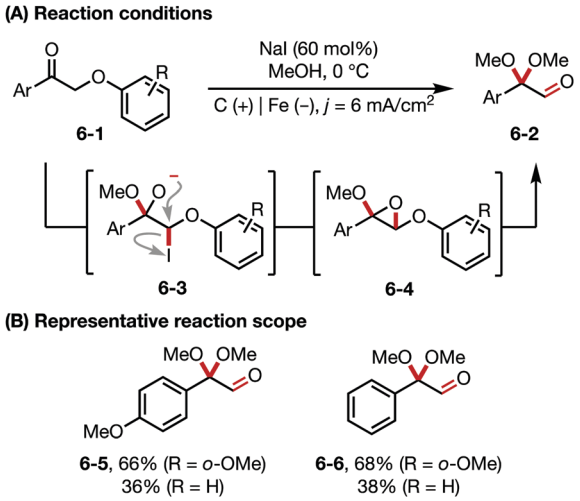


Fig. 6 (A and B) Iodide-mediated oxidation of lignin model compounds.

of nucleophiles in an S_N2 fashion. Appending a nucleophile in the same molecule has been employed to generate cyclic motifs intramolecularly (Fig. 4), such as cyclopropanes,[27–30] cyclobutanes,[31] cyclopentanes,[32] β-lactams,[33] and dihydrofurans.[34] In the intermolecular realm, carbon, nitrogen, and sulfur nucleophiles have been explored, including nitrile anions,[35] enolates,[36] amines,[37] sulfinates[38] and carbamodithioates.[39] Although several of these methods use high loadings or even stoichiometric amounts (see example **4–6**, Fig. 4) of halide mediators, halide salts are fairly inexpensive. In 2021, the scalability of these methods was explored by Baran and Sabatini,[25] where compound **4–5** was synthesized on a hundred-gram scale.

During the 2010s, a different approach towards the electrocatalytic α-functionalization of ketones was reported by Zha, Wang, and co-workers, where the electrolysis of arylmethylketones and iodide is carried out under aerobic conditions (Fig. 5). The authors propose the intermediacy of a peroxyl radical (**5-4**), which could be later converted to different functionalities,

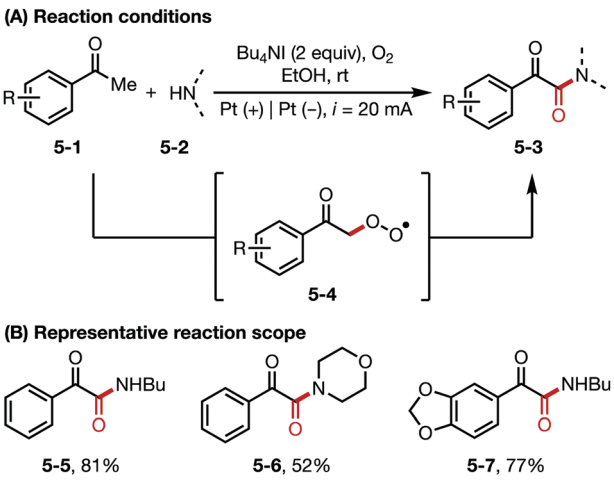


Fig. 5 (A and B) Iodide-mediated oxidation of methylketones.

such as α-keto-esters,[40] α-keto-amides,[41] enaminones,[42] and isatins.[43] Although the role of the iodide mediator is not fully understood for these reactions, we hypothesize that *in situ* generated iodine could react with an enolate, and the resultant C–I bond could undergo homolytic cleavage followed by O_2 trapping to give the peroxyl radical intermediate.

Elinson and co-workers reported the electrochemical conversion of ketones to α-carbonyl-acetals.[44–46] In this reaction, an enolate reacts with anodically generated iodine to form a C–I bond. Addition of cathodically generated methoxide to the carbonyl of **6-1** gives intermediate **6-3**, which undergoes epoxide formation followed by methanolysis, releasing a phenol leaving group to generate **6-2**. In 2017, a similar reactivity was explored by Zeng, Sun, and co-workers during the selective oxidation of lignin-type model compounds (Fig. 6).[47]

2.1.3. Periodate as mediator. The periodate anion is a versatile oxidant and is typically employed in the oxidative cleavage of diols or the *in situ* regeneration of catalysts such as osmium tetroxide or ruthenium tetroxide. Oxidative cleavage of vicinal diols, vicinal aminoalcohols, and α-hydroxyketones was studied by Pillai and co-workers using anodically generated periodate.[48] The production of this hypervalent iodine reagent requires the use of a divided cell to prevent its unproductive cathodic reduction. This mediator was also employed by Schäfer and co-workers to promote regeneration of ruthenium tetroxide, which was used in the electrochemical oxidative cleavage of alkenes[49] (Fig. 7). In 2020, Waldvogel and co-workers reported an efficient method for generating periodate electrochemically from iodide for *ex situ* applications.[50]

2.1.4. Oxidation of sulfur functional groups. The use of halides and hypervalent iodine compounds as electrochemical mediators has been useful for the selective oxidation of different sulfur functional groups, including sulfinate salts, thiols, dithianes, and dithiolanes.[51,52] For example, upon anodic oxidation of halides, sulfinate salts can form adducts with a labile heteroatom-halogen bond (O–I or S–I), which can be homolytically cleaved by light or heat. The newly generated

Published on 01 June 2021. Downloaded by University of Cambridge on 12/3/2022 1:39:05 PM.

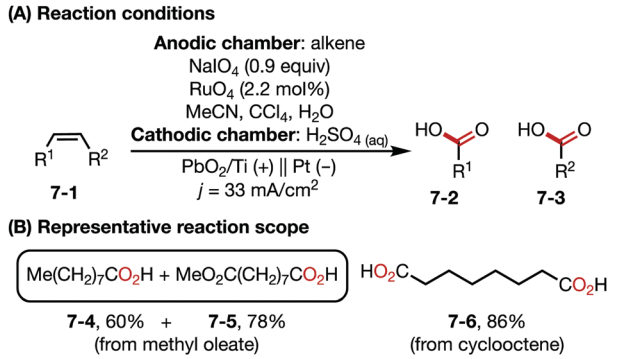


Fig. 7 (A and B) Oxidative cleavage of alkenes using electrochemical generated periodate.

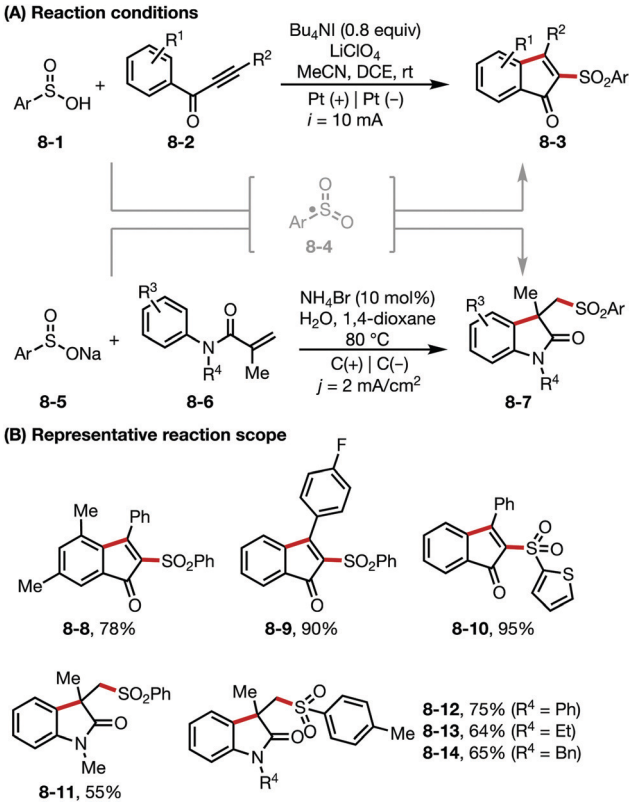


Fig. 8 (A and B) Radical cyclization triggered by electrochemical generated sulfur centered radicals.

sulfur-centered radicals (**8-4**) can then add to the π systems of alkynes[53] or alkenes[54] (Fig. 8), and this protocol can also be used for the construction of sulfonamides.[55]

In 2010, Fuchigami and co-workers reported an electrochemical approach to convert dithiolanes to geminal difluoride groups (Fig. 9). This transformation is mediated by **9-2**, which can undergo anodic oxidation in the presence of Et_3N-5HF electrolyte to generate hypervalent iodine species **9-4** with a tethered imidazolium ion. **9-4** then reacts with substrate **9-1** to give the *gem*-difluorinated product **9-3**. At the end of the reaction, the aryl iodide mediator can be recovered with a simple extraction and reused.[56] Fuchigami has also developed

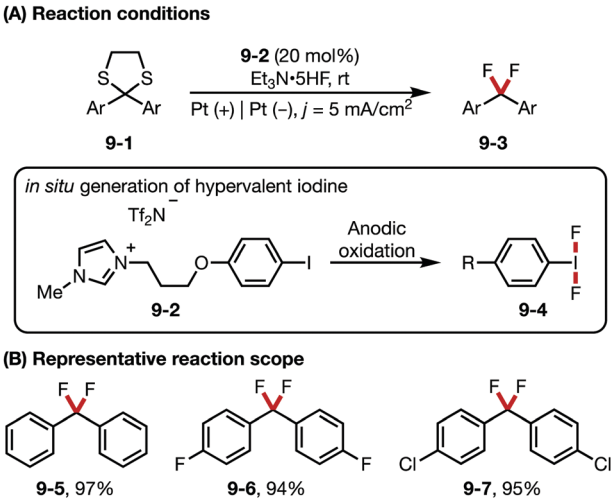


Fig. 9 (A and B) Hypervalent iodine-mediated fluorodesulfurization of dithiolanes.

a fluorodesulfurization employing chloride as an electrochemical mediator, which can aid in the generation of hypervalent iodine species from polystyrene-supported iodobenzene.[57]

2.1.5. Oxidation of nitrogenated functional groups. The cleavage of weak nitrogen–halogen bonds is the basis for the development of a wide range of reactions. Two possible mechanisms for this reactivity have been proposed. In an ionic mechanism, upon formation of the iodinated amine intermediate, a simple beta-H^+ elimination step promoted by base will generate a C=N group to complete the mediated dehydrogenation.[58–60] In radical mechanisms, an N-centered radical is generated from the halogenated amine by modes of single-electron activation such as photoirradiation (see Section 7: Electrophotocatalysis).[61,62] As an example of the ionic scenario, in 2014, Little and co-workers demonstrated the use of anodically generated electrophilic iodine species to promote the formation of benzoxazoles from 2-aminobenzoxazolines *via* key intermediate **10-4**[52] (Fig. 10).

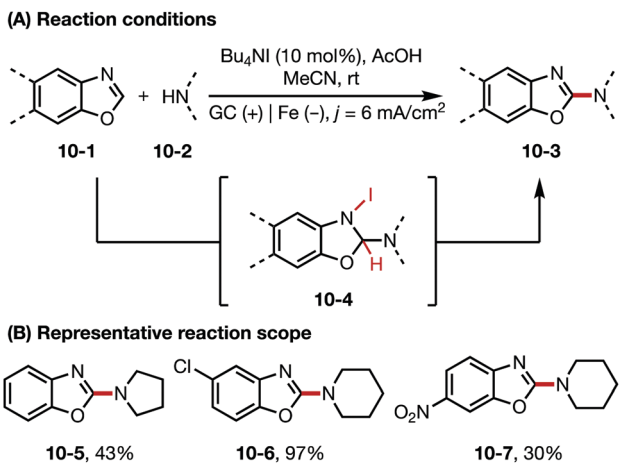


Fig. 10 (A and B) Iodide-mediated synthesis of 2-aminobenzoxazoles.

 This journal is © The Royal Society of Chemistry 2021

Published on 01 June 2021. Downloaded by University of Cambridge on 12/3/2022 1:39:05 PM.

2.2. Nitrate mediators

The nitrate radical was first identified in the atmosphere during the late 1800s and has been shown to play an important role in atmospheric chemistry. It can be formed by reaction of NO_2 with ozone or through the decomposition of N_2O_5.[63] Nitrate radicals can react with aldehydes *via* an HAT process, resulting in acyl radicals and nitric acid. Nitrate radicals can also add to alkenes, to furnish organic nitrate functional groups.

2.2.1. Alcohol oxidation. Nitrate radicals can also be generated electrochemically *via* anodic oxidation of nitrate anions. Despite this interesting reactivities, this species has been rarely used in synthetic electrochemistry. One of these examples was reported in 2012 by Raja and co-workers, where an electrochemical oxidation of alcohols to aldehydes or ketones was mediated by nitrate radical[64,65] (Fig. 11). This reaction is thought to proceed by an HAT event, whereby a nitrate radical removes a hydrogen from the carbinolic position, followed by a second oxidation proceeding through direct anodic oxidation of the carbon centered radical or a second oxidation mediated by nitrate radical.

2.2.2. Fluorination of unactivated C(sp^3)–H bonds. In 2019, Baran and co-workers employed nitrate radicals to achieve fluorination of unactivated C(sp^3)–H bonds[66] (Fig. 12). The proposed mechanism starts with a HAT process mediated by a nitrate radical, which leads to a radical chain process that is sustained by the nitrogen-centered radical cation **12-4** derived from Selectfluor (**12-3**), the fluorinating agent. This methodology provided good yields for substrates containing ketones, esters, carboxylic acids, and imides.

2.3. Nitroxyl mediators

Stable nitroxyl radicals have been reported since the 1960s[67–71] and have since attracted the attention of synthetic chemists. These radicals can be oxidized electrochemically to oxoammonium cations, which have been extensively studied for the oxidation of alcohols and amines. In 2015, Minteer, Sigman,

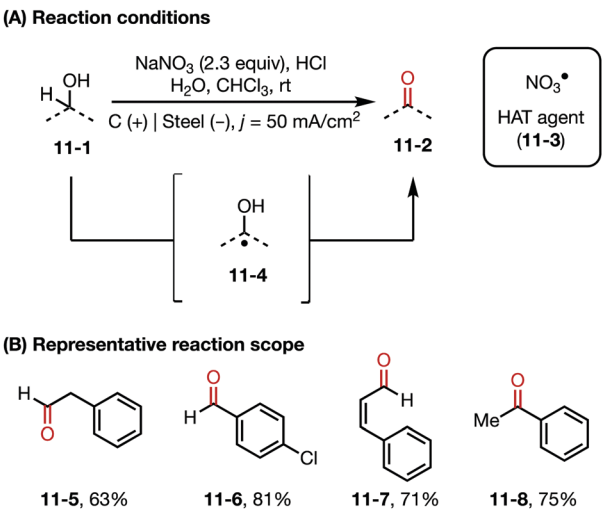


Fig. 11 (A and B) Nitrate-mediated oxidation of alcohols.

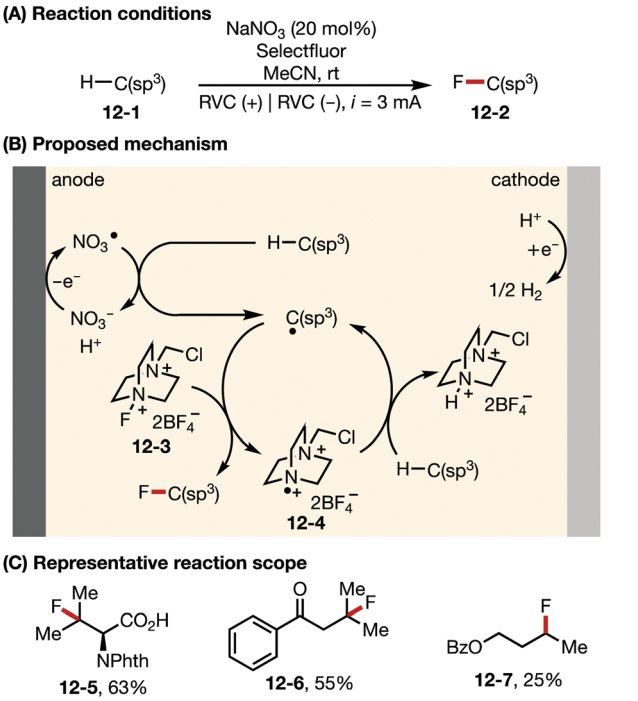


Fig. 12 (A–C) Nitrate-mediated C(sp^3)–H fluorination.

and co-workers combined experimental and computational techniques to group nitroxyl mediators into four distinct classes, matching high or low oxidation potentials of the mediator with high or low catalytic activity for alcohol oxidation (Fig. 13).[72] The top left quadrant of the graph originated from this study contains nitroxyls with high activity that can be generated at low potential, which is desirable for energy applications. On the other extreme, the bottom right corner contains poorly active mediators that require high oxidation potentials, which are useful as EPR labels. Curiously, TEMPO (labeled as number **1** in Fig. 13), the most frequently employed nitroxyl catalyst and EPR label, is not the best option for either applications, and its common use can be understood due to its relative ease of access. In 2018, Stahl, Rafiee, and co-workers extensively reviewed the use of nitroxyl radicals in electrocatalytic reactions.[73]

2.3.1. Alcohol oxidation. During the 2000's, the research groups of Tanaka,[74–76] Onomura,[77] and Frontana-Uribe[78] reported cooperative electrochemical systems involving bromide and nitroxyl radicals, which could generate oxoammonium cations capable of oxidizing primary and secondary alcohols to the corresponding carbonyl compounds. Tanaka[79] and Brown[80] also reported direct oxidation of TEMPO to induce oxidation of alcohols to carboxylic acids, or aldehydes, and ketones.

During the last decade, Stahl and co-workers have explored the oxidation of alcohols mediated by anodically generated oxoammonium cations.[81–84] Stahl observed that ACT (4-acetamido-TEMPO) (E = 0.65 V *vs.* Ag/AgCl) is more electrocatalytic active than AZADO (2-azaadamantane-*N*-oxyl) and ABNO (9-azabicyclo[3.3.1]nonane *N*-oxyl) (E_{AZADO} = 0.45 V, E_{ABNO} = 0.48 V, *vs.* Ag/AgCl) which are less sterically hindered.[81] The higher

Published on 01 June 2021. Downloaded by University of Cambridge on 12/3/2022 1:39:05 PM.

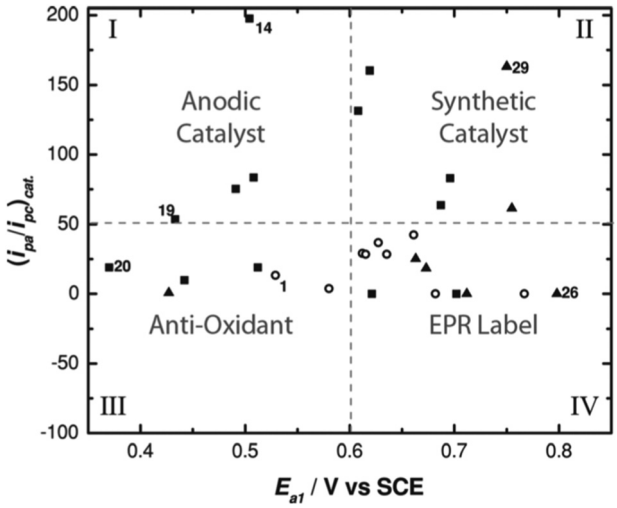


Fig. 13 Minteer and Sigman's model for nitroxyl mediators. This figure has been reproduced from ref. 72 with permission from American Chemical Society, copyright 2015.

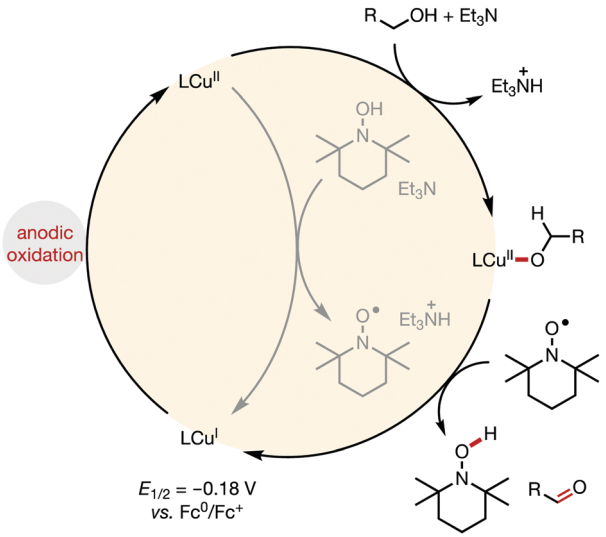


Fig. 15 Cooperative copper-nitroxyl system for oxidation of alcohols to aldehydes.

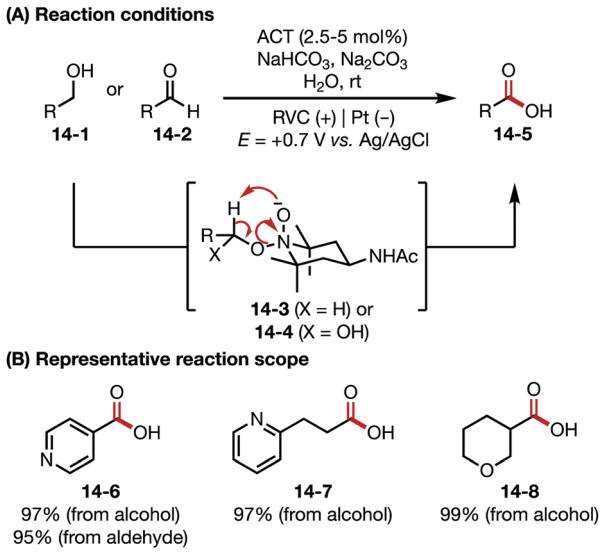


Fig. 14 (A and B) Nitroxyl-mediated oxidation of alcohols and aldehydes to carboxylic acids.

activity of ACT is attributed to the fact that its corresponding oxoammonium cation is generated at a higher potential. A higher pH environment further contributes to the increase of turnover frequency of the electrocatalyst. This finding was explored for oxidation of alcohols and aldehydes into the corresponding carboxylic acids[82,83] (Fig. 14).

Identification of electrocatalytic systems that operate at low potentials and exhibit high turnover frequencies is highly relevant to the energy-conversion field. In 2016, Stahl and co-workers demonstrated an elegant example with a cooperative electrochemical system, composed of Cu^{II}(bpy) and TEMPO, for oxidation of alcohols[85] (Fig. 15). This system combines Cu^{II}'s ability to promote single-electron oxidations with the electron-proton acceptor property of nitroxyl radicals. Since high energy intermediates are avoided in this catalytic cycle, this reaction can be realized with an anodic potential 500 mV lower than a system using only TEMPO, which would involve oxoammonium cations (−0.14 V and +0.36 V, *vs.* Fc^0/Fc^+). This cooperative system also proved to be advantageous in terms of kinetics, with a k_{obs} (11.6 s^{-1}) nearly 5 times higher than the corresponding k_{obs} (2.3 s^{-1}) for the TEMPO-only system.

2.3.2. Oxidation of amines and carbamates. The electrochemical generation of oxoammonium cations has been applied to oxidation of amines and carbamates, yielding amides and imides, respectively. While Little[86] used a cooperative system formed by bromide/TEMPO, Kashiwagi[87] and Stahl[88] employed modified versions of TEMPO to accomplish this type of transformation (Fig. 16). The proposed mechanism first involves a two-electron-one-proton transfer to generate a stabilized iminium species **16-3** which is subsequently trapped by water to form a hemiaminal **16-4.** In a second step, the hemiaminal **16-4** is subjected to a two-electron-one-proton transfer, forming the carbonyl group.

2.3.3. Generation of nitrogen-centered radicals. New reactivities of nitroxyl radicals and the corresponding oxoammonium cations have emerged recently. In 2014, Xu and co-workers reported the formation of nitrogen-centered radicals *via* the oxidation of amides by $TEMPO^+$ under basic conditions[89] (Fig. 17). Mechanistic investigation suggests that this process might involve a single-electron transfer from a nitrogen-centered anion to an oxoammonium cation. The nitrogenated radical was employed in a subsequent intramolecular reaction with an olefin to produce bicyclic products. In this reaction, TEMPO is used in stoichiometric amounts, since it is also employed as a radical trap.

The formation of nitroxyl radicals was also explored by Lin and co-workers. During the investigation of an electrochemical alkene azidooxygenation,[90] Lin postulated the anodically generation of a metastable charge-transfer complex (CTC) arising from the combination of azide anion with $TEMPO^+$. This structure was confirmed by X-ray crystallography in 2021.[91] When CTC is in

 This journal is © The Royal Society of Chemistry 2021

Published on 01 June 2021. Downloaded by University of Cambridge on 12/3/2022 1:39:05 PM.

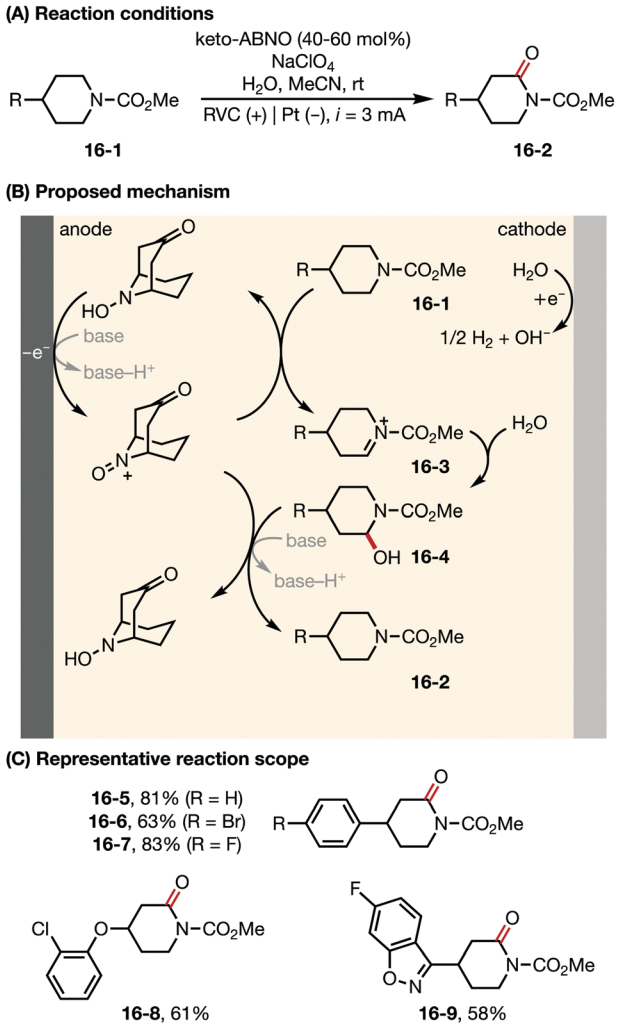


Fig. 16 (A–C) Nitroxyl-mediated oxidation of carbamates.

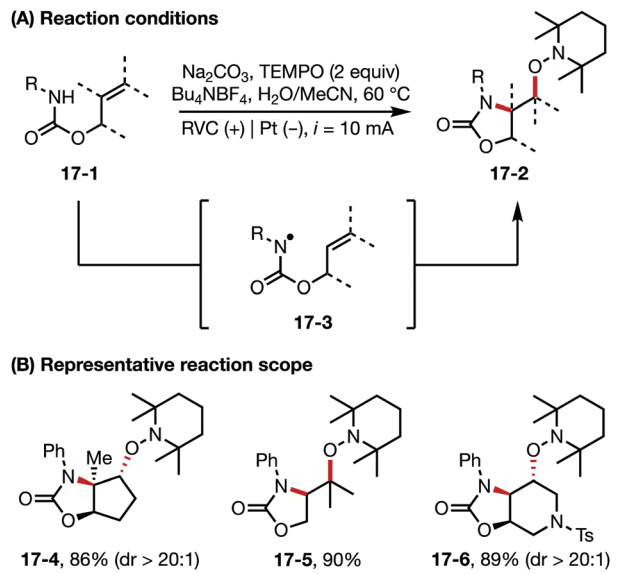


Fig. 17 (A and B) Radical cyclization triggered by electrochemical generated nitrogen centered radicals.

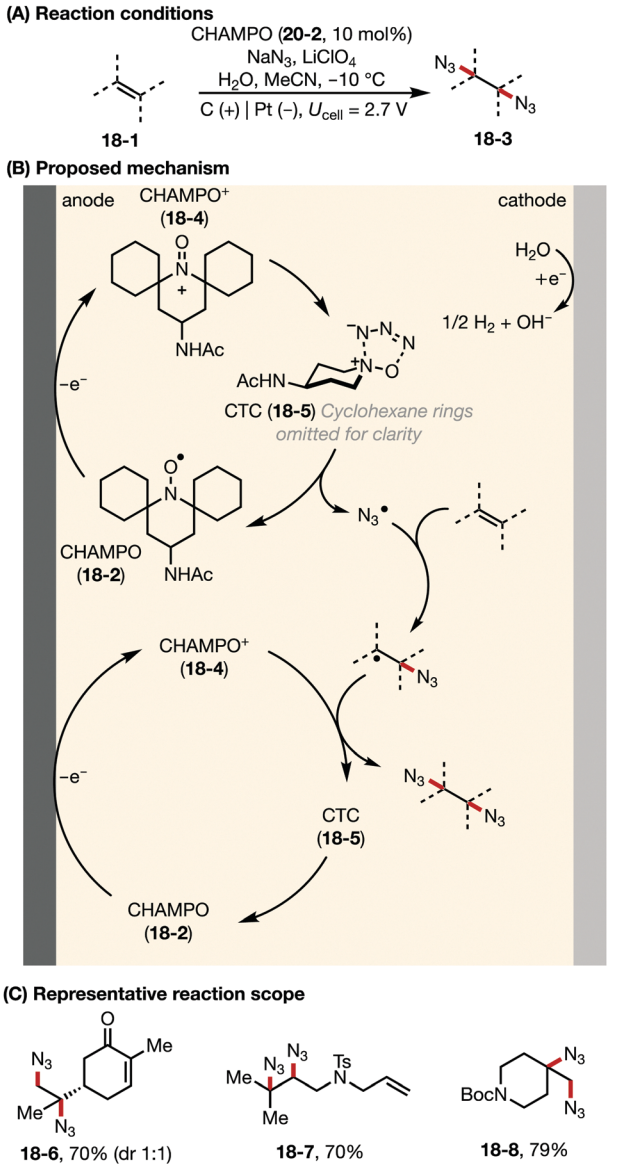


Fig. 18 (A–C) Nitroxyl-mediated diazidation of alkenes.

solution, an equilibrium is established with formation of small amounts of azidyl radical, which can add to an alkene, generating a carbon centered radical that can be trapped by TEMPO.

During the development of this azidooxygenation of alkenes, minor amounts of vicinal diazides were frequently identified as side-products. In order to favor the formation of the diazides, Lin designed a new sterically hindered nitroxyl catalyst (CHAMPO, Fig. 18).[92] Once the carbon-centered radical is generated, CHAMPO would be too sterically hindered to form a C–O bond, and a second azidyl group could be transferred, possibly *via* an inner-sphere mechanism.

2.4. Phthalimide *N*-oxyl radical (PINO) and quinuclidine radical cation as HAT agents

The phthalimide *N*-oxyl radical (PINO) has been used in radical reactions since 1977, beginning with a seminal report by

Published on 01 June 2021. Downloaded by University of Cambridge on 12/3/2022 1:39:05 PM.

Grochowski and co-workers.[93,94] The majority of reactions employing PINO take advantage of the high BDE of *N*-hydroxyphthalimide's O–H bond (NHPI). Pedulli and co-workers[95] measured a BDE equal to 88.1 kcal mol^{-1}, which is similar to the C–H bonds of allylic (88.8 kcal mol^{-1}) and benzylic (89.7 kcal mol^{-1}) positions.[96]

During the 1980s, Masui and co-workers pioneered the electrochemical generation of PINO from catalytic amounts of NHPI, and employed this radical for a wide range of oxidative reactions, including the oxidation of alcohols to carbonyl compounds,[97,98] conversion of acetals and ethers to esters,[96,99,100] generation of imides from amides,[101] and early examples of allylic and benzylic oxidations.[96,102] Kinetic studies of the oxidation of benzhydrol to benzophenone mediated by electrochemically-generated PINO revealed a large primary KIE (k_H/k_D = 10.6 at 25 °C), indicating that a HAT process should be the rate-determining step.[103]

2.4.1. Allylic oxidation. Oxidation of allylic C–H bonds offers a convenient and often selective approach for the functionalization of complex molecules[104] and thus has been widely employed in total synthesis of natural products. In 2016, Baran and co-workers studied this transformation taking Masui's pioneering work as a foundation to develop an optimized protocol. Baran incorporated two major modifications in their system[105] (Fig. 19). Firstly, ^{t}BuOOH replaced O_2 as terminal oxidant, which contributed to a substantial improvement in reaction conversion and reproducibility. Secondly, after the evaluation of different redox mediators, tetrachloro-*N*-hydroxyphthalimide (Cl_4NHPI) was identified as an optimal choice. Cyclic voltammetry analysis showed that the *N*-oxyl radical derived from Cl_4NHPI should be higher in energy and more reactive than the PINO radical, which facilitates the HAT step. Following the formation of an allylic peroxide intermediate, this peroxide was subsequently converted into the enone product. Control experiments showed that this final step can proceed without electrochemical assistance. This method was also employed in the oxidation of a wide range of terpenes and olefins.

2.4.2. Benzylic oxidations. In 2017, Stahl and co-workers studied a cooperative catalytic system employing cobalt(II) acetate and NHPI under aerobic conditions to promote benzylic oxidation.[106] During the development of this chemical method, a few substrates showed poor reactivity, and the authors hypothesized that the oxidation product would chelate cobalt, inhibiting the catalytic cycle. To overcome this limitation, the authors explored an electrochemical route for the generation of the PINO radical without cobalt, leading to improved yields.

In a subsequent work, Stahl and co-workers utilized anodically generated PINO to produce benzyl radicals, which were trapped by iodine, yielding benzylic iodides[107] (Fig. 20). The choice of base was shown to be decisive in regulating the outcome of this reaction; when the sterically hindered 2,6-lutidine is used as base, the benzylic iodides can be generated efficiently. However, the use of pyridine as base leads to the unproductive formation of benzyl-pyridinium salts. Competition between hydrogen evolution and the reduction of iodine to iodide at the cathode required the use of a divided cell for these experiments, keeping all iodine in the anodic chamber.

2.4.3. Oxidation of unactivated C(sp^3)–H bonds. The oxygenation of unactivated C(sp^3)–H bonds is a challenging transformation in organic synthesis and is typically approached through the use of highly reactive species. Curci and co-workers have studied the utilization of dioxiranes to promote these challenging oxidations,[108] the most common members of this class of compounds, DMDO (dimethyldioxirane) and TFDO (methyltrifluoromethyldioxirane), are not commercially available due to their tendency to easily decompose. In 2007, White and co-workers reported the use of a new iron-oxo complex to achieve

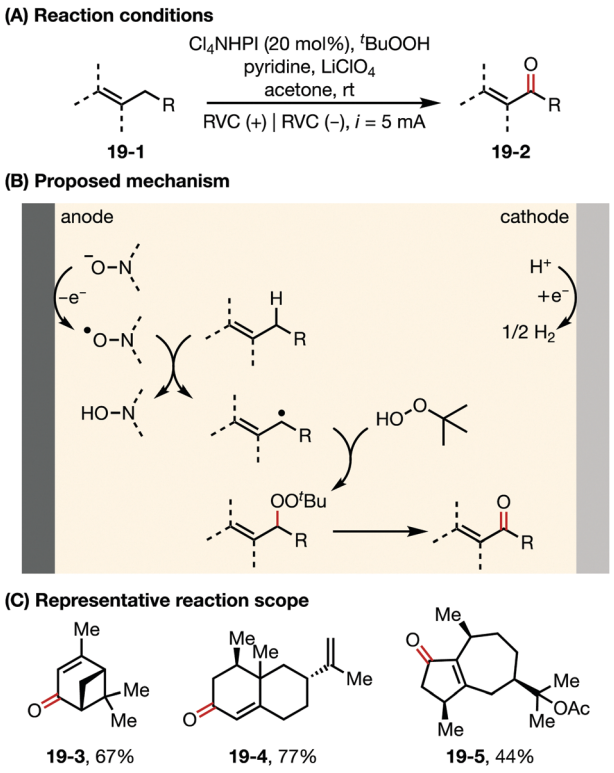


Fig. 19 (A–C) *N*-hydroxy phthalimide-mediated allylic oxidation.

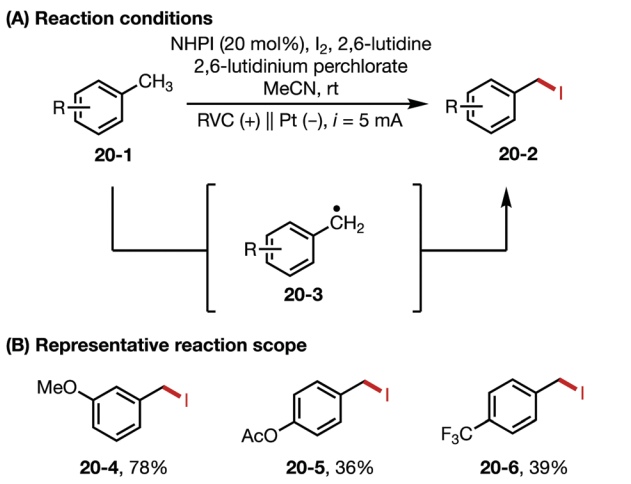


Fig. 20 (A and B) *N*-hydroxy phthalimide-mediated benzylic iodination.

 This journal is © The Royal Society of Chemistry 2021

Published on 01 June 2021. Downloaded by University of Cambridge on 12/3/2022 1:39:05 PM.

selective oxidation in complex architectures.[109] These developments are transformative in the selective oxidation of complex molecules, especially in medicinal chemistry. Nevertheless, the application of many existing chemical methods in large-scale synthesis can still be challenging considering the cost of the required oxidants (*e.g.*, trifluoroacetone) and catalysts.

In 2017, Baran and co-workers used PINO radicals and *N*-oxyl radicals derived from Cl_4NHPI to promote a HAT process on unactivated C(sp^3)–H bonds.[110] However, this approach was unsuccessful, likely due to the inert nature of such C–H bonds. During an evaluation of different mediators, a stoichiometric amount of quinuclidine was identified as a promising option. Quinuclidine can be anodically oxidized to the corresponding radical cation (**21-5**), which is reactive enough to abstract hydrogen from electron-rich C(sp^3)–H bonds, forming alkyl radicals that can be later trapped by O_2. Use of this methodology culminated in the total synthesis of (+)-2-oxo-yahazunone (**21-13**; Fig. 21) by employing sclareolide (**21-11**) as a substrate. In 2019, Magauer and co-workers explored the electrochemical generation of the radical cation of quinuclidine to synthesize the natural product mitrephorone A (**21-15**).[111]

2.5. Dehydrogenation mediated by DDQ

DDQ (2,3-dichloro-5,6-dicyano-1,4-benzoquinone) is a useful oxidant used to mediate the dehydrogenation of different functional groups. DDQ produces a hydroquinone (DDHQ) as a by-product, which can be anodically oxidized back to DDQ, allowing for a catalytic process (Fig. 22). This approach has been explored for the oxidation of alcohols to aldehydes,[112] secondary amines to imines,[113] and for the synthesis of benzoxazoles.[114]

2.6. Nitrogen centered radical cation as electron transfer agents

In the 1960s, Nelson and co-workers demonstrated that anodic oxidation of triphenylamine (**23-1**) led to a rapid coupling to form tetraphenylbenzidine (**23-4**), which would undergo subsequent oxidation to form radical cation and dication species (Fig. 23). Notably, the addition of a *para*-substituent on the three aromatic rings (**23-6**) would alter the reactivity and allow the formation of a very stable nitrogen centered radical cation (**23-7**), which was observed by a reversible profile on cyclic voltammetry analysis.[115,116] Introduction of electron-donating

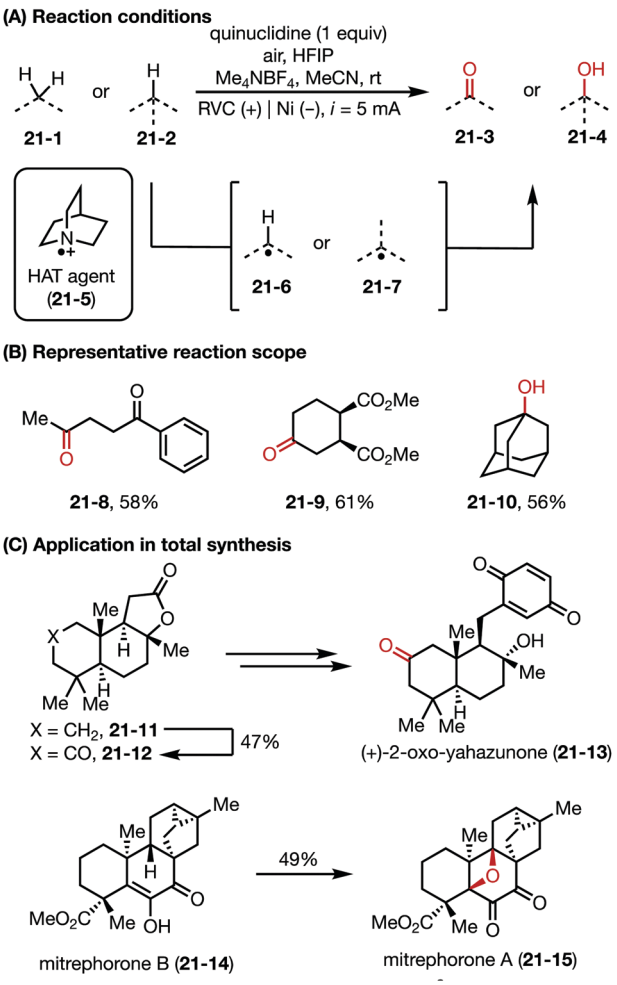


Fig. 21 (A–C) Quinuclidine-mediated C(sp^3)–H oxidation.

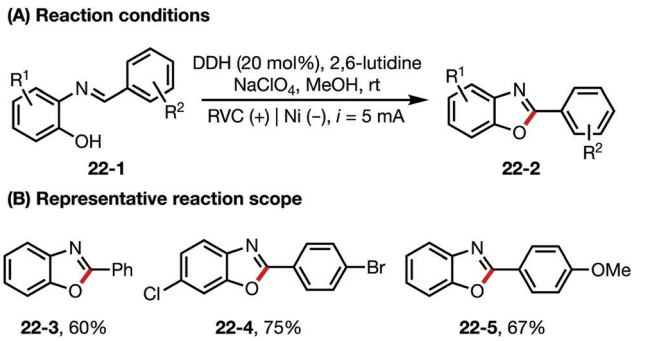


Fig. 22 (A and B) DDQ-mediated generation of benzoxazoles.

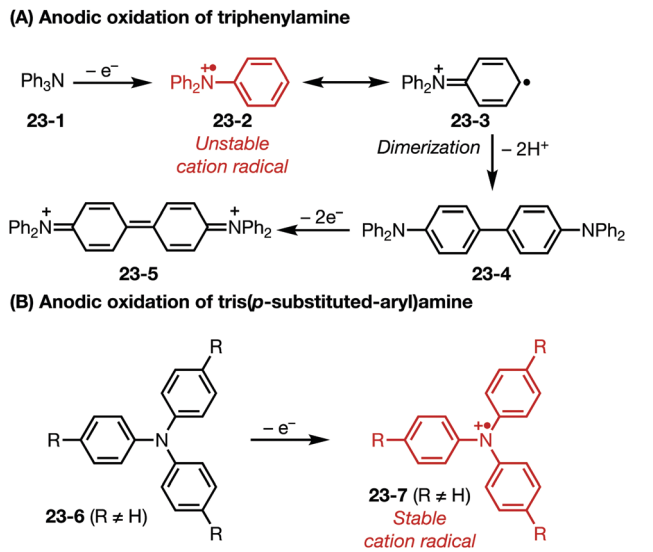


Fig. 23 (A and B) Different stability profiles of triarylamine cation-radicals.

Published on 01 June 2021. Downloaded by University of Cambridge on 12/3/2022 1:39:05 PM.

or electron-withdrawing groups on the *para* position of the aryl rings allows easy modulation of the oxidation potential. These mediators have been employed in a wide range of transformations to promote electron transfer events, such as the oxidation of sulfides,[117,118] stilbenes,[119] and strained bicycles.[120,121]

2.6.1. Oxidation of electron-rich aromatics. In 2015, Little and co-workers explored the use of the cation-radical of tris(*p*-bromophenyl)amine to oxidize benzylic alcohols to aldehydes and benzylic ethers to benzoate esters, among other transformations (Fig. 24).[122] The use of a triarylamine allowed the authors to perform the oxidation at a much lower potential than the oxidation potential of the substrate, which enables higher yields and broader functional group compatibility. In this work, a polymeric ionic liquid was employed as electrolyte, which could be recovered and reused, simplifying product isolation and minimizing waste generation.

Inspired by the useful properties of radical cations derived from triarylamines, Zeng, Little, and co-workers developed analogue redox mediators using a triarylimidazole (TAI) scaffold that can be easily synthesized.[123,124] The radical cation derived from TAI was able to oxidize benzylic alcohols and *p*-methoxytoluene to the corresponding benzaldehydes, benzylic ethers to benzoate esters, and chalcone epoxides (**25-1**) to radical cations (**25-4**) that can further engage in a Friedel–Crafts mechanism (Fig. 25).[125]

Little and co-workers also explored a fused-ring form of TAI mediator (2-aryl-1-methylphenanthro[9,10-*d*]imidazole, see **26-2**), which yields a more stable radical cation than original TAIs. The higher stability of this radical cation was observed by cyclic voltammetry analysis: when the scan rate was decreased from 100 mV s^{-1} to 10 mV s^{-1} (a longer analysis time), the fused mediator **26-2** still presented a quasi-reversible profile, indicating a longer lifetime of the corresponding radical cation as compared to the radical cation derived from mediator **26-1**[126] (Fig. 26). Another analogue redox mediator, *N*-aryl-carbazole, was studied by Ma and co-workers, and the corresponding N-centered radical cation was also suggested as the key reactive species in oxidative transformations.[127]

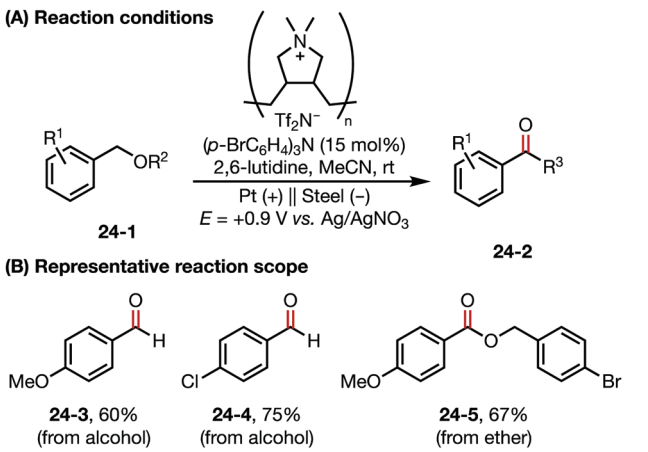


Fig. 24 (A and B) Triarylamine-mediated oxidation of alcohols and ethers.

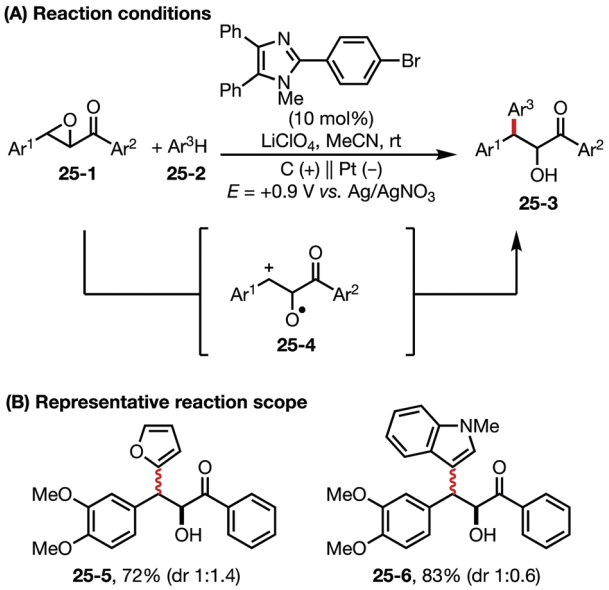


Fig. 25 (A and B) Triarylimidazole-mediated oxidation of chalcone epoxides mediated by TAI cation-radical.

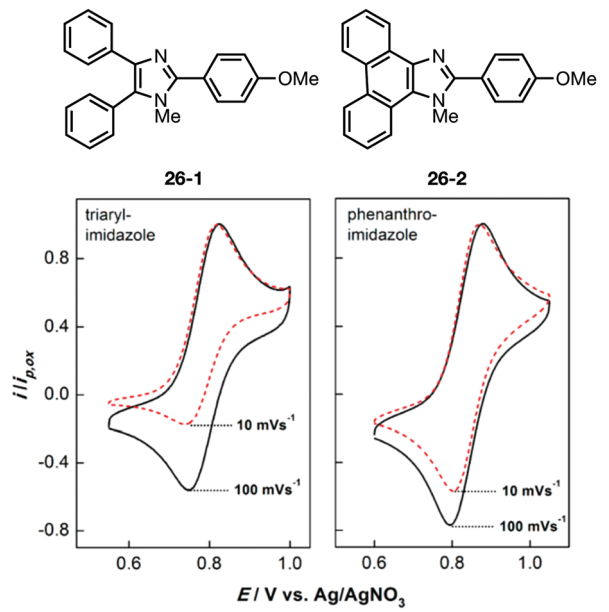


Fig. 26 Cyclic voltammogram of TAI **26-1** and its cyclized analogue **26-2**. This figure has been adapted from ref. 126 with permission from American Chemical Society, copyright 2014.

2.6.2. Oxidation of anions into radicals. In 2018, Xu and co-workers developed a radical cascade to produce imidazo-fused N-heterocycles[128] (Fig. 27). Their approach relies on the generation of a nitrogen-centered radical by oxidation of the corresponding anion, which has an oxidation potential ($E_{p/2}$ = 0.66 V *vs.* SCE) significantly lower than common triarylamines (TBPA, $E_{p/2}$ = 1.08 V *vs.* SCE). This difference in potentials indicates that the substrate would likely undergo a direct oxidation, and that the triarylamine radical cation would play a minor role in the mechanism. Since triarylamines gave low

 This journal is © The Royal Society of Chemistry 2021

Published on 01 June 2021. Downloaded by University of Cambridge on 12/3/2022 1:39:05 PM.

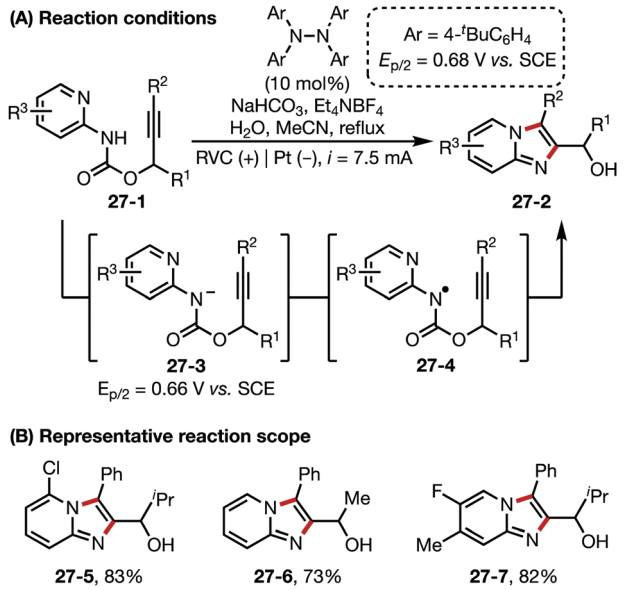


Fig. 27 (A and B) Tetraarylhydrazine-mediated synthesis of imidazo-fused N-heterocycles.

yields (11–39%) of the desired product, the authors turned to tetraarylhydrazine mediators which proved more efficient. Tetra-(4-*tert*-butylphenyl)hydrazine showed an oxidation potential ($E_{p/2}$ = 0.68 V *vs.* SCE) lower than that of triarylamines, and could generate the desired bicyclic product in 89% yield. This was the first application of this mediator in synthetic electrochemistry.

Xu and co-workers also explored mediated oxidation of enolates derived from dimethyl malonate and methyl acetoacetate (Fig. 28), which have low oxidation potential (enolate of dimethylmalonate, $E_{p/2}$ = 0.31 V *vs.* SCE).[129] In order to achieve a mediated process, a phenothiazine (**28-4**; $E_{p/2}$ = 0.52 V *vs.* SCE) was employed, which has a lower oxidation potential than triarylamines, despite architectural similarities. The concentration of enolate **28-5** was kept small, as it was generated continuously by deprotonation of the dicarbonyl compound with cathodically generated hydroxide, which is an important feature to guarantee a mediated process. The resultant carbon-centered radical **28-6** was employed on the construction of substituted pyrrolidines and tetrahydropyridines.

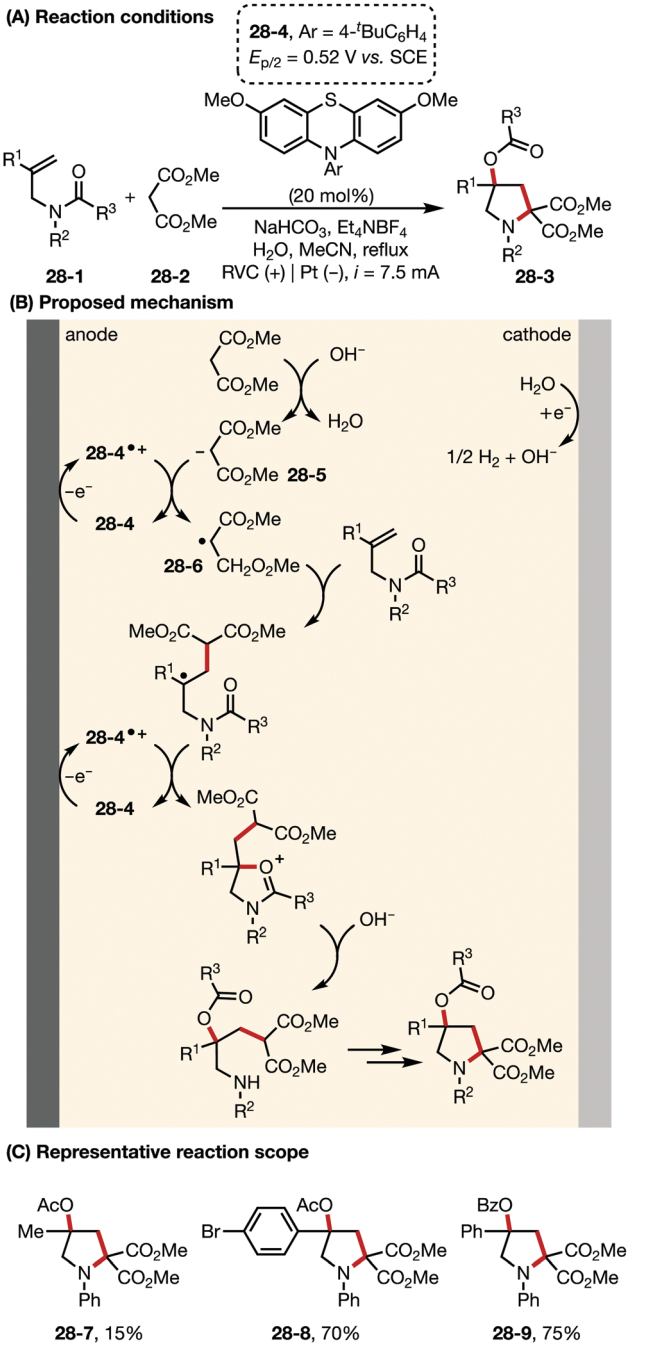


Fig. 28 (A–C) Phenothiazine-mediated synthesis of substituted pyrrolidines.

Transition metal complex as mediators

The combination of transition metal catalysis and electrochemistry offers the advantages of higher atom efficiency, milder reaction conditions, and safer protocols in place of using stoichiometric chemical oxidants to induce catalyst turnover. Furthermore, using electrochemistry to activate metal catalysts or key reactive intermediates derived from these catalysts has been shown to promote new reactivities that were previously challenging or unknown.

Metalla-electrochemical reactions fall into two broad categories. First, transition-metal complexes can serve as direct mediators to transfer electrons between electrodes and target substrates. Specifically, transition metal-bound substrate adducts exhibit lower oxidation potentials, and the oxidized open-shell species possess characteristics of persistent radicals, thus rendering the group transfer process to the substrates more selective and efficient. This type of metalla-electrochemical methods has given rise to numerous new transformations that were impossible or challenging to accomplish otherwise. A more detailed review on these methods can be found in a recent account.[130]

Second, electrochemistry supports traditional transition-metal catalyzed C–H activations, leading to a variety of transformations forging carbon–carbon and carbon–halogen bonds. In a transition-metal-catalyzed C–H activation, anodic oxidation can

Published on 01 June 2021. Downloaded by University of Cambridge on 12/3/2022 1:39:05 PM.

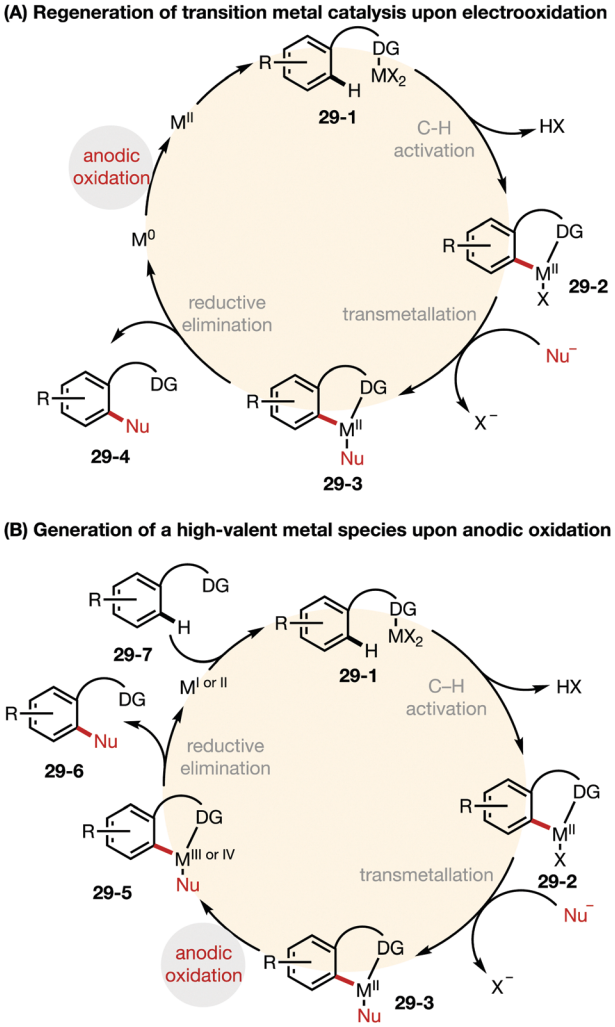


Fig. 29 (A and B) Modes of electrochemical transition metal-catalyzed C–H functionalization.

typically play two roles: to enable regeneration of the active transition metal catalyst (Fig. 29A) and to oxidize the transition metal catalyst intermediate to a high-valent species to induce subsequent reductive elimination (Fig. 29B). Detailed discussion on transition-metal catalyzed C–activation reactions can be found in recent reviews.[131] An important advantage of metalla-electrochemistry is that C–H activation reactions employ electricity as the oxidizing equivalent, thus avoiding the use of external chemical oxidants and generation of wasteful by-products.

Traditionally, anodic C–H activation has been dominated by precious transition metal catalysts based on palladium, ruthenium, iridium, and rhodium; more recently, however, 3d earth-abundant metals such as nickel and cobalt have seen increasing use in electrochemical C–H activation. In the following section we will discuss recent advances in metalla-electrochemical reactions grouped by different metal mediators.

2.7. Manganese

Manganese is a particularly attractive mediator in electrocatalytic systems due to its abundance, low toxicity, and low cost. Traditionally, manganese complexes have been employed in alkene and C–H functionalizations to form C–N, C–O, and C–halogen bonds *via* radical pathways.[132] However, it was not until recently that redox-active manganese complexes matured as competent mediators for electrochemically-driven transformations. Mechanistic investigation of these catalytic cycles suggest that a Mn^{II}/Mn^{III} redox pair is operating in many of these transformations.

2.7.1. Olefin functionalization. In 1998, Snider reported the diazidation of alkenes and glycals using 3 equivalents of $Mn(OAc)_3{\cdot}H_2O$.[133] Snider proposed that the diazidation of alkene occurs *via* rapid azide transfer from Mn^{III}-azide to the alkene and subsequently to the incipient alkyl radical intermediate. This pioneering discovery has provided inspiration for several recent developments in electrocatalysis.

In 2017, the Lin lab developed an electrochemical diazidation of alkenes using Mn^{II} salts as efficient and selective electrocatalysts.[134] The resulting vicinal diazides can be easily reduced to form diamines, which are prevalent motifs in a variety of bioactive natural products, pharmaceuticals, and molecular catalysts. Unlike Snider's reaction system, the Mn^{II} salt was added as precatalyst, and was then oxidized under electrochemical conditions to generate a Mn^{III}–N_3 intermediate (Fig. 30B). This oxidized intermediate serves as a latent azidyl radical source that delivers a first azide equivalent to the alkene

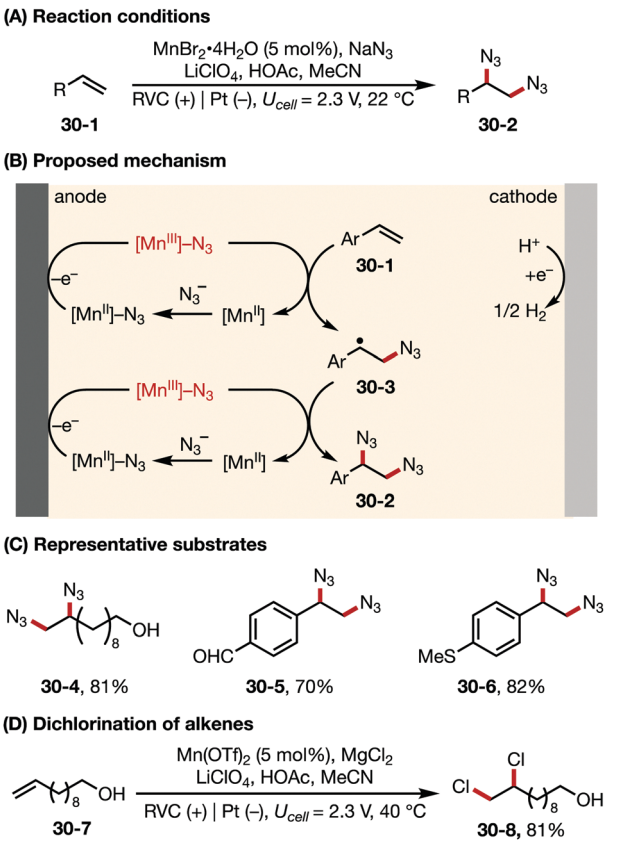


Fig. 30 (A–D) Manganese-catalyzed electrocatalytic diazidation and dichlorination of alkenes.

 This journal is © The Royal Society of Chemistry 2021

Published on 01 June 2021. Downloaded by University of Cambridge on 12/3/2022 1:39:05 PM.

(**30-1**), followed by addition of a second azide equivalent to the resultant alkyl radical (**30-3**) to furnish the diazide product **30-2**. This work also features significantly milder reaction conditions than those reported by Snider. The Lin group later applied this strategy to the dichlorination of alkenes (Fig. 30D).[135]

To extend the utility of the strategy used for this electrochemical diazidation protocol, the Lin group developed an additional electrochemical method for the heterodifunctionalization of alkenes based on anodically coupled electrolysis (ACE) strategy.[136] The implementation of ACE strategy relies on the appropriate pairing of radical precursors $(X1)^-$ and $(X2)^-$ with a suitable metal catalyst. Two parallel anodic oxidations will take place: one radical precursor would undergo single-electron oxidation to generate a transient free radical $(X1)^\bullet$ while the other precursor $(X2)^-$ would undergo catalyst-assisted anodic oxidation to form a $(X2)^\bullet$ equivalent in the form of a metal-bound adduct. This adduct could then transfer the functional group of interest to the alkene substrate. The persistent radical effect would dictate the order in which radicals $(X1)^\bullet$ and $(X2)^\bullet$ add to the substrate, thereby inducing a highly chemo- and regioselective strategy for the heterodifunctionalization of alkenes. In the reaction reported by Lin, two different radical intermediates including a transient CF_3 radical and a Mn^{III}–Cl adduct were generated simultaneously *via* ACE from Langlois's reagent and $MgCl_2$ in the presence of Mn^{II} precatalyst. As shown in Fig. 31, the anodically generated CF_3 radical adds to the alkene, which is followed by transfer of chlorine from Mn^{III}–Cl to deliver the chlorotrifluoromethylated product **31-2**. The use of ACE as a mechanistic design principle has also been utilized for the chlorophosphinoylation (Fig. 31C),[137] and haloalkylation of alkenes (Fig. 31D).[138]

The Lin group applied their strategy for the electrochemical heterodifunctionalization of alkenes to the radical cyclization of 1,6-enynes.[139] In this reaction, the Langlois reagent (CF_3SO_2Na) and $MgCl_2$ served as functional group donors and Mn^{II} served as the electrocatalyst. As depicted in Fig. 32, the 1,6-enyne substrate undergoes consecutive trifluoromethylation, radical ene–yne cyclization, and chlorination to furnish the substituted cyclized product (Fig. 32). The *E*/*Z* selectivity observed in the product was proposed to be sterically controlled. To explore the validity of this proposal, addition of bulky ligand (*e.g.* 2,2,-bipyridine) yielded near-complete selectivity for a single product isomer.

The Mo group developed an electrochemical method to make trifluoromethylated oxindoles and related heterocycles.[140] Langlois' reagent is used as the CF_3 source. Upon anodic oxidation, this reagent releases a CF_3 radical which adds to the substrate to generate a tertiary alkyl radical and triggers cyclization onto the aromatic ring (Fig. 33). This protocol has been employed to forge complex ring systems through cascade cyclization (Fig. 33C).

The Lei group has also used the Mn^{II}/Mn^{III} redox pair to enable electrochemically driven radical cyclization reactions.[141] In this work, the authors reported an electrochemically-driven, Mn-catalyzed coupling reaction between N-substituted 2-arylbenzoimidazoles (**34-1**) and alkylboronic acids (Fig. 34). EPR and

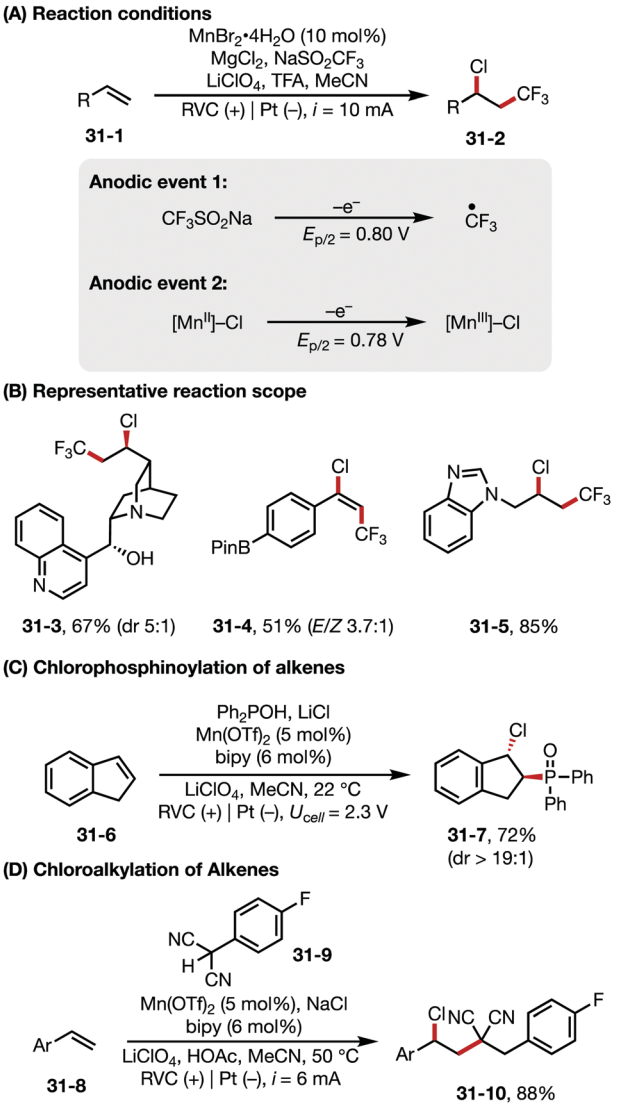


Fig. 31 (A–D) Manganese-catalyzed electrocatalytic heterofunctionalization of alkenes.

CV data led them to propose a mechanism including the direct anodic oxidation of alkylboronic acids to alkyl radicals. Subsequent addition of these alkyl radicals to substrate **34-1** was proposed to be facilitated by a Mn^{III} species, ultimately leading to the formation of cyclized product **34-2**.

2.7.2. C(sp³)–H functionalization. In addition to alkene functionalization, manganese electrochemical mediators have been utilized in C(sp^3)–H functionalization. An interesting example from the Lei group described an electrochemical azidation of C(sp^3)–H bonds facilitated by visible light catalysis (Fig. 35).[142] In this work, DDQ was utilized as a HAT reagent to activate inert tertiary C–H bonds, which is then trapped by the azide-transfer complex Mn^{III}–N_3 formed *in situ* on the anode. Mechanistic studies suggested that both excited photocatalyst DDQ and the anodically generated azidyl radicals are capable of HAT to form alkyl or benzyl radicals. This reaction technically belongs to the electrophotocatalysis section (see Section 7) but

Published on 01 June 2021. Downloaded by University of Cambridge on 12/3/2022 1:39:05 PM.

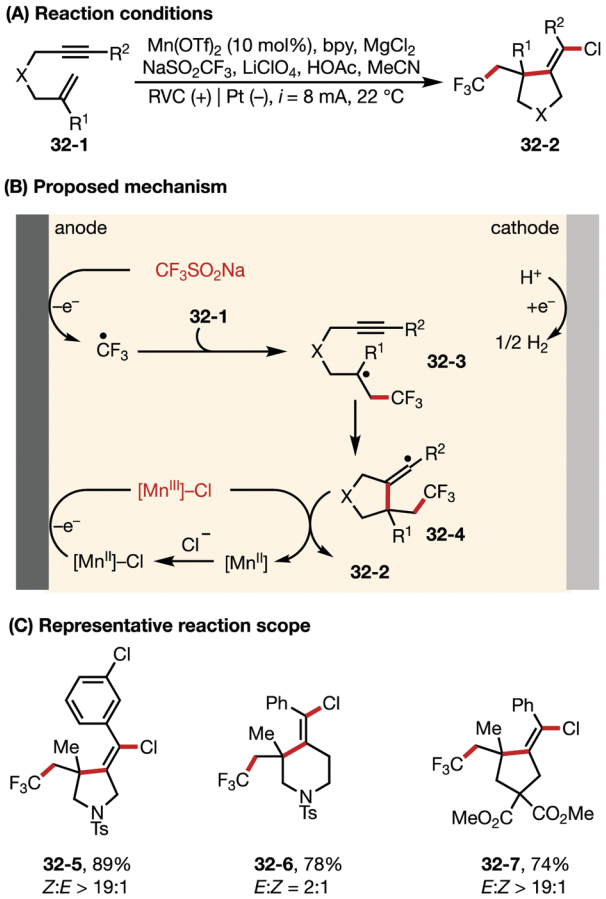


Fig. 32 (A–C) Synthesis of chlorotrifluoromethylated pyrrolidines *via* electrocatalytic radical ene–yne cyclization.

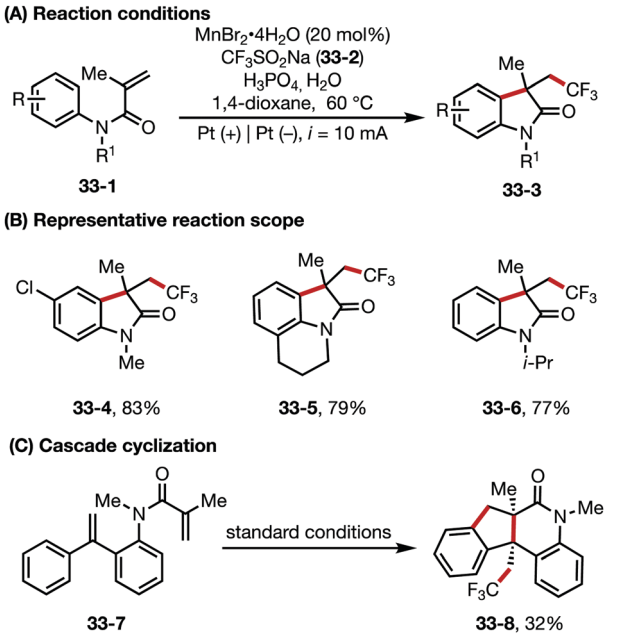


Fig. 33 (A–C) Manganese-mediated electrochemical trifluoromethylation for the synthesis of azaheterocycles.

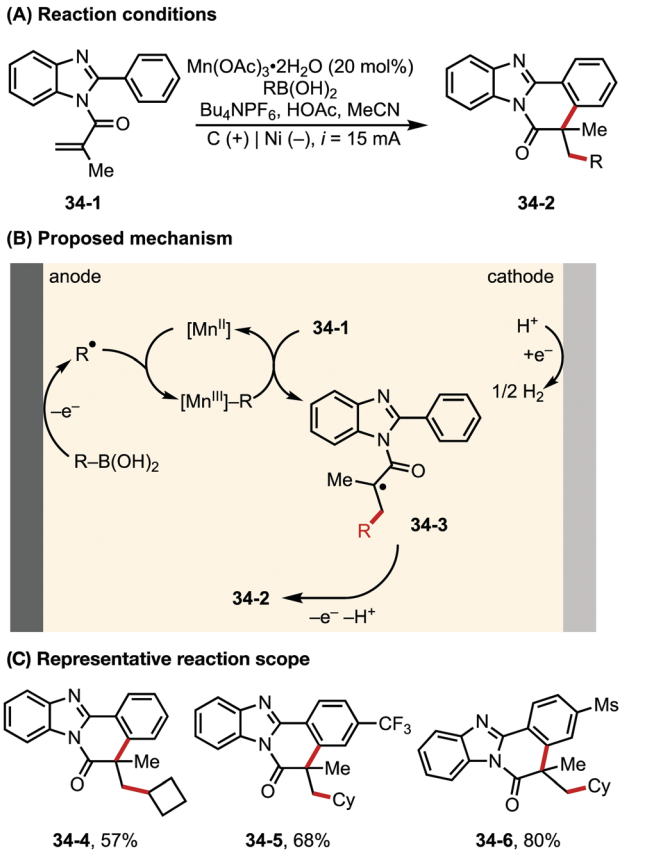


Fig. 34 (A–C) Manganese-catalyzed electrochemical cyclization reaction of N-substituted 2-arylbenzoimidazoles with alkylboronic acids.

is discussed here owing to its similarity in catalytic mechanism to other examples in this section.

In 2021, the Ackermann group reported an electrochemical manganese porphyrin/salen complex-catalyzed azidation of unactivated secondary, tertiary, and benzylic C–H bonds.[143] In this work, mechanistic studies suggest that a Mn^{III}/Mn^{IV} redox pair is in operation.

A similar mechanism was proposed in another example by Morrill and co-workers that used a Mn^{II} catalyst to mediate an electrochemical synthesis of β- and γ-chlorinated ketones (Fig. 36).[144] In this system, anodically generated Mn^{III}–Cl is responsible for the activation of a cyclopropanol or cyclobutanol substrate (**36-1**) to afford alkoxy radical **36-3**, which undergoes C–C bond homolysis to generate a primary alkyl radical **36-4**. The release of ring strain is thought to be the driving force for cleavage of the C–C bond. In an alternative pathway, a Mn^{III}-alkoxide resulting from ligand exchange between Mn^{III}–Cl and **36-1** may undergo reversible β-scission to form **36-4**. Trapping of this transient primary carbon-centered radical with the persistent Mn^{III}–Cl species forms a new C–Cl bond.

2.7.3. Manganese-catalyzed alcohol oxidation. Mn-Based mediators have also been shown to mediate alcohol oxidation reactions. Huang and co-workers developed an electrochemical Mn-catalyzed cyclization reaction to construct quinazolinones from aminobenzamides and alcohols in an undivided cell (Fig. 37).[145] The authors proposed that the Mn^{III} species

 This journal is © The Royal Society of Chemistry 2021

Published on 01 June 2021. Downloaded by University of Cambridge on 12/3/2022 1:39:05 PM.

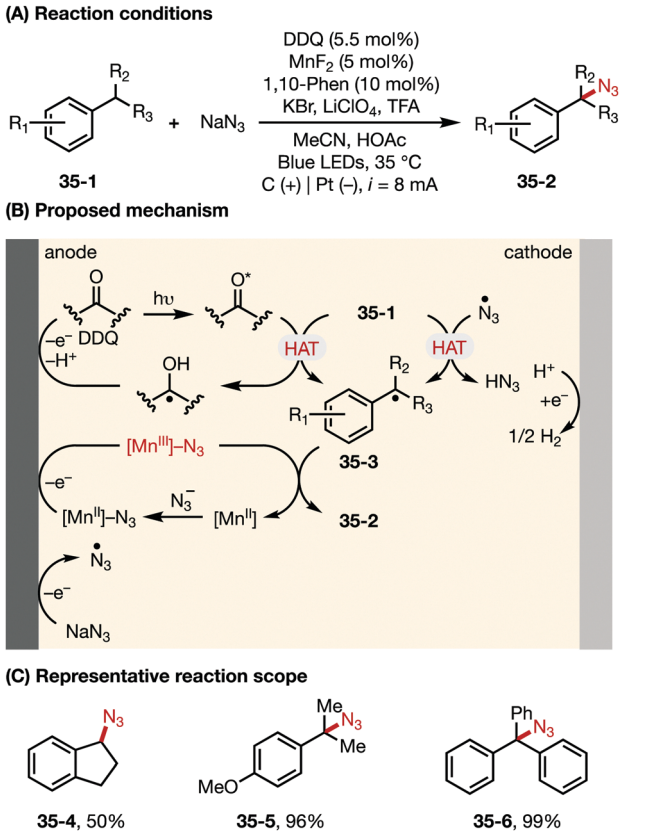


Fig. 35 (A–C) Manganese-catalyzed oxidative azidation of C(sp^3)–H bonds under electrophotocatalytic conditions.

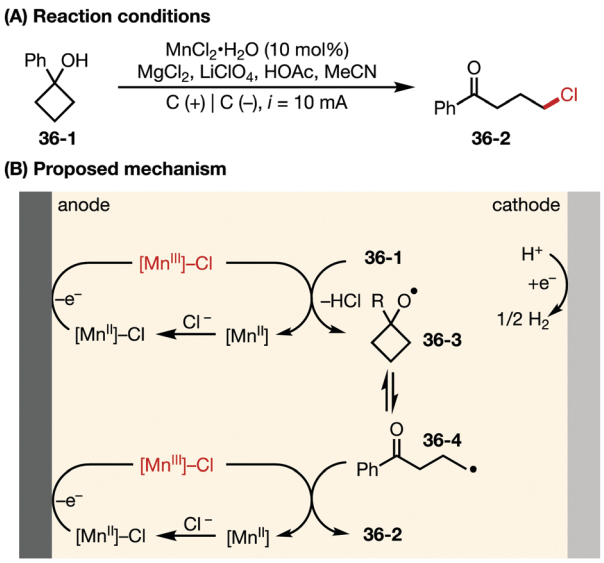


Fig. 36 (A and B) Manganese-catalyzed electrochemical deconstructive chlorination of cycloalkanols *via* alkoxy radicals.

generated on the anode can oxidize the alcohol to benzaldehyde, which then condenses with aminobenzamides to be further transformed into the cyclized product **37-3**.

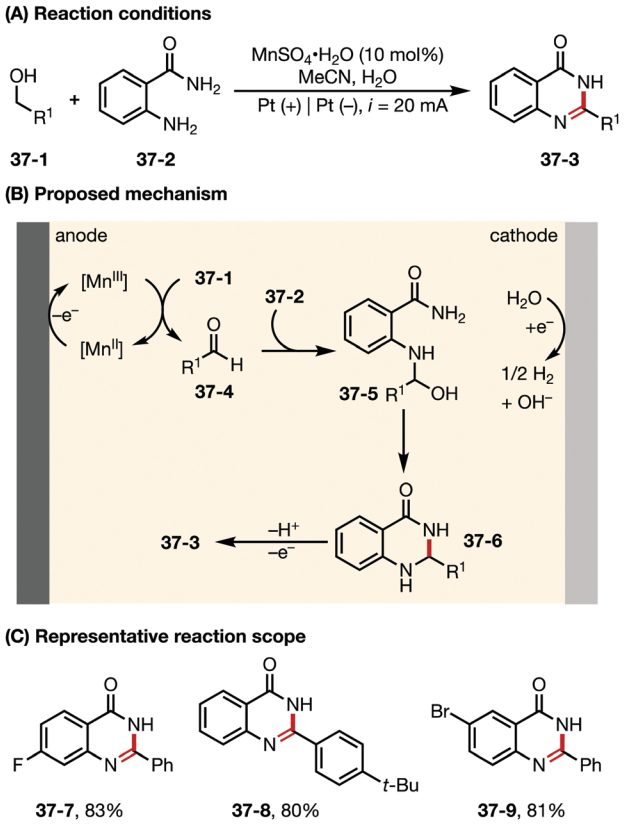


Fig. 37 (A–C) Manganese-catalyzed electrochemical synthesis of quinazolinones.

2.8. Iron

The relatively low oxidation potential of ferrocene ($E_{1/2}(Cp_2Fe)$ = 0.34 V *vs.* SCE in 9 : 1 MeCN : H_2O) makes it a selective redox catalyst that bears a broad functional group tolerance.[146] Ferrocene has been utilized in numerous transformations to activate N–H bonds to generate highly reactive amidyl radicals. Additionally, other iron complexes have found applications in electrochemical C–H activation reactions.

2.8.1. Radical cyclization. In 2018, the Xu group reported a ferrocene-mediated electrochemical alkyne functionalization to access fluorinated dibenzazepines[147] using $CF_2HSO_2NHNHBoc$ as a CF_2H radical precursor (Fig. 38). The electrolytic process commences with the anodic oxidation of Cp_2Fe to Cp_2Fe^+. At the same time, methanol is reduced on the cathode to generate H_2 and MeO^-. The deprotonation and subsequent oxidation of $CF_2HSO_2NHNHBoc$ (**38-2**) generates intermediate **38-5**, which further loses an electron and a proton to afford diazene **38-6**. The following decomposition of **38-6** releases a CF_2H radical which can react with an alkyne group to furnish vinyl radical **38-8**. This vinyl radical then cyclizes onto phenyl rings to afford a 7-member ring structure **38-9**. Lastly, oxidative rearomatization of the cyclized intermediate affords the dibenzazepine product **38-3**.

In another work by the Xu group, Lewis acids were used to acidify the tertiary C–H bond on malonate amides, which was then deprotonated by electrochemically generated methoxide (Fig. 39).

Published on 01 June 2021. Downloaded by University of Cambridge on 12/3/2022 1:39:05 PM.

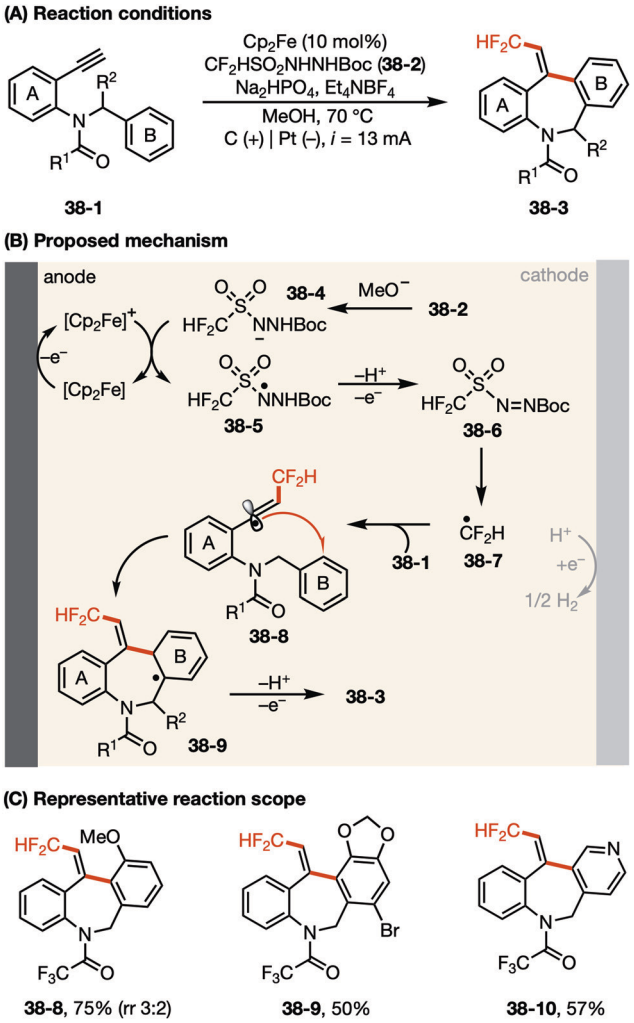


Fig. 38 (A–C) Electrochemical difluoromethylarylation of alkynes.

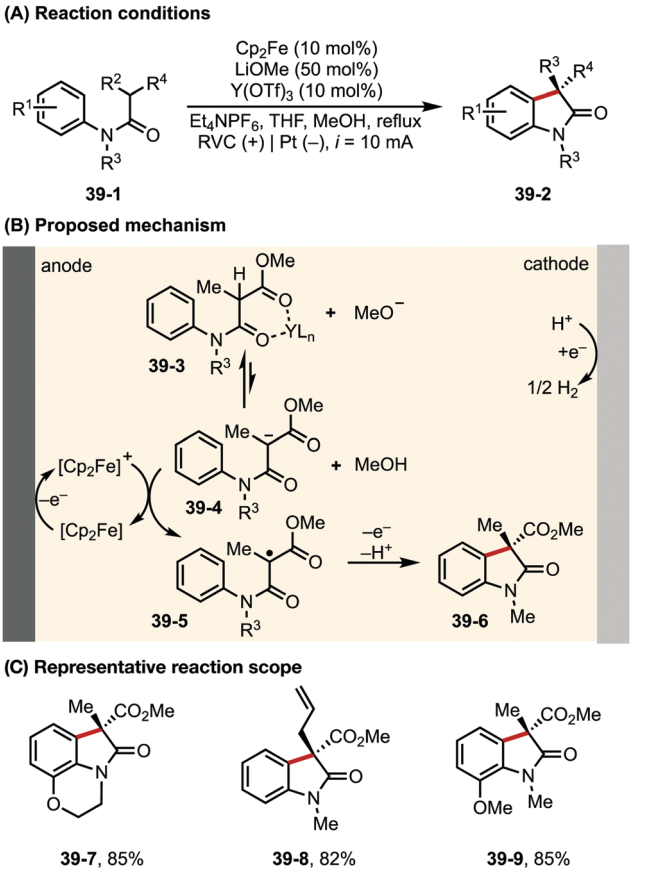


Fig. 39 (A–C) Electrochemical dehydrogenative cyclization of 1,3-dicarbonyls.

Oxidation of the resulting anion **39-4** by a Fc/Fc^+ couple then generates the alkyl radical intermediate **39-5**, which subsequently undergoes cyclization to deliver product **39-6**.[148]

The Xu group employed a similar strategy for radical cascade cyclization reaction to access functionalized 7-member carbocyclic compounds (Fig. 40).[149] The anodically generated amidyl radical by means of Cp_2Fe^+ catalysis undergoes stepwise 5-exo-trig and 7-endo-trig cyclization followed by HAT from 1,4-cyclohexadiene (1,4-CHD) to deliver product **40-2**. It was concluded that the trans disposition of the alkyl radical and the alkene in the intermediate **40-4** is critical to inducing an 7-endo-trig cyclization pathway instead of the 6-exo-trig cyclization pathway in the second radical addition event.[150] The typically favored 6-exo-trig cyclization is likely inhibited by the ring strain from the resultant trans-fused bicyclic ring system.

2.8.2. Aromatic C–H functionalization. $Fe(acac)_3$ has also been used as a catalyst in electrochemical C–H activation. The Ackermann group described a ferraelectrocatalytic C–H arylation in 2019.[151] As shown in Fig. 41, this transformation is thought to proceed through a C–H cleavage (*via* a sigma bond metathesis pathway or through a base-assisted internal electrophilic substitution). After this initial event, the resultant Fe^{II} intermediate goes through an anodic single-electron-transfer (SET) and transmetallation to generate five-membered Fe^{III} intermediate **41-4**, which then reductively eliminates to release the arylated product. The iron catalyst is then regenerated on the anode.

2.8.3. Various amination reactions. In a similar report in 2018, Luo and co-workers demonstrated an Fe-catalyzed electrochemical cycloaddition of diaza-oxyallyl cations to synthesize diamines.[152] Like some previous examples in this section, this reaction also featured cathodic reduction of methanol paired with the anodic oxidation of ferrocene (Fig. 42). On the anodic side, the oxidized ferrocenium serves as a mediator to oxidize the deprotonated *N*,*N*-dibenzyloxyurea (**42-4**). As such, diaza-oxyallyl cation **42-5** is generated in an efficient fashion and reacts with a variety of heteroarenes to form value-added diamine products.

Furthermore, Banerjee and co-workers reported a synthesis of benzimidazolone and oxazinones from aryl benzyloxyureas using a ferrocene catalyst and paired electrolysis.[153] Here, water was reduced cathodically and the resultant hydroxide ion acts as the active base to remove the proton on urea **43-1** (Fig. 43). The resultant species then undergoes Fc^+-mediated oxidation to form zwitterionic nitrenium intermediate **43-3**. Loss of a nitrene leaving group gives rise to an isocyanate intermediate **43-4**, which undergoes 5-exo cyclization to give the desired product.

 This journal is © The Royal Society of Chemistry 2021

Published on 01 June 2021. Downloaded by University of Cambridge on 12/3/2022 1:39:05 PM.

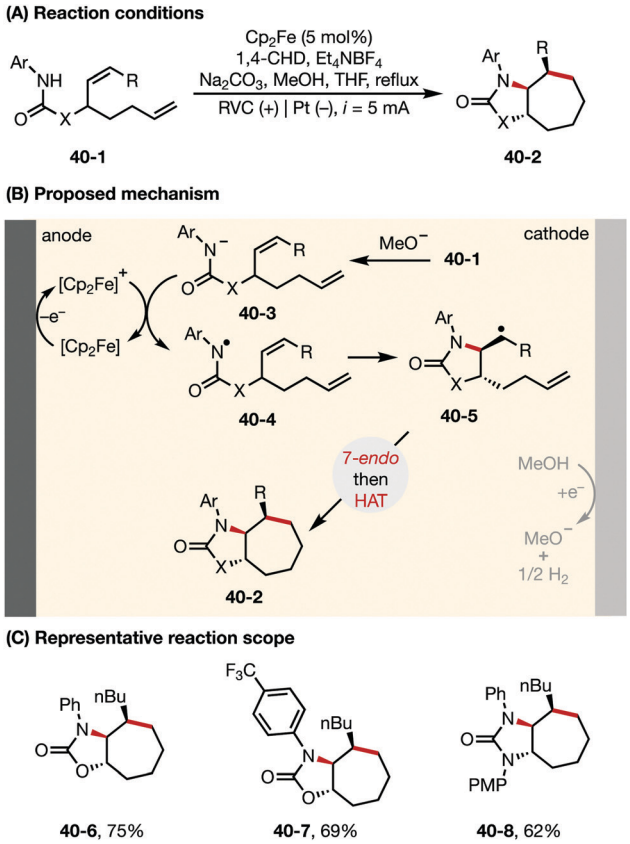


Fig. 40 (A–C) Electrochemical synthesis of 7-membered carbocycles through cascade 7-endo-trig radical cyclization.

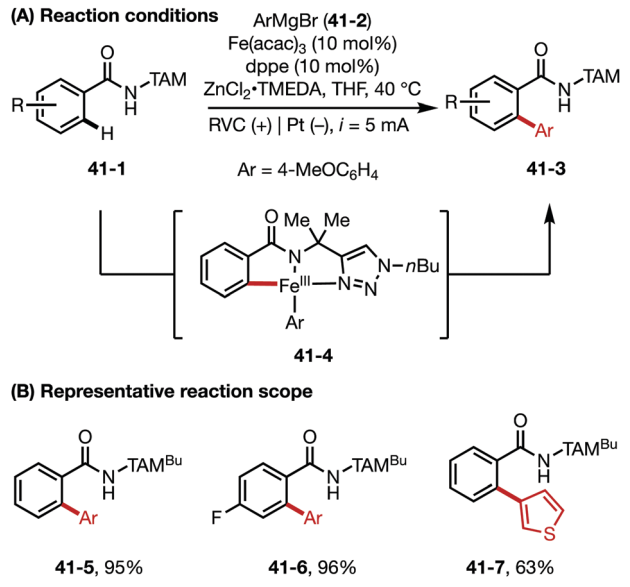


Fig. 41 (A and B) Electrochemistry-driven iron-catalyzed C–H arylation.

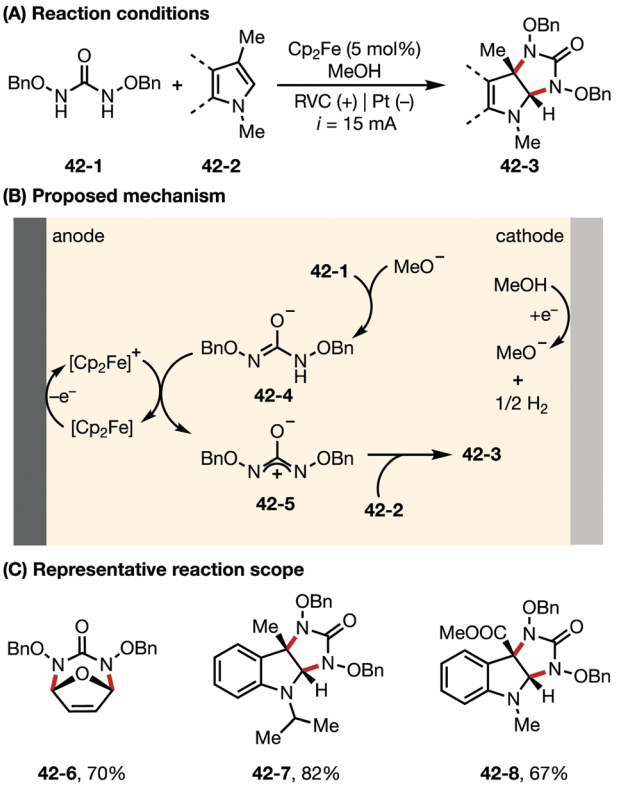


Fig. 42 (A–C) Electro-oxidative generation of diaza-oxy-allyl cation toward the synthesis of diamine.

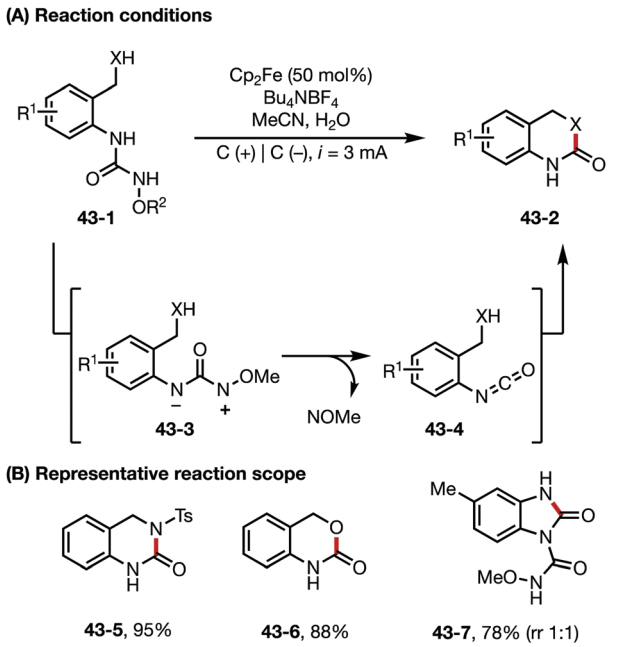


Fig. 43 (A and B) Electrochemical access to benzimidazolone and quinazolinone *via in situ* generation of isocyanates.

2.9. Copper

2.9.1. Cyanation of alkenes. In 2019, the Lin group reported a Cu-catalyzed enantioselective electrocatalytic cyanophosphinoylation of vinylarenes that made use of ACE strategy (Fig. 44). A secondary phosphine is oxidized in a Cu-mediated process to form a P-centered transient radical **44-4** and meanwhile Cu^{II}–CN is oxidized to Cu^{III}–CN. This pair of open-shell intermediates will then react

Published on 01 June 2021. Downloaded by University of Cambridge on 12/3/2022 1:39:05 PM.

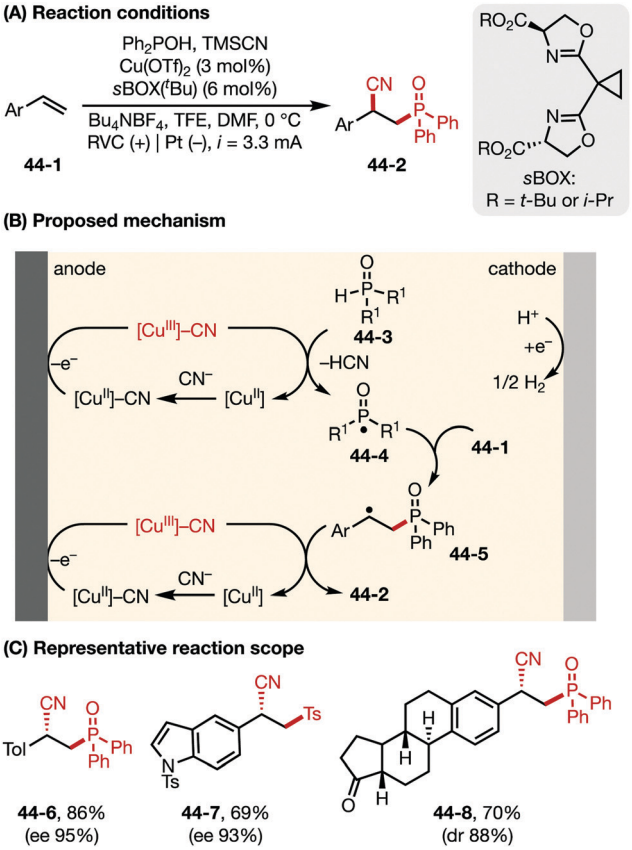


Fig. 44 (A–C) Enantioselective electrocatalytic cyanophosphorylation of vinylarenes.

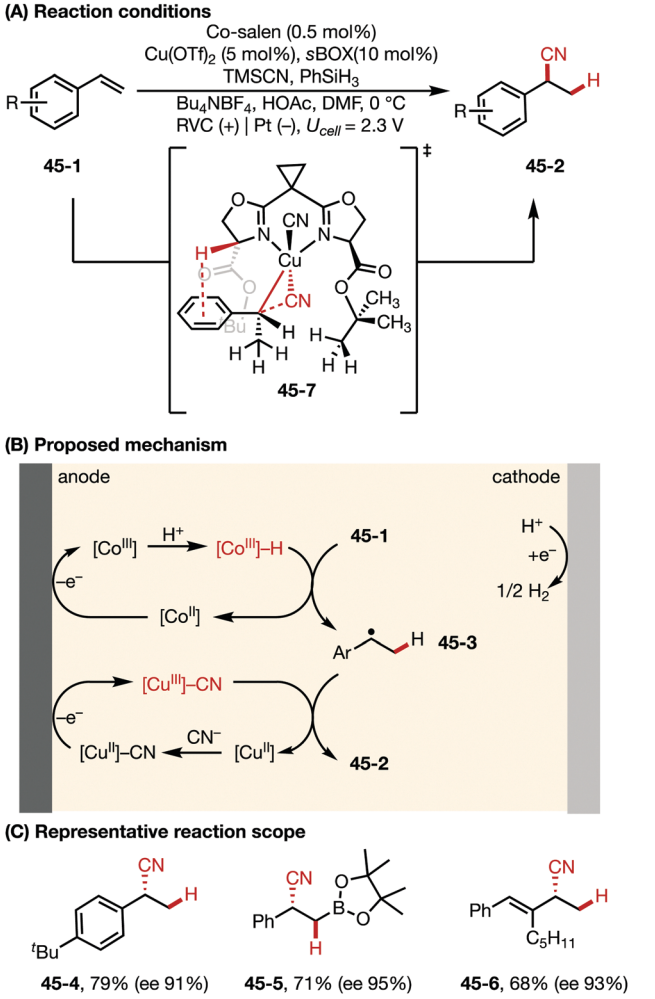


Fig. 45 (A–C) Dual electrocatalysis enables enantioselective hydrocyanation of conjugated alkenes.

with the alkene sequentially following the persistent radical effect to give product **44-2**. The bisoxazoline (BOX) ligands along with CN^- play a key role in preventing the cathodic reduction of copper ions, which will result in Cu metal plating out.[149] The high enantioselectivity of this transformation was found to be related to the structure of the ester groups on the sBOX ligand.

In 2020, the Lin group reported a dual electrocatalytic approach for the asymmetric hydrocyanation of conjugated alkenes (Fig. 45).[154] Anodic oxidation generates a Co^{III}–H complex and a Cu^{III}–CN complex in a concerted fashion. The Co^{III}–H species enables hydrogen-atom transfer to the alkene substrate, and Cu^{III}–CN delivers a cyanide radical equivalent to the resultant alkyl radical. The enantioselectivity of the hydrocyanation reaction was again induced by the use of chiral Cu(sBOX) catalysts. Electrochemistry turns over both catalysts so that an external oxidant is not necessary. Notably, performing the same hydrocyanation reaction using traditional chemical oxidants without electrical input has not proven successful to give comparable efficiencies or enantioselectivities to the electrocatalytic protocol. This reaction is broadly applicable to the functionalization of conjugated alkenes, including alkenylarenes, dienes, enynes, and allenes. Computational studies using DFT unravelled the mechanism of enantioinduction facilitated by the Cu(sBOX) catalyst: the pendant ester group played a key part in enhancing the enantioselectivity of this reaction *via* a C–H···π interaction with the aryl group of the alkene substrate as illustrated in transition state **45-7**.

2.9.2. C–H functionalization. Ackermann and co-workers developed a Cu catalyzed C–H functionalization of benzamides to access isoindolones (Fig. 46).[155] The Cu^I catalyst was oxidized on the anode the first time to Cu^{II}, which complexes with substrate **46-1**, and a second oxidation occurs to generate a Cu^{III} species (**46-6**) which is responsible for C–H activation. Thereafter, metalation of the terminal alkyne *via* ligand exchange and subsequent reductive elimination delivers the C–H alkynylated arene **46-10**, which readily undergoes base-promoted cyclization to form isoindolone **46-3**.

In 2020, the Mei group reported a Cu/TEMPO co-catalyzed asymmetric Shono-type electrooxidation reaction. TEMPO acts as the redox mediator while copper with bisoxazoline ligands induce high enantioselectivities to afford C1-alkynylated tetrahydroisoquinolines (Fig. 47).[156]

Mei's group also demonstrated a Cu-catalyzed electrochemical C–H amination of arenes (Fig. 48).[157] Another redox

 This journal is © The Royal Society of Chemistry 2021

Published on 01 June 2021. Downloaded by University of Cambridge on 12/3/2022 1:39:05 PM.

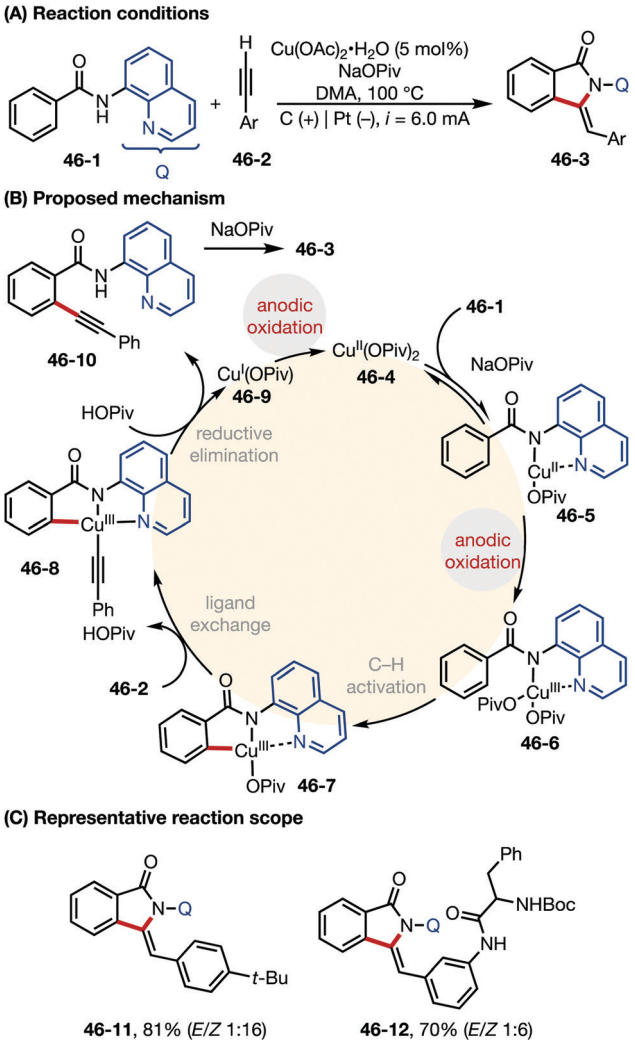


Fig. 46 (A–C) Copper-catalyzed alkyne annulation.

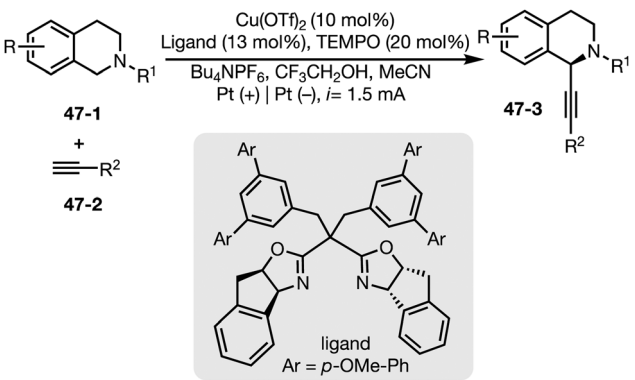


Fig. 47 Cu(II)/TEMPO-coatalyzed enantioselective C(sp^3)–H alkynylation of tertiary cyclic amines.

mediator used in this system is *n*-Bu_4NI, which is directly recycled on the anode. Kinetic studies indicated that the electron transfer event between the iodine radical and copper complex is the rate-determining step. The authors proposed that the catalytic cycle

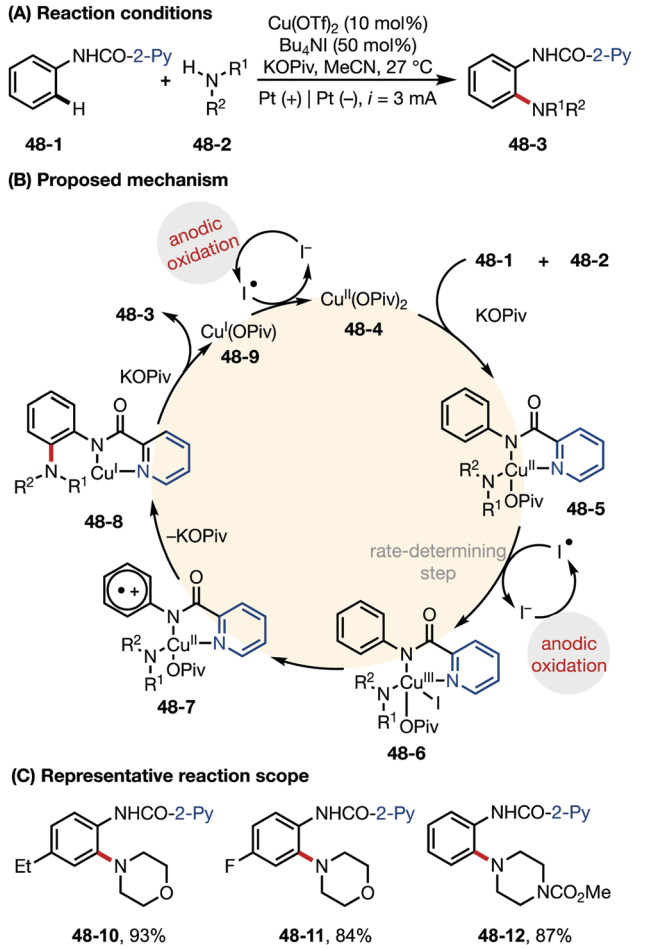


Fig. 48 (A–C) Copper-catalyzed electrochemical C–H amination of arenes with secondary amines.

starts with the coordination of substrates **48-1** and **48-2** to Cu^{II} catalyst to generate intermediate **48-5**, and this complex is then oxidized by an iodine radical to form a Cu^{III} species **48-6.** Complex **48-6** then undergoes metal-to-ligand electron transfer to form radical cation **48-7.** Subsequent intramolecular amine transfer to the radical cation and ligand exchange affords product **48-3** and generate a Cu^{I} species, which is oxidized on the anode to restore the catalyst to its active form. In a related report, Nicholls and co-workers disclosed a $Cu(OAc)_2$ catalyzed directed C–H amination of benzamides with morpholine.[158]

2.9.3. Allylic amination. The Hu group described an electrochemical method to accomplish a formal aza-Wacker cyclization of internal alkenes.[159] In this protocol, as shown in Fig. 49, electrochemical oxidation generates amidyl radical **49-4** which subsequently cyclizes to generate alkyl radical **49-5.** This radical intermediate is then trapped by the Cu catalytic cycle, and an elimination assisted by base yields the alkene product. After releasing the product, the resultant Cu^{I} catalyst is oxidized at the electrode to Cu^{II} to re-enter the catalytic cycle. A wide range of 5-membered N-heterocycles including oxazolidinone and pyrrolidinone-containing functionalizable alkenes can be prepared under mild conditions.

Published on 01 June 2021. Downloaded by University of Cambridge on 12/3/2022 1:39:05 PM.

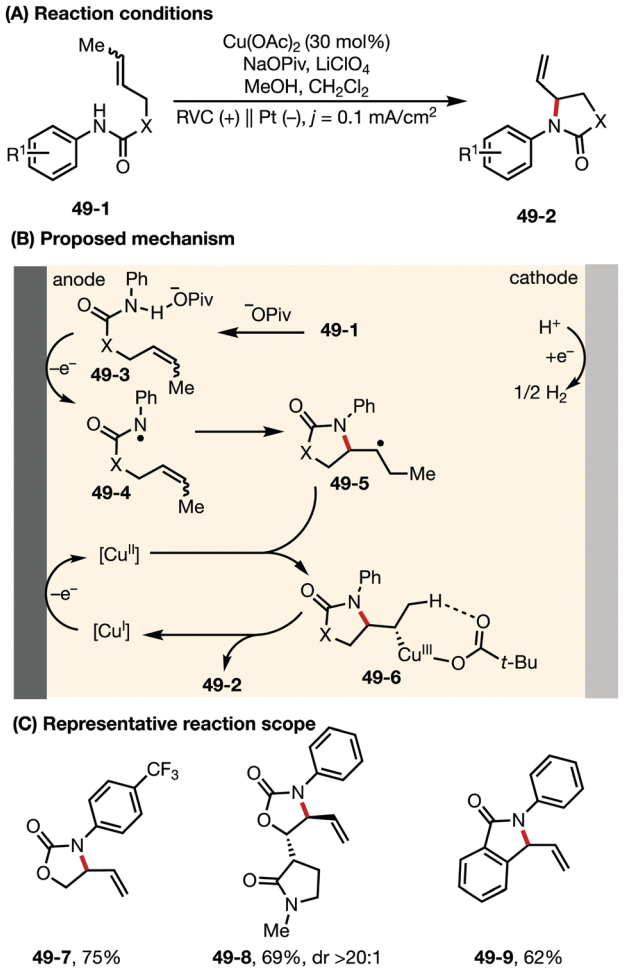


Fig. 49 (A–C) Formal aza-Wacker cyclization by tandem electrochemical oxidation and copper catalysis.

2.10. Palladium

In 2007, Amatore, Jutand, and co-workers reported an electrochemical Pd^{II}-catalyzed C–H bond olefination reaction of *N*-acetylanilines.[160] In this reaction, benzoquinone acts as a sub-stoichiometric redox mediator, which is electrochemically recycled.

Pd-Catalyzed electrocatalytic reactions have also enabled the strategic formation of C–O bonds. In 2013, the Budnikova group reported the electrochemical Pd-catalyzed C–H oxygenation of 2-phenylpyridine using perfluoroalkyl carboxylic acids (Fig. 50A).[161] Cyclic voltammograms and NMR data suggested that this C–H functionalization reaction proceed through monometallic Pd^{III} intermediates in acetonitrile or through bimetallic fluorinated Pd^{II} intermediates in dichloromethane.

The same group later developed an electrooxidative Pd-catalyzed phosphonation reaction of 2-phenylpyridine (Fig. 50B).[162] The authors postulated and subsequently isolated a key intermediate, binuclear phosphonate bipalladium $[(PhPy)Pd(EtO)_2P(O)]_2$, whose structure was confirmed by X-ray analysis. This species could be electrochemically oxidized to a Pd^{III} or Pd^{IV} reactive intermediate that undergoes reductive elimination to afford the phosphonated product.

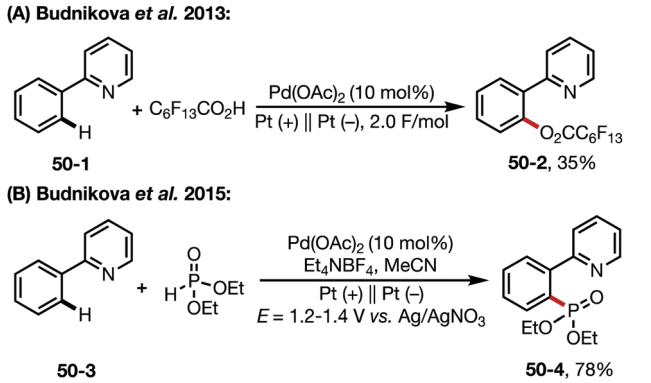


Fig. 50 (A) Electrochemical palladium-catalyzed *ortho*-oxygenation of 2-phenylpyridines with perfluorocarboxylic acids. (B) Electrochemical palladium-catalyzed phosphonation of pyridines.

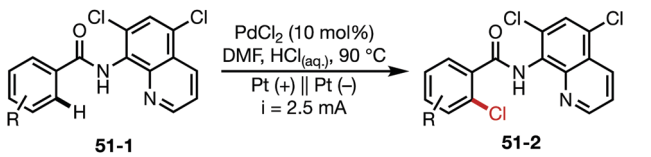


Fig. 51 Electrochemical palladium-catalyzed chlorination of *N*-quinolinylbenzamide derivatives.

Electrochemical Pd-catalyzed transformations have also been applied in carbon–halogen bond formation. In 2017, the Kakiuchi group reported a palladium-catalyzed *ortho*-selective chlorination of *N*-quinolinylbenzamide derivatives under anodic oxidation conditions (Fig. 51).[163]

The breadth of Pd electrocatalysis is further showcased in C–C bond formation. In 2017, the Mei group reported Pd-catalyzed $C(sp^2)$–H functionalization of oximes using organoboron reagents or benzoyl acetic acids, providing *ortho*-methylated or *ortho*-acylated products, respectively.[164] The proposed reaction mechanism starts with C–H activation to generate palladacycle **52-5**. It is proposed that $MeBF_3K$ can be directly oxidized to afford a methyl radical, which is then trapped by palladacycle **52-5**. Alternatively, **52-5** can undergo direct transmetallation with $MeBF_3K$ followed by anodic oxidation to form a Pd^{III} or Pd^{IV} intermediate **52-6**. This high-valent intermediate readily undergoes reductive elimination to deliver the methylated product and regenerate the Pd^{II} catalyst (Fig. 52).

In 2017, Surendranath and co-workers developed an electrochemical strategy to oxidize methane with $PdSO_4$ as the mediator.[165] Mechanistic studies support an electrochemical oxidation of Pd^{II} catalyst to a putative bimetallic $Pd_2^{III,III}$ intermediate, which rapidly functionalizes methane to generate CH_3OSO_3H and CH_3SO_3H *via* concurrent faradaic and non-faradaic pathways, respectively. Both CH_3OSO_3H and CH_3SO_3H can be thermally and hydrolytically converted to methanol (Fig. 53).

The Lei group reported a Pd-catalyzed electrochemical aminocarbonylation of alkynes under atmospheric pressure of CO in an undivided cell (Fig. 54).[166] Based on cyclic voltammetry,

 This journal is © The Royal Society of Chemistry 2021

Published on 01 June 2021. Downloaded by University of Cambridge on 12/3/2022 1:39:05 PM.

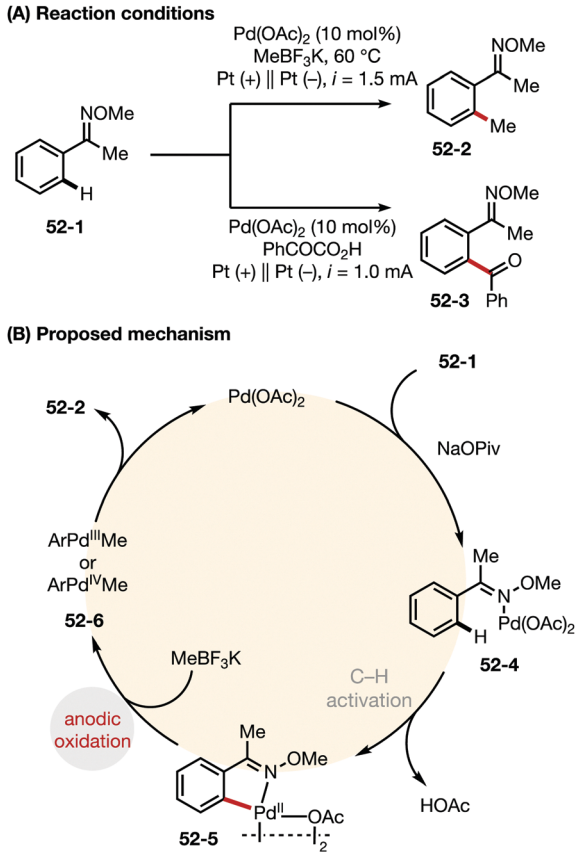


Fig. 52 (A and B) Palladium-catalyzed electrooxidative C–C bond formation of oximes.

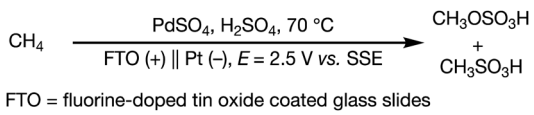


Fig. 53 Electrochemical palladium-catalyzed methane monofunctionalization.

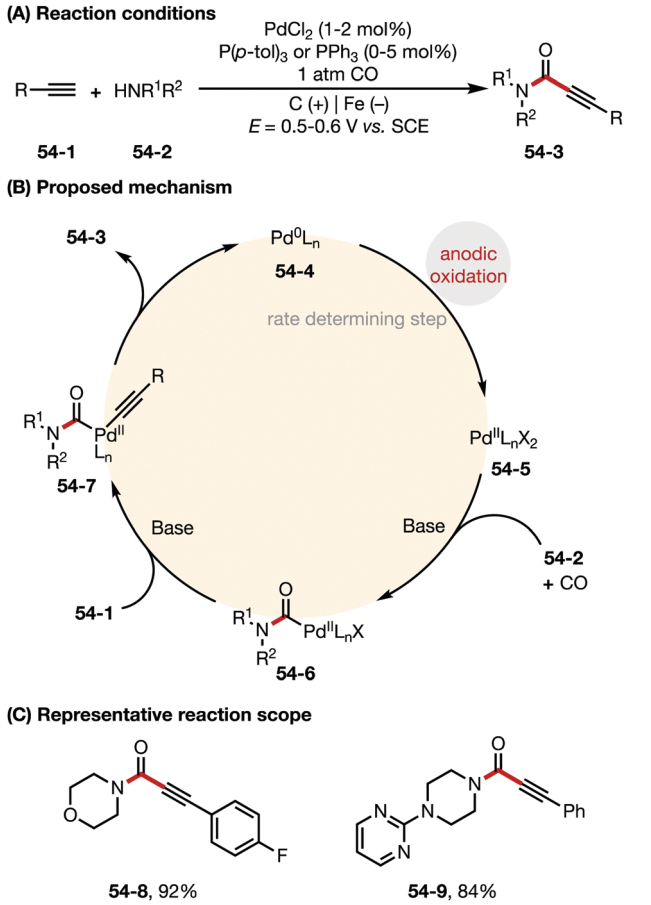


Fig. 54 (A–C) Electrochemical oxidative aminocarbonylation of terminal alkynes.

kinetic analysis, and XAFS spectroscopy data, the authors proposed that the catalytic cycle proceeds through a Pd^0/Pd^{II} redox pair. The reaction starts with amine substrate **54-2** binding to Pd^{II} catalyst **54-4**, followed by CO insertion to generate intermediate **54-6**, which reacts with alkyne **54-1** to give the palladium acetylide **54-7**. This species then undergoes reductive elimination to release 2-ynamide **54-3**. The resultant Pd^0 subsequently gets oxidized on the anode to regenerate the catalytic cycle. Diverse primary and secondary amines with various functional groups are viable substrates for this reactivity.

In 2017, the Mei group reported a Pd^{II}-catalyzed C(sp^3)–H oxygenation *via* anodic oxidation. According to the proposed mechanism, electrochemical oxidation of divalent palladacycle **55-4** to a Pd^{III} or Pd^{IV} intermediate (**55-5**) occurs to induce the subsequent reductive elimination (Fig. 55).[167] Kinetic isotope effect (KIE) experiments suggested that the C–H activation of the substrate is the rate-limiting step (k_H/k_D = 3.7). The acylated product can re-enter the catalytic cycle to undergo an additional C–H activation, eventually resulting in di- or tri-acetoxylation products. The Sanford group has also applied electrochemistry in Pd-catalyzed electrochemical acetoxylations of C(sp^2)–H and C(sp^3)–H bonds.[168]

2.11. Ruthenium

A common practice for inducing C–H activation is to utilize nitrogen-based directing groups. In 2018, the Ackermann group reported a Ru-catalyzed electrocatalytic C–H activation with aromatic carbamates and phenols (Fig. 56).[169] Based on mechanistic studies, the authors proposed that the catalytic cycle starts with the coordination of aromatic carbamates accompanied by C–H activation to generate ruthena(II)cycle intermediate **56-5**. Subsequent coordination of an alkyne followed by migratory insertion affords the seven-membered ruthena(II)cycle **56-7**. This species then undergoes reductive elimination to deliver the product and Ru^0 intermediate **56-8**. The anodic oxidation of intermediate **56-8** back to the active Ru^{II} species **56-4** completes the catalytic cycle.

The Ackermann group later reported a Ru-catalyzed C–H activation to enable annulations between alkynes and benzoic acids.[170] The proposed mechanism is similar to that of the previous example. In 2021, the group published an electrochemical three-component assembly of isoquinolines catalyzed by a Ru^{II} catalyst, shown in Fig. 57.[171]

Published on 01 June 2021. Downloaded by University of Cambridge on 12/3/2022 1:39:05 PM.

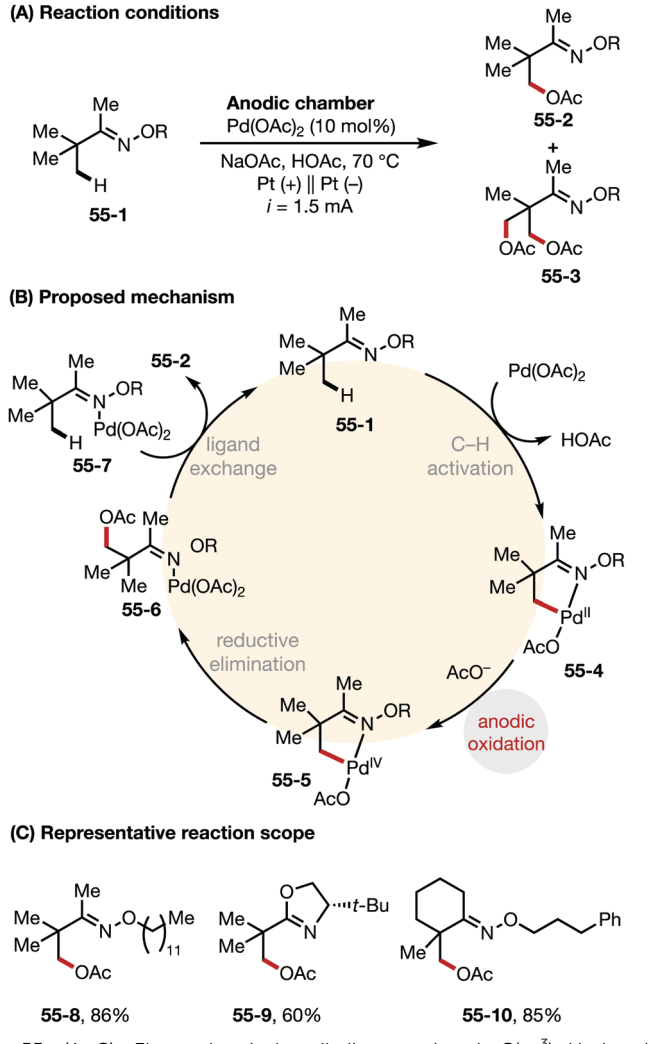


Fig. 55 (A–C) Electrochemical palladium-catalyzed C(sp^3)–H bond acetoxylation.

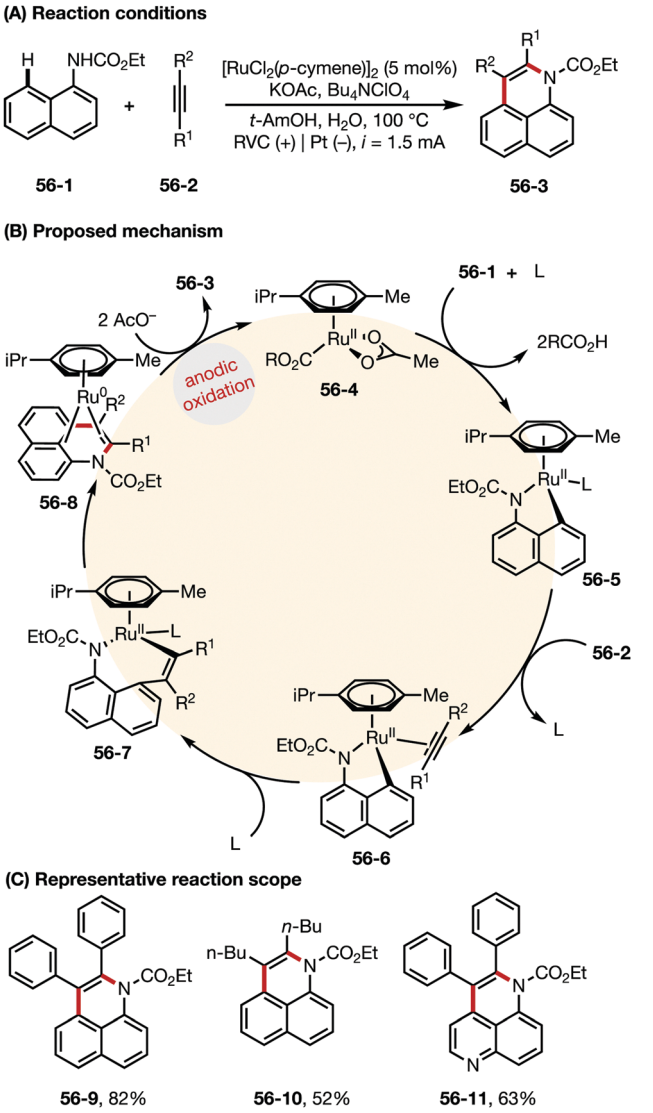


Fig. 56 (A–C) Electrochemical ruthenium-catalyzed alkyne annulations of arylcarbamates.

In 2018, the Xu group described a Ru-catalyzed electrochemical dehydrogenative annulation reaction of aniline derivatives and alkynes for the synthesis of indoles (Fig. 58).[172] Similar to Ackermann's work, an electric current is used to oxidize Ru^0 precatalyst **58-9** to its active form. Xu proposed that NaOAc converts precatalyst $[RuCl_2(p\text{-cymene})]_2$ into ruthenium diacetate complex **58-4**. Coordination with the pyrimidine directing group promotes reversible C–H activation to form the six-membered ruthenacycle **58-6**. Subsequently, intermediate **58-6** goes through ligand exchange, and migratory insertion of the bound alkyne into the Ru–C bond triggers the metal center to dissociate from the pyrimidyl nitrogen and instead complex with the amino group of the aniline moiety to obtain the six-membered ruthenacycle in the resultant intermediate **58-8**. Eventually, reductive elimination delivers the product.

2.12. Iridium

In 2018, the Ackermann group developed an Ir/benzoquinone co-catalyzed electrochemical C–H alkenylation of benzoic acids *via ortho*-coordination.[173] Mechanistic studies in Fig. 59 suggested a facile C–H cleavage and the subsequent formation of Ir^{III} cycle **59-7**, which undergoes β-H elimination and reductive elimination to form Ir^{I} intermediate **59-8**. Benzoquinone-mediated anodic oxidation then restores the Ir^{I} species to the active catalyst **59-4**.

In 2019, Mei and co-workers demonstrated that the synergistic combination of iridium catalysis and electrochemistry enables vinylic C–H activation of acrylic acids for alkyne annulation, producing α-pyrones in an undivided cell (Fig. 60).[174] Without electricity, traditional chemical oxidants such as Ag^0 or Cu^{II} did not give significant amounts of the desired product.

2.13. Cobalt

Cobalt electrocatalysis is a particularly powerful platform for a variety of C–H transformations and has been applied for the construction of C–O, C–N, and C–C bonds.

 This journal is © The Royal Society of Chemistry 2021

Published on 01 June 2021. Downloaded by University of Cambridge on 12/3/2022 1:39:05 PM.

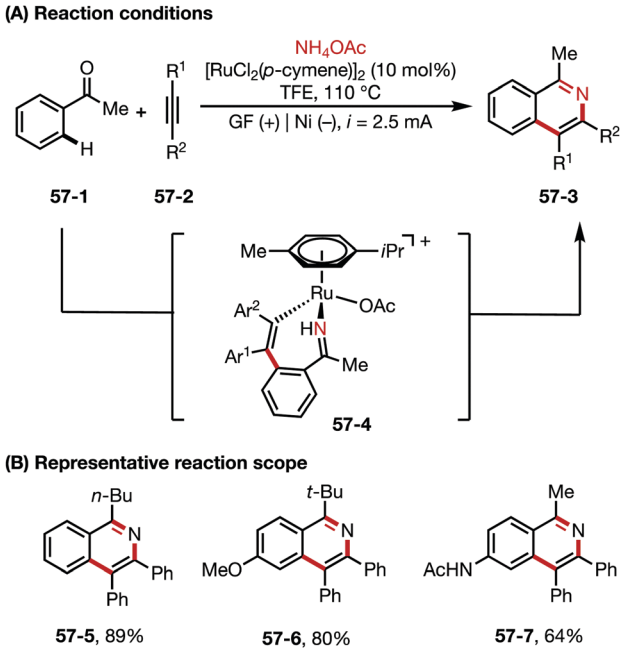


Fig. 57 (A and B) Ruthenaelectro-catalyzed three-component alkyne annulation.

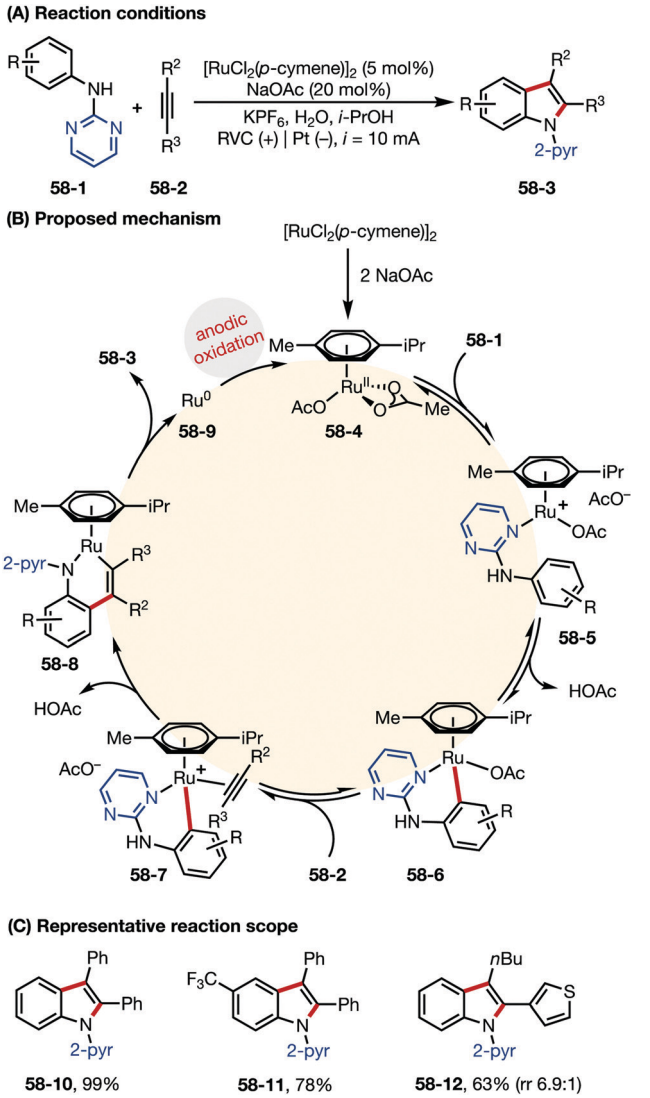


Fig. 58 (A–C) Ruthenium-catalyzed Electrochemical dehydrogenative alkyne annulation.

The Ackermann group has pioneered the development of cobalt-catalyzed metalla-electrochemical C–H activations.[175] In 2018, the group reported a Co-catalyzed electrochemical C–H/N–H annulation of alkynes at room temperature.[176] The proposed mechanism is shown in Fig. 61, the catalytic cycle starts with the anodic oxidation of Co^{I} or Co^{II} to an active Co^{III} carboxylate species **61-4**. Thereafter, this species engages in carboxylate-assisted C–H activation of benzamides to generate intermediate **61-5**, which then binds to phenyl alkyne to provide Co^{III} intermediate **61-6**. Lastly, reductive elimination affords the desired product and form the putative Co^{I} species **61-7**. The catalytically active Co^{III} carboxylate complex is regenerated by anodic oxidation, thereby avoiding the use of sacrificial stoichiometric oxidants.

In 2020, the same group reported a cobalt-catalyzed electrochemical C–H allylation of benzamides with electronically unactivated alkenes.[177] A similar mechanism involving $Co^{II/III}$ intermediates is proposed.

The Lei group has described several Co-catalyzed electrochemical C–H activation protocols.[178] In 2018, Lei published a cobalt-catalyzed C–H amination of arenes to access synthetically useful arylamines (Fig. 62).[179] Later, the authors reported a Co-catalyzed electrochemical [4+2] annulation of sulfonamides with alkynes to make a variety of sultams (Fig. 63).[180] In this work, it was proposed that the [4+2] annulation reaction possibly proceeds through the following pathway: Co^{II} species first coordinates with substrate **63-1** to generate Co^{II} complex **63-4** and then undergoes single electron oxidation to access the Co^{III} complex **63-5**. It is noteworthy that oxygen is critical for the reaction to proceed, and the authors hypothesize that H_2O_2 generated from O_2 reduction could also oxidize Co^{II} complex **63-4** to Co^{III} complex **63-5**. Next, C–H activation followed by phenylacetylene insertion to generate intermediate **63-7**, which undergoes reductive elimination to form the annulation product and Co^{I} species. The generated Co^{I} species is oxidized at anode to regenerate Co^{II}. At the same time, O_2 is reduced at the cathode to generate the superoxide radical anion, which then reacts with the solvent mixture to produce H_2O_2.

In 2019, the Yu group described a Co-catalyzed electrochemical oxidative C–H/N–H intramolecular annulation with isocyanides to synthesize iminoisoindolinone derivatives (Fig. 64).[181] Anodic oxidation serves a similar role as in the previous examples.

2.14. Nickel

In an early work, the Budnikova group developed a Ni- or Pd-catalyzed electrochemical *ortho*-fluoroalkylation of 2-phenylpyridine.[182] Based on the cyclic voltammogram of $[Ni(bpy)_3]^{2+}$ catalyst, the authors proposed that the C–H functionalization process goes through a Ni^{II}/Ni^{III} redox pair.

Published on 01 June 2021. Downloaded by University of Cambridge on 12/3/2022 1:39:05 PM.

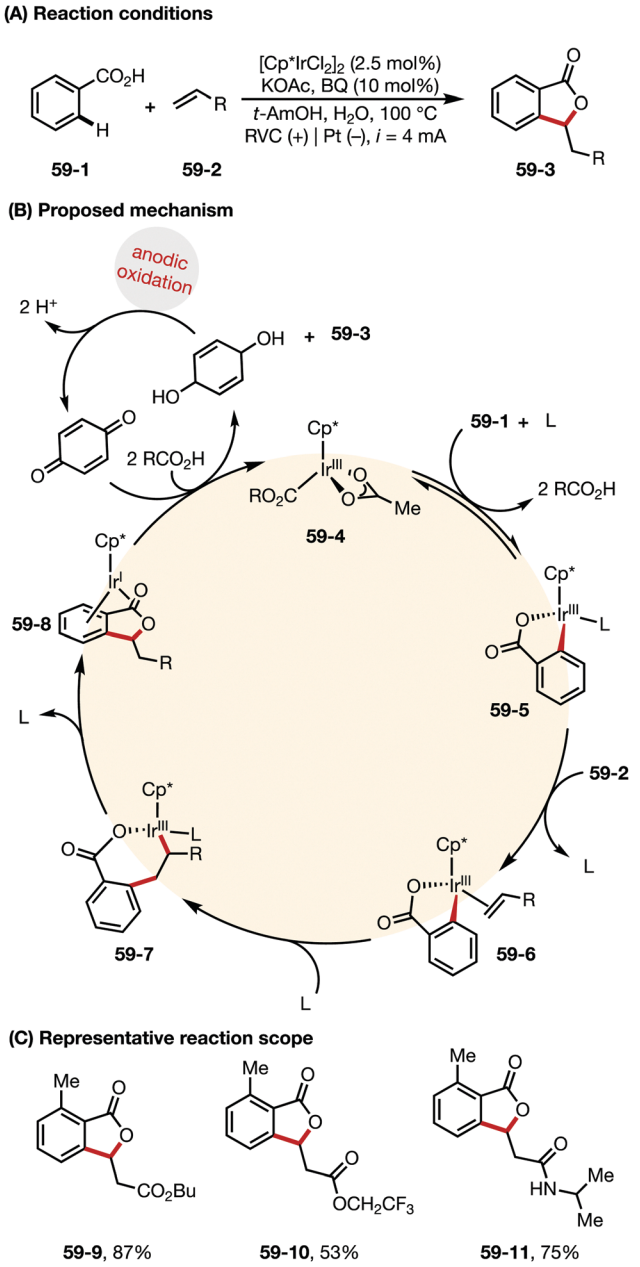


Fig. 59 (A–C) Cooperative iridium-catalyzed electrooxidative C–H alkenylations.

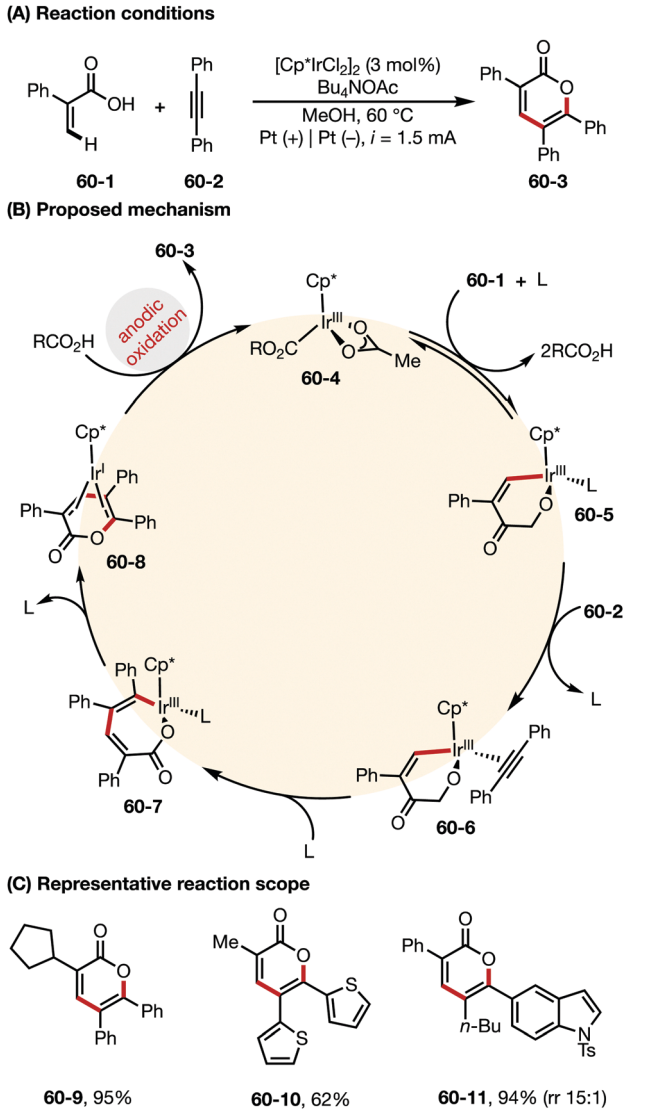


Fig. 60 (A–C) Electrochemistry-enabled Ir-Catalyzed vinylic C–H Functionalization for alkyne annulation.

In 2019, the Ackermann group reported Ni-catalyzed electrochemical alkoxylations of benzamides and secondary alcohols.[183] Notably, this reaction has not been shown possible with other transition metal catalysts prior to this work. Anodic oxidation is used to induce reductive elimination of a high valent Ni^{III} or Ni^{IV} complex. In order to rationalize the C–O bond formation process, the well-defined Ni^{III} complex **65-4** was synthesized and fully characterized, including X-ray diffraction analysis. Cyclic voltammetric studies of **65-4** revealed an oxidation feature at a potential of 0.50 V *vs.* $Fc^{0/+}$, suggesting the formation of a higher valent complex **65-5** (Fig. 65). DFT calculations indicate the redox non-innocence of the ligand during oxidation; thus the oxidation is best described as a ligand-centered process. Reductive elimination of this species gave the final product.

2.15. Rhodium

In 2018, the Ackermann group reported a Rh-catalyzed electrochemical C–H alkenylation of benzoic acids mediated by a rhodium catalyst.[184] As shown in Fig. 66, the authors proposed a catalytic cycle that proceeds *via* an *ortho* C–H activation of benzoic acid **66-1** followed by migratory insertion of alkene **66-2**. Intermediate **66-7** subsequently undergoes β-hydride elimination and reductive elimination. Finally, anodic oxidation of Rh^{I} intermediate **66-8** regenerates the catalytically active complex **66-4** while generating the desired product **66-3**. Based on competition experiments with CF_3-substituted and CH_3-substituted benzoic acids and isotope labelling experiments, it is believed that the C–H activation proceeds through a base-assisted internal electrophilic substitution mechanism.

 This journal is © The Royal Society of Chemistry 2021

Published on 01 June 2021. Downloaded by University of Cambridge on 12/3/2022 1:39:05 PM.

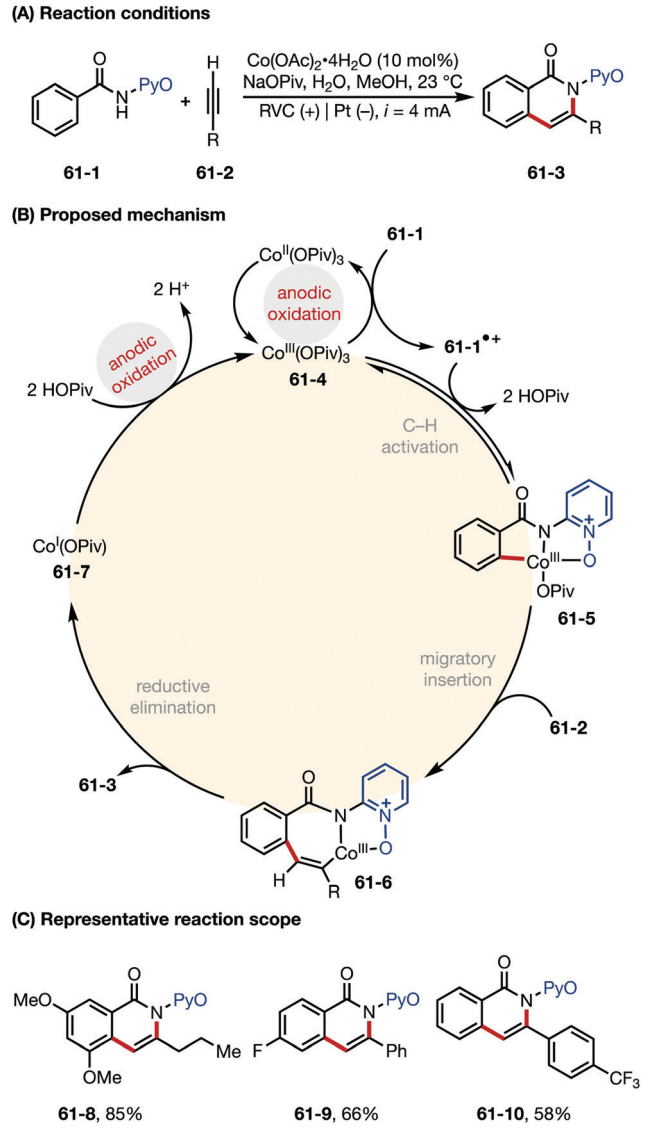


Fig. 61 (A–C) Electrochemistry-enabled cobalt-catalyzed C–H/N–H Activation. PyO = 2-pyridyl *N*-oxide.

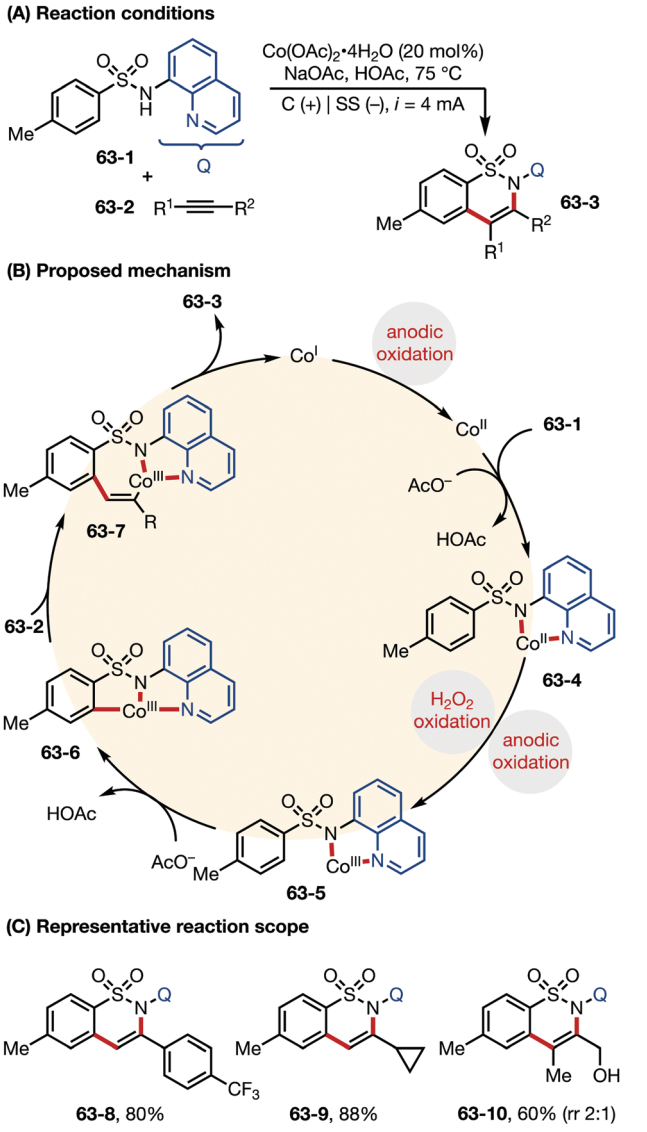


Fig. 63 (A–C) Electrochemistry-enabled cobalt-catalyzed [4+2] annulation for the synthesis of sultams.

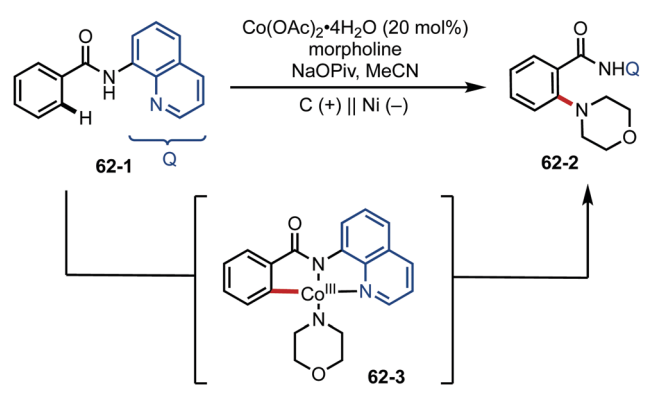


Fig. 62 Cobalt-catalyzed electrooxidative C–H amination of arenes with alkylamines.

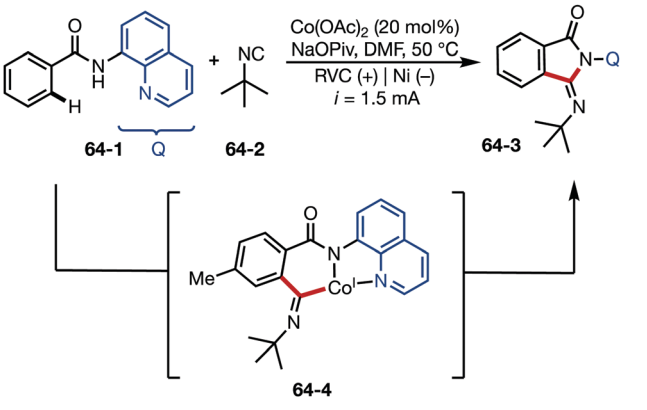


Fig. 64 Electrochemical oxidative C–H/N–H intramolecular annulation with isocyanides for iminoisoindolinone synthesis.

Published on 01 June 2021. Downloaded by University of Cambridge on 12/3/2022 1:39:05 PM.

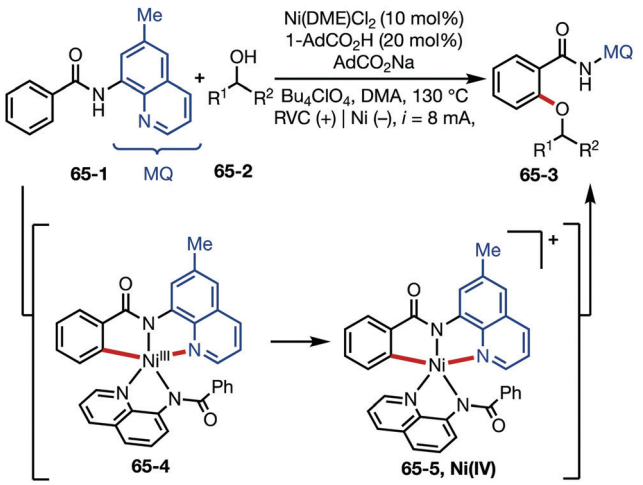


Fig. 65 Nickellaelectro-catalyzed C–H alkoxylation with secondary alcohols.

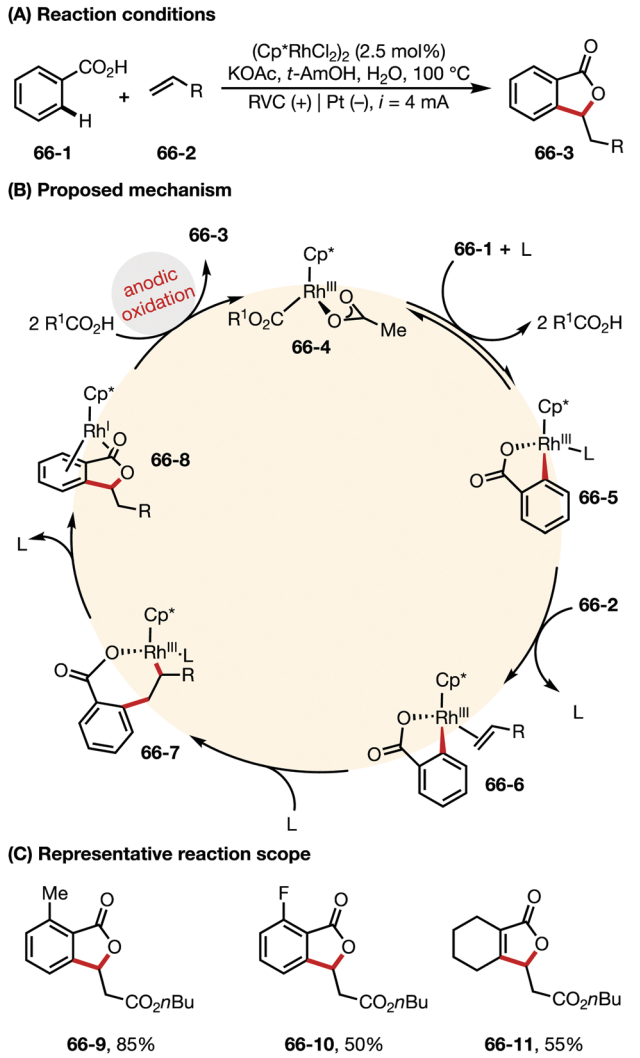


Fig. 66 (A–C) Electrooxidative rhodium-catalyzed C–H/C–H activation for dehydrogenative alkenylation.

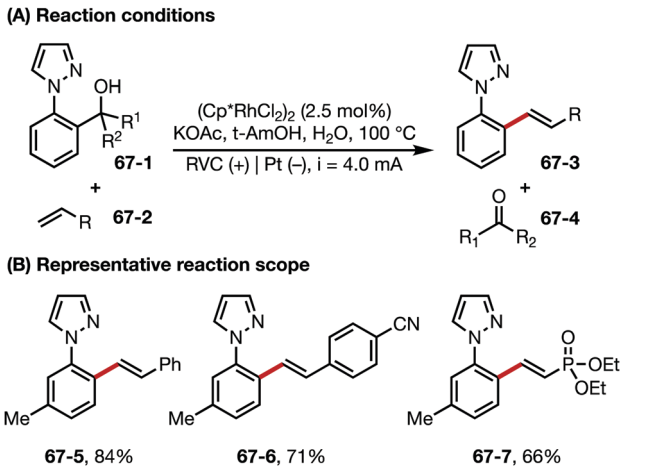


Fig. 67 (A and B) Electrochemical C–C bond activation C–C bond alkenylation by rhodium(III) catalysis.

The Ackermann group also published an electrochemical arene alkenylation reaction catalyzed by a Rh complex. Like the previous example, this catalytic cycle also involves a Rh^{I}/Rh^{III} redox pair. The proposed mechanism includes a key C–C bond activation step that leads to the formation of ketone by-product **67-4** (Fig. 67).[185]

The Xu group reported a Rh-catalyzed electrocatalytic C–H phosphorylation reaction in 2019.[186] This method enabled the synthesis of triarylphosphine oxides from diarylphosphine oxides. In this work, electricity is used to oxidize Rh^{III} intermediate **68-6** to facilitate reductive elimination towards C–P bond formation (Fig. 68). However, the authors stated that the exact oxidation state of intermediate **68-7** prior to reductive elimination remains unknown. Pyrazole, pyridazine, purines, and pyrrolo-pyrimidine directing groups were shown to be compatible with the C–H activation step.

3. Cathodic reduction

Compared to electrooxidative methodologies, the utility of electroreductive chemistry remains relatively underexplored. In recent years, electrochemistry has emerged as a powerful and efficient method for achieving challenging transformations at deeply reducing potentials.[187–190] In contrast to traditional reductive reactions which use heterogeneous reducing metals or homogenous organic compounds as stoichiometric reductants, electroreductive chemistry provides several advantages including highly efficient electron transfer, tunable reducing potential, and good scalability. Nevertheless, these approaches rely on the direct reduction of reactants on the cathode surface, which may result in electrode passivation leading to lower selectivity. As such, reductive electrocatalysis has attracted increasing attention in synthetic chemistry for its ability to decrease reaction overpotential and regulate downstream chemical pathways. Currently, nickel complexes are the most predominant catalysts used in electroreductive chemistry. However, a variety of 3d block metals such as cobalt and zinc

 This journal is © The Royal Society of Chemistry 2021

Published on 01 June 2021. Downloaded by University of Cambridge on 12/3/2022 1:39:05 PM.

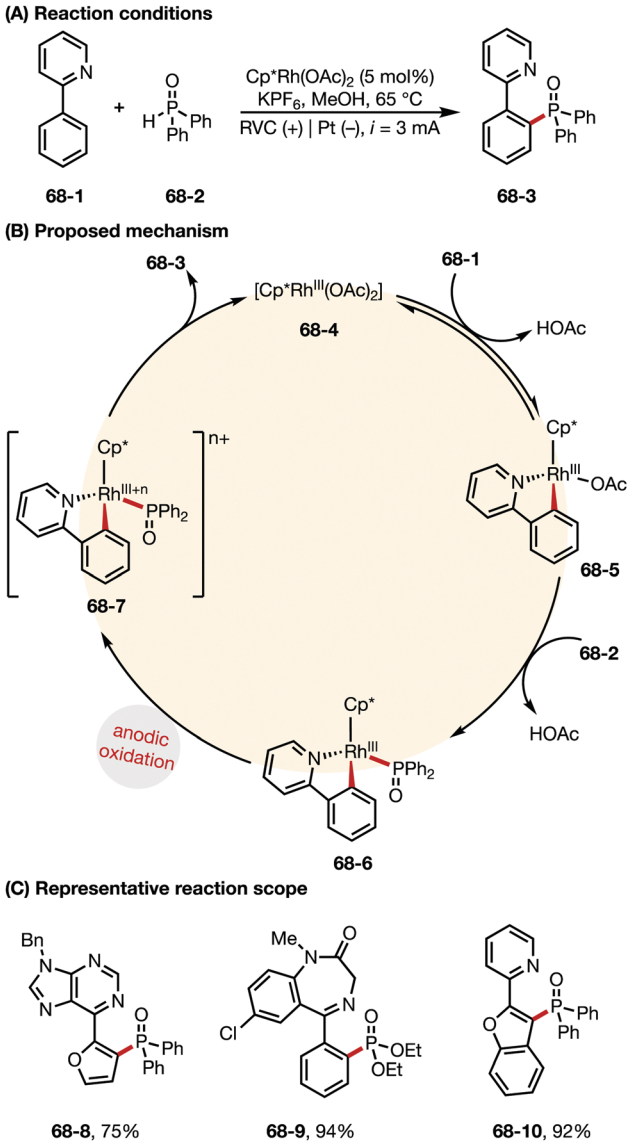


Fig. 68 (A–C) Rhodium(III)-catalyzed aryl C–H phosphorylation enabled by anodic oxidation induced reductive elimination.

as well as organic compounds have also been demonstrated as efficient reductive mediators. Electroreductive transformations are usually coupled with the oxidation of sacrificial anodes, such as Mg, Zn or Fe, or readily oxidizable additives such as triethyl amine (Et_3N). During electrolysis, the anodic oxidation of these sacrificial reductants generates metal salts or amine radical cations, which are typically innocuous. In addition, sacrificial reductants may also prevent the undesired oxidation of substrates or reactive intermediates when the electrolysis is carried out in an undivided cell.

3.1. Nickel

In this section, cathodic reduction utilizing nickel complexes is discussed. Electrochemistry advantageously supports the *in situ* generation of often sensitive Ni species, resulting in more practical conditions for Ni-catalyzed transformations compared to traditional methods. Consequently, a wide variety of protocols have been reported in this direction including cross-electrophile coupling (XEC), alkene difunctionalization, C–H activation, as well as C–N, C–S, and C–P bond formation.

3.1.1. Homocoupling of aryl halides. Among the earliest examples of electrochemically promoted homocoupling of electrophiles was Ban's work using cathodically generated Ni^0 species **69-3** (Fig. 69A).[191] When used stoichiometrically, this nickel species was shown to facilitate the homocoupling of bromobenzene, which had previously been accomplished *via* chemical reductants such as Zn or $AlEt_3$. This seminal work led to a number of further developments in Ni-catalyzed electrochemical coupling reactions.[192–200]

In 2018, the Léonel group reported an electrocatalytic homocoupling of aryl and heteroaryl halides mediated by a nickel bipyridine catalyst (Fig. 69B).[201] In the proposed catalytic cycle, nickel pre-catalyst **69-11** is first reduced to Ni^0 complex **69-12**

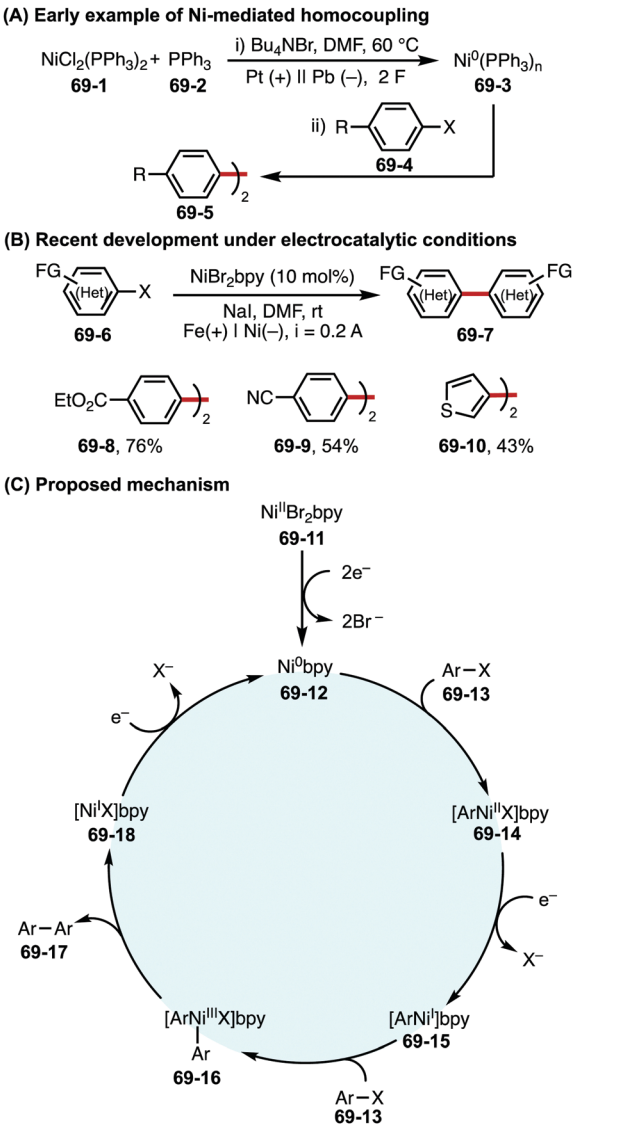


Fig. 69 (A–C) Nickel-catalyzed electrochemical homocoupling reaction.

Published on 01 June 2021. Downloaded by University of Cambridge on 12/3/2022 1:39:05 PM.

via cathodic reduction. Oxidative addition of this intermediate to the C–X bond of the aryl halide **69-13** then furnishes intermediate **69-14**. Cathodic single-electron reduction of this intermediate, followed by oxidative addition to a second aryl halide equivalent, furnishes Ni^{III} complex **69-16**. A reductive elimination step provides the desired coupling product **69-17**. This step also generates Ni^{I} species **69-18** which is further reduced electrochemically to regenerate Ni^{0} complex **69-12** (Fig. 69C). The authors achieved the desired homocoupling in good yields and demonstrated functional group tolerance of esters, nitriles, and thiophenes.

In 2020, the Mei group reported a Ni-catalyzed enantioselective homocoupling of aryl bromides using chiral pyridineoxazoline ligands, providing biaryls in good yields and enantioselectivities using an undivided cell (Fig. 70A).[202] This transformation provides protected BINOL derivatives that could not be easily generated *via* traditional reductants (such as Mn dust). The reaction also tolerates a variety of functional groups including boronic esters and aryl chlorides (Fig. 70B).

3.1.2. C(sp^2)–C(sp^2) XEC. Early examples of Ni-catalyzed XEC were disclosed by Périchon and co-workers.[203,204] In these reports, an N-heteroaryl halide and a simple aryl halide can be cross coupled in good yields. The authors attributed the cross-coupling selectivity to the intrinsic reactivity of the nickel catalyst employed: (1) Ni^{0} undergoes oxidative addition to a simple aryl halide faster than an N-heteroaryl halide, giving rise to Ni^{II} aryl, and (2) the Ni^{I} aryl complex upon a single-electron reduction is more reactive towards oxidative addition to an N-heteroaryl halide than to another equivalent of the simple aryl halide. Depending on the electronic property of the substrates and the identity of the leaving group, homocoupling products can sometimes also be observed. Sengmany and co-workers also extended the scope of this XEC to reactions between phenyl halides and chloropyrimidines or chloropyridazines.[205–208] The corresponding products resemble fragments of pharmaceutical and bioactive compounds (Fig. 71).

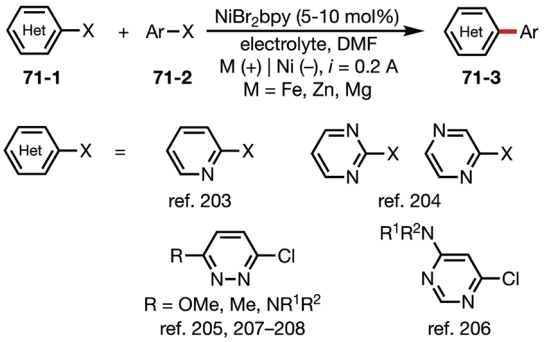


Fig. 71 Nickel-catalyzed electrochemical cross coupling reaction. X = Br or Cl.

In 2019, Sevov reported a Mizoroki–Heck coupling with aryl halides and alkenes, which was achieved by combining electrochemistry and nickel catalysis in lieu of the traditional Pd catalyst (Fig. 72A).[209] To overcome the slow kinetics that is

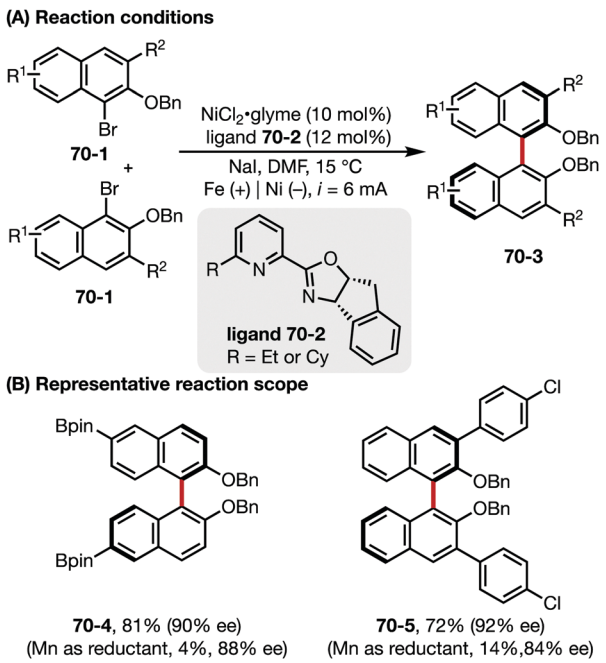


Fig. 70 (A and B) Nickel-catalyzed electrochemical enantioselective homocoupling reaction.

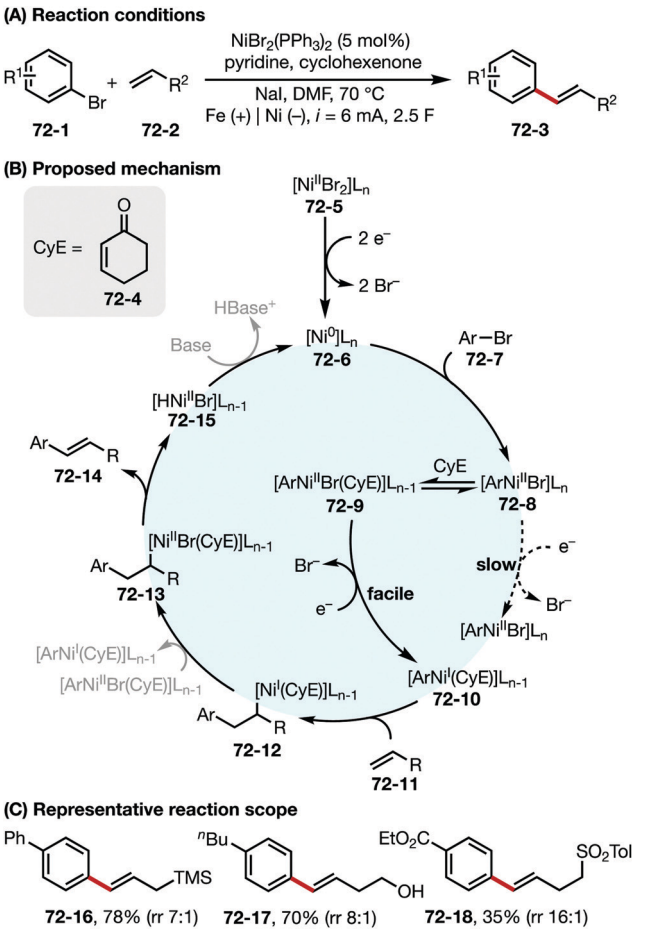


Fig. 72 (A–C) Nickel-catalyzed electrochemical Mizoroki–Heck coupling reaction.

This journal is © The Royal Society of Chemistry 2021

Published on 01 June 2021. Downloaded by University of Cambridge on 12/3/2022 1:39:05 PM.

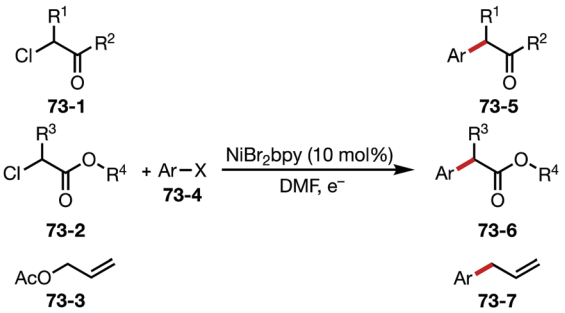


Fig. 73 Nickel-catalyzed electrochemical cross coupling of aryl, heteroaryl or vinyl halides with activated alkyl chlorides.

characteristic of Ni^{II} aryl complexes in the Heck reaction, the authors employed cyclohexenone (**72-4**) as an additive to transform the redox inert Ni^{II} aryl complex **72-8** to a redox active Ni^{II} species **72-9**. This intermediate thus undergoes single-electron reduction on the cathode and subsequent migratory insertion into the corresponding alkenes followed by β-H elimination to give coupling product **72-14**. Good selectivity towards the linear products over the branched products was observed. A wide range of simple alkenes containing functional groups such as silyl, hydroxy, and sulfone are compatible in this system (Fig. 72C).

3.1.3. $C(sp^2)$–$C(sp^3)$ XEC. Nickel electrocatalysis has also been demonstrated to promote $C(sp^2)$–$C(sp^3)$ coupling with α-haloketones (**73-1**), α-haloesters (**73-2**), or allyl acetate (**73-3**) as a coupling partner (Fig. 73).[210–213] Early developments in this area are discussed in a review by Périchon.[214]

In 2017, Hansen and co-workers further extended the scope of this reactivity to cross coupling between unactivated alkyl bromides and aryl bromides (Fig. 74A).[215] The group reported that electrochemistry offered improved reproducibility over traditional metal reductants for Ni-catalyzed cross coupling reactions. Inspired by the mechanism that Weix proposed for reducing metal-promoted cross coupling,[216] the authors suggested a reaction pathway that is distinct from Perichón's original hypothesis.[207] In this mechanism, the Ni(alkyl)(aryl) intermediate (**74-6**) formed prior to reductive elimination is generated in a radical recombination process instead of traditional oxidative addition of Ni^{I} to the alkyl halide. Specifically, Ni^{I} intermediate **74-8** reacts with alkyl halide **74-2** *via* halogen abstraction to form an alkyl radical **74-9**, which then adds to Ni^{II} aryl species **74-5** to furnish Ni^{III} intermediate **74-6**. The rest of the catalytic cycle is analogous to the previous proposal (Fig. 74B). The same group also reported a modified protocol using MeCN as a more process-friendly solvent instead of DMA and a secondary amine as the sacrificial oxidant instead of a sacrificial anode to avoid the production of stoichiometric metal salts (*e.g.*, ZnX_2, MnX_2 or NiX_2).[217]

In 2018, Bio and co-workers reported nickel-catalyzed electroreductive coupling using N-hydroxyphthalimide esters (**75-1**) as coupling agents (Fig. 75A).[218] The cathodic reduction potential of the redox active ester **75-1** is −1.2 V (*vs.* Ag/AgCl), which matches the reduction potential of the Ni^{I} complex **75-9**, thus enabling the cathodic reduction of both species to take

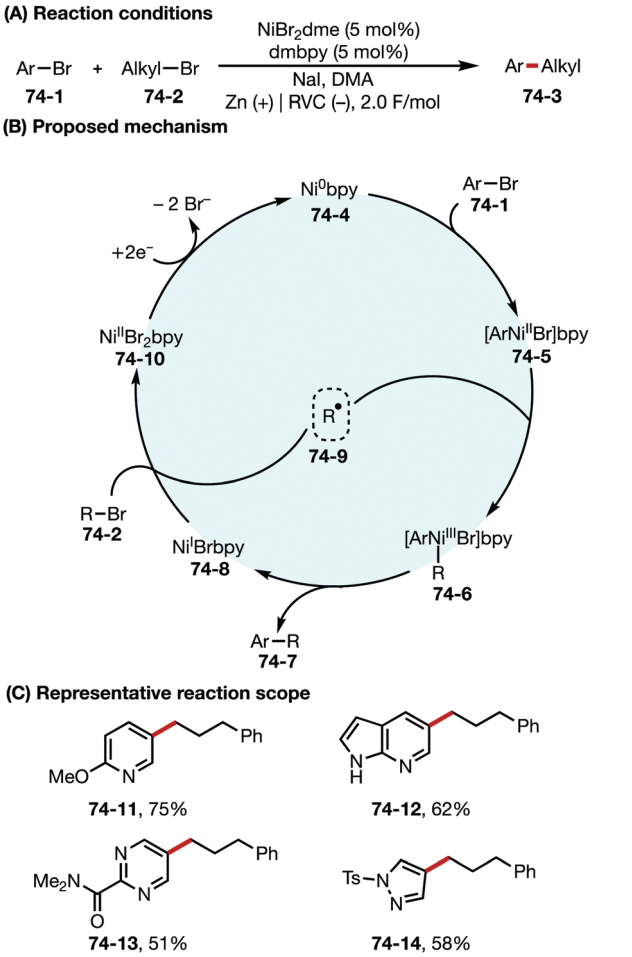


Fig. 74 (A–C) Nickel-catalyzed electrochemical cross-electrophile coupling reactions of unactivated alkyl halides.

place simultaneously in a cathodically coupled electrolysis (CaCE) towards the desired reactivity (Fig. 75B). The $C(sp^3)$ radical **75-5** generated from **75-1** reduction is intercepted by a nickel catalyst **75-7**, which arises from the oxidative addition of electrogenerated Ni^{0} **75-6** to aryl halide **75-2**. The resultant Ni^{III} species **75-8** undergoes reductive elimination to form the $C(sp^2)$–$C(sp^3)$ coupled product **75-3**. Notably, electron-rich tertiary amines are used as sacrificial reductants, as they can easily undergo anodic oxidation to complete the full electrochemical reaction. The authors also carried out this reaction in a continuous flow system, showing that reaction yield and chemoselectivity can be optimized through systematic tuning of flow rate and current density. In 2019, Loren's group reported a one-pot strategy for the same transformation involving premixing of alkyl carboxylates and *N*-hydroxyphthalimide tetramethyluronium hexafluorophosphate (PITU) to form the corresponding *N*-hydroxyphthalimide esters prior to electrolysis.[219]

In 2020, the Mei group and the Rueping group independently reported Ni-catalyzed electroreductive XEC *via* a chain-walking mechanism (Fig. 76A).[220,221] These two groups used terminal alkyl bromides **76-1** as the $C(sp^3)$ electrophiles. Upon formation of Ni^{I}(alkyl)(aryl) intermediate **76-3**, a series of β-H

Published on 01 June 2021. Downloaded by University of Cambridge on 12/3/2022 1:39:05 PM.

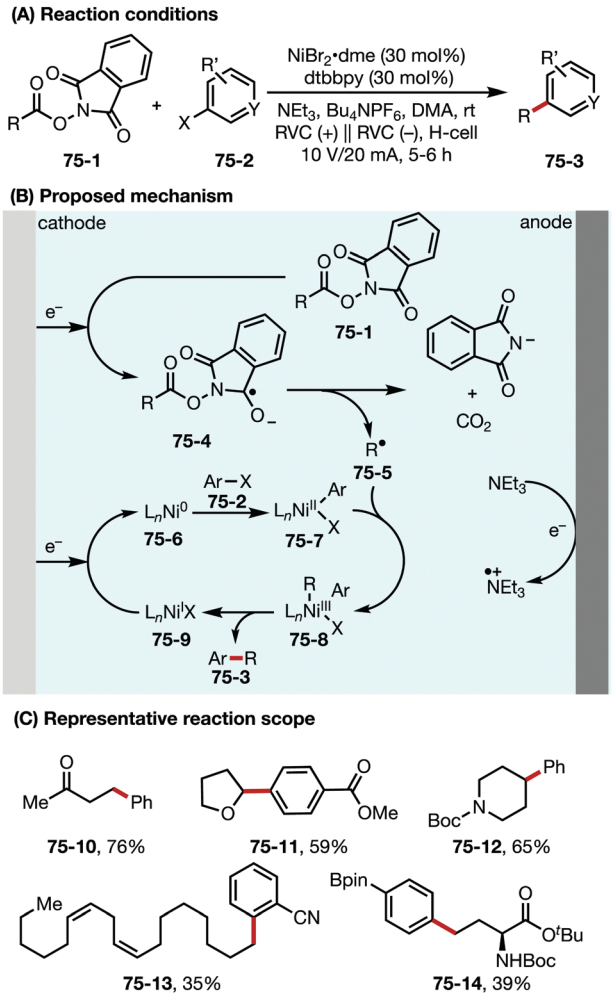


Fig. 75 (A–C) Nickel-catalyzed electrochemical cathodically coupled electrolysis.

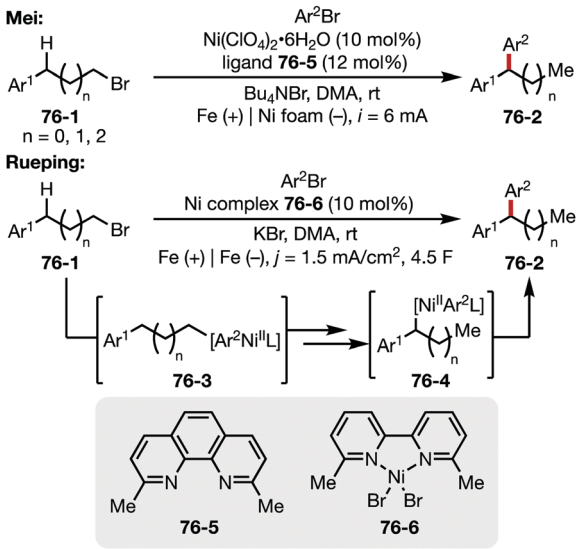


Fig. 76 Nickel-catalyzed chain-walking cross-electrophile coupling reaction.

elimination and migratory insertion processes took place to complete "chain walking," eventually giving rise to thermodynamically stable benzyl nickel species **76-4**. Subsequent reductive elimination furnished the products **76-2**. This system was initially susceptible to several unproductive pathways such as early reductive elimination of Ni^{II} complex **76-3** homocoupling between two aryl halides, and generation of alkenes *via* β-H elimination. However, both groups were able to tackle these problems through the use of a bipyridine ligand which drastically changed the catalyst's CV profile (as shown in Mei's work) and smoothly facilitated the chain-walking mechanism.

In 2020, the Sevov group introduced a redox shuttle (**77-5**) strategy in a Ni-catalyzed electroreductive XEC reaction that serves to mitigate overreduction and degradation of the catalyst (Fig. 77A).[222] The authors found that the difference between the cathodic potential required for XEC coupling and the potential needed to induce catalyst degradation, which leads to protonation and homocoupling, is minimal. Taking advantage of the redox shuttles developed by the energy-storage community, the reaction yield improved substantially (from 43% to 97% for bromobiphenyl and from 5% to 89% for bromobenzoate) (Fig. 77B). The reaction tolerates sulfones, nitriles, amides, esters, and heteroarenes such as pyridines and quinolines. The authors later found that maintaining a proper concentration of these redox shuttles is crucial for achieving both high reactivity and overcharge protection, as high concentration of

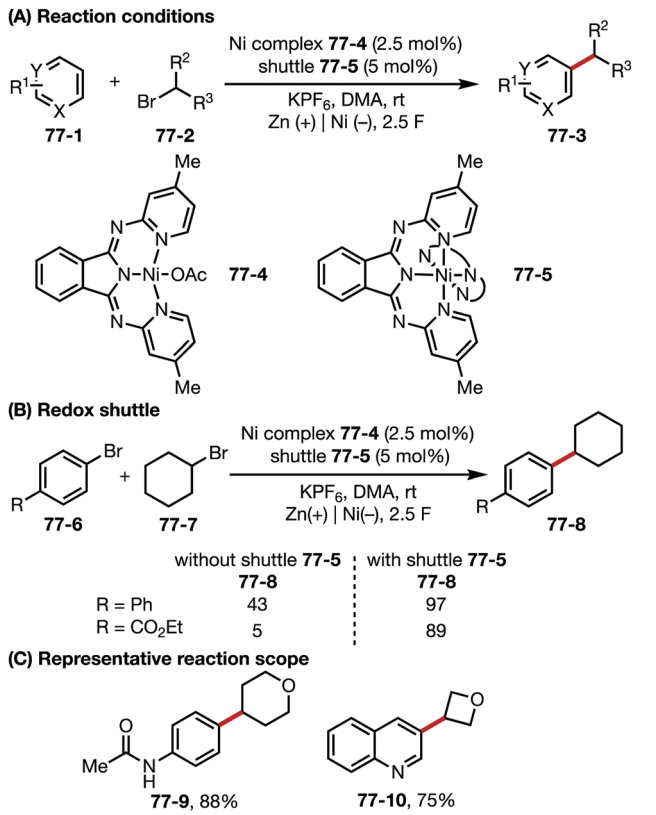


Fig. 77 (A–C) Nickel-catalyzed electroreductive electrophile cross coupling reaction *via* redox shuttles.

This journal is © The Royal Society of Chemistry 2021

Published on 01 June 2021. Downloaded by University of Cambridge on 12/3/2022 1:39:05 PM.

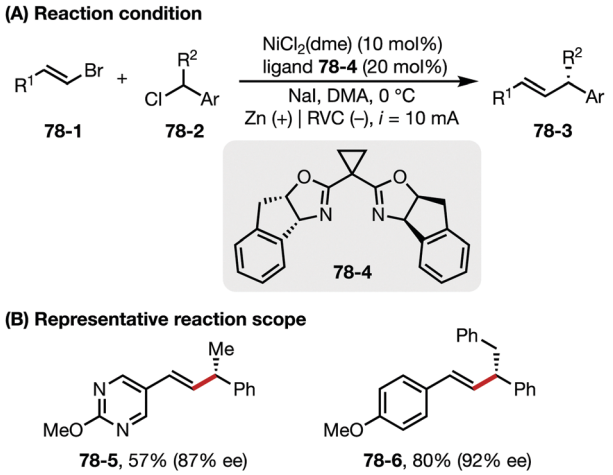


Fig. 78 (A and B) Nickel-catalyzed electrochemical enantioselective cross coupling reaction.

77-5 inhibits product formation whereas low concentration cannot sufficiently suppress catalyst overreduction.

In 2019, Reisman and co-workers reported an enantioselective variant of Ni catalyzed C(sp^3)–C(sp^2) XEC (Fig. 78A), where the asymmetric electroreductive coupling between alkenyl bromides (**78-1**) and benzyl chlorides (**78-2**) was explored.[223] The high enantioselectivity of this transformation was achieved using an aminoindanol-derived bis(oxazoline) ligand.

3.1.4. Alkene/alkyne functionalization. An early example of Nickel-catalyzed electroreductive alkene/alkyne functionalization was achieved by the Périchon group in 1995 using aryl bromides and ethyl acrylate.[224] The pioneering work led to a variety of intramolecular variations of this reactivity.[225–227] These developments served to expand the scope of the starting materials to alkynes[228,229] and other Michael acceptors,[230,231] as well as to perfluorinated organohalides.[232] In 2005, Little *et al.* employed a Ni(salen) catalyst to achieve the electroreductive cyclization of an aldehyde or ketone onto a pendant Michael acceptor (Fig. 79).[233]

In 2020, the Findlater group reported electroreductive pyridylation of electron-deficient alkenes, utilizing *para*-cyanopyridine as the heterocycle donor (Fig. 80A).[234] Through CV experiments, the authors proposed two possible pathways, both of which include the reduction of the Michael acceptor to the corresponding radical anion. Subsequently, either radical cross coupling with a cathodically generated cyanopyridyl radical anion or radical addition to Ni-activated cyanopyridine results in C–C bond formation.

3.1.5. C–N bond formation. In 2017, the Baran group reported the electrochemical nickel-catalyzed coupling between aryl halides and amines (Fig. 81A).[235] This work features mild

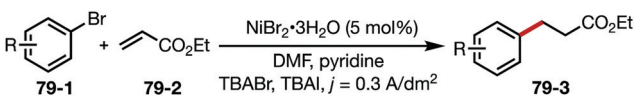


Fig. 79 Nickel-catalyzed electroreductive alkene fuctionalization.

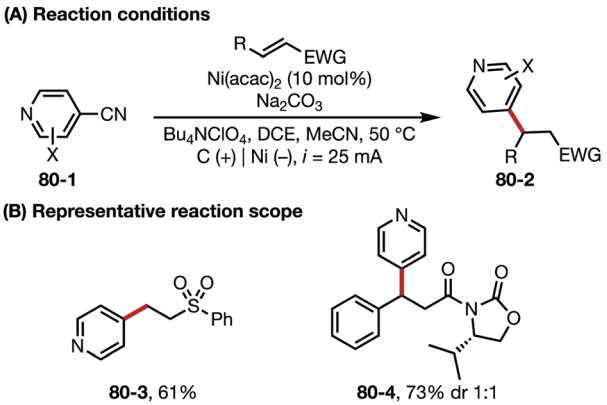


Fig. 80 (A and B) Electroreductive pyridylation of electron-deficient alkenes. The anodic reaction is not discussed by the authors.

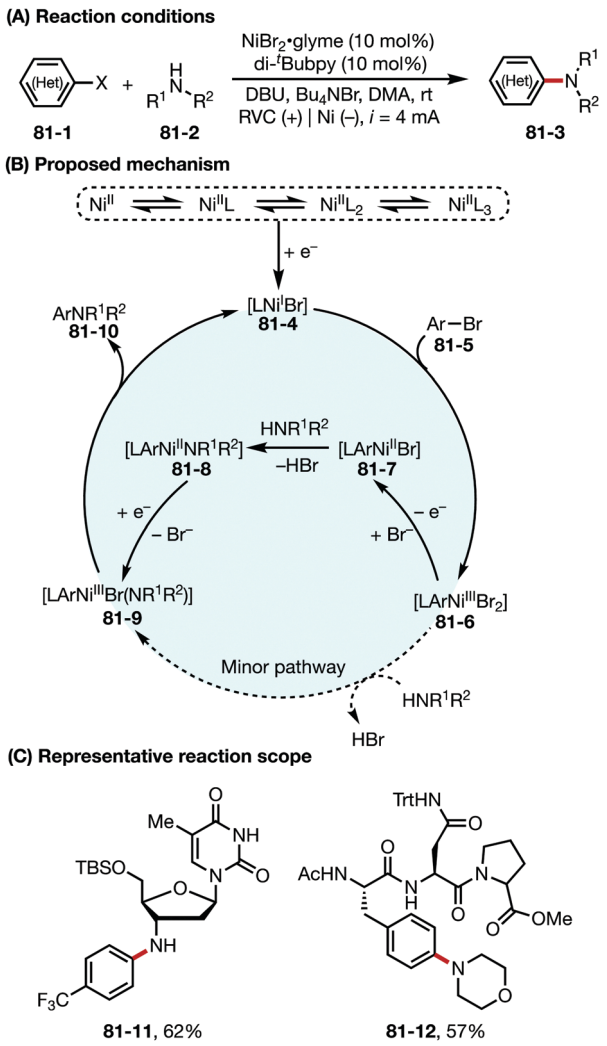


Fig. 81 (A–C) Electrochemical nickel-catalyzed coupling between aryl halides and amines.

conditions, is amenable to large scale preparation, and exhibits complementary substrate suitability to established methods

Published on 01 June 2021. Downloaded by University of Cambridge on 12/3/2022 1:39:05 PM.

facilitated by transition metal catalysis or photochemistry. Baran, Minteer, and Neurock subsequently carried out mechanistic studies and demonstrated additional applications of this reaction in the modification of medicinally relevant compounds.[236] The reaction is proposed to begin with cathodic reduction of the nickel precatalyst to form **81-4**, followed by oxidative addition of **81-4** to aryl bromide **81-5**. Upon formation of **81-6**, ligand exchange between bromide and free amine was proposed to be inefficient. Consequently, cathodic reduction take place to form **81-7** as a stable intermediate. With assistance from a base (1,8-diazabicyclo[5.4.0]undec-7-ene, DBU), ligand exchange occurs to yield amine-coordinated **81-8**. Subsequent anodic oxidation and reductive elimination provide the desired product and turn over the Ni catalyst (Fig. 81B). The authors applied this reaction towards the derivatization of nucleosides and oligopeptides (Fig. 81C). This reaction technically adopts a paired electrolysis mechanism (see Section 4) but is discussed here owing to its similarity in catalytic mechanism to other examples in this section.

3.1.6. C–S and C–P bond formation. The Mei group reported a Ni-catalyzed thiolation of aryl bromides and chlorides *via* electrocatalysis (Fig. 82A).[237] The work features mild and base-free reaction conditions and exhibits good tolerance with heterocycles (Fig. 82C). The authors proposed a mechanism that is distinct from that of the aforementioned amination. Specifically, electrogenerated Ni^0 **82-5** is hypothesized to add to aryl halide **82-6**, and the resultant Ni^{II} intermediate **82-7** then undergoes ligand exchange with thiol **82-11** to form product **82-9**. However, the participation of an electrogenerated thiyl radical **82-12** as a possible pathway has not been definitively ruled out (Fig. 82B).

Meanwhile, the Pan group reported a similar transformation using aryl iodides as the coupling partner (Fig. 83).[238] In this work, a mechanism involving the addition of a thiyl radical to Ni is proposed, which was based on CV data and control experiments. In 2020, the Messaoudi group further expanded the scope of thiol coupling partners to various anomeric glycosyl thiols, achieving coupling with aryl, alkenyl, and alkynyl bromides (Fig. 83).[239]

Analogously, Ni has been shown to catalyze C–P bond formation using organophosphites as the nucleophile. An electrochemical version of this reaction was reported in 2018 by the Léonel (Fig. 84A).[240] Several dialkylphosphites and trimethyl

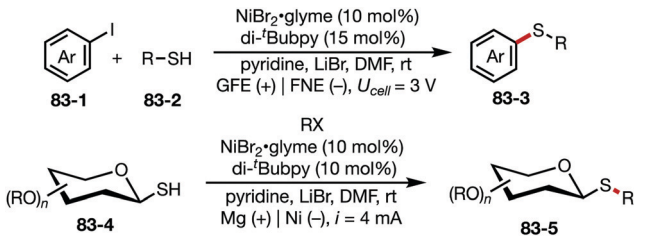


Fig. 83 Electrochemical nickel-catalyzed carbon–sulfur bond formation.

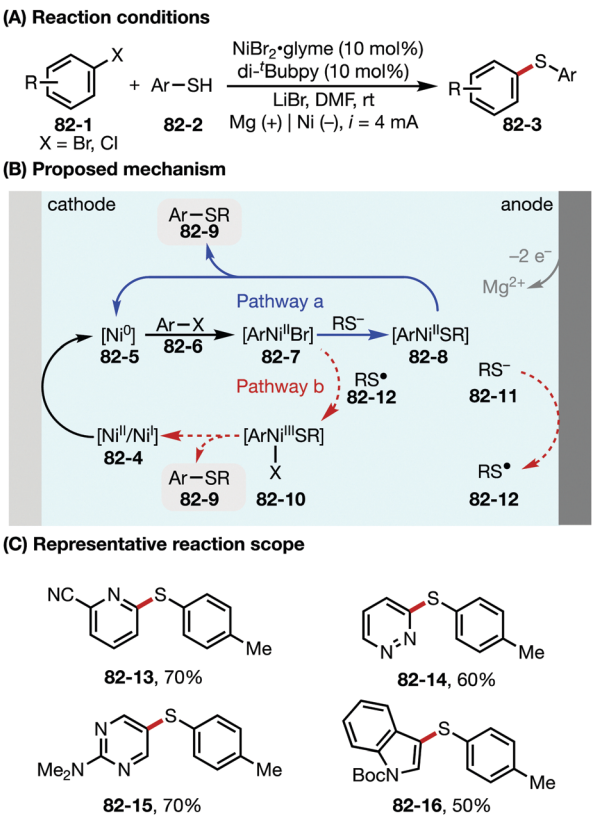


Fig. 82 (A–C) Electrochemical nickel-catalyzed thiolation of aryl halides and heteroaryl halides.

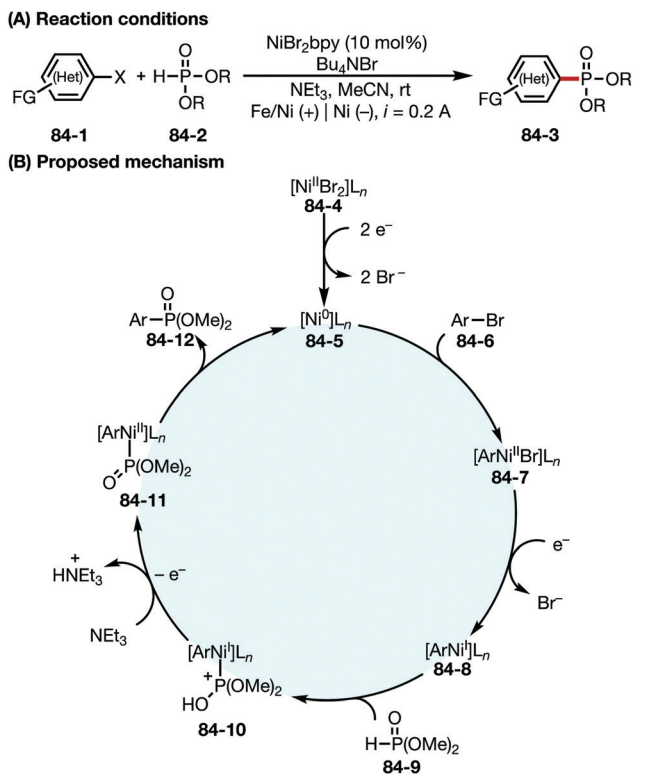


Fig. 84 (A and B) Electrochemical nickel-catalyzed phosphorination of aryl halides and heteroaryl halides.

 This journal is © The Royal Society of Chemistry 2021

Published on 01 June 2021. Downloaded by University of Cambridge on 12/3/2022 1:39:05 PM.

phosphites proved suitable coupling partners, providing the corresponding aryl phosphonates in good efficiency. The proposed mechanism is analogous to the thiolation reaction described previously (Fig. 84B).

The Xiang group reported a similar system with a scope that extended to nitriles, esters, ketones, pyrimidines, thiophenes, and benzo[*d*]thiazoles without the use of a sacrificial anode (Fig. 85A).[241] A different mechanism is proposed for this transformation in which dialkyl phosphite **85-17** undergoes proton-transfer/electron-transfer on the anode to generate P-centered radical **85-18.** Meanwhile, Ni species **85-13** is formed from cathodic reduction of the catalyst precursor and oxidative addition with the aryl halide. The radical addition of **85-18** to **85-13** precedes reductive elimination to deliver the product **85-16** and Ni^{I} **85-15**, the latter of which is reduced on the cathode to regenerate Ni^{0} **85-11** (Fig. 85B). This reaction technically adopts a paired electrolysis mechanism (see Section 4) but is discussed here owing to its similarity in catalytic mechanism to other examples in this section.

The Léonel group later published a follow-up work on electrochemical nickel-catalyzed C–P formation and further extended the scope of P-donors.[242] The Rueping group also reported a similar transformation as well as a C–Se coupling protocol.[243]

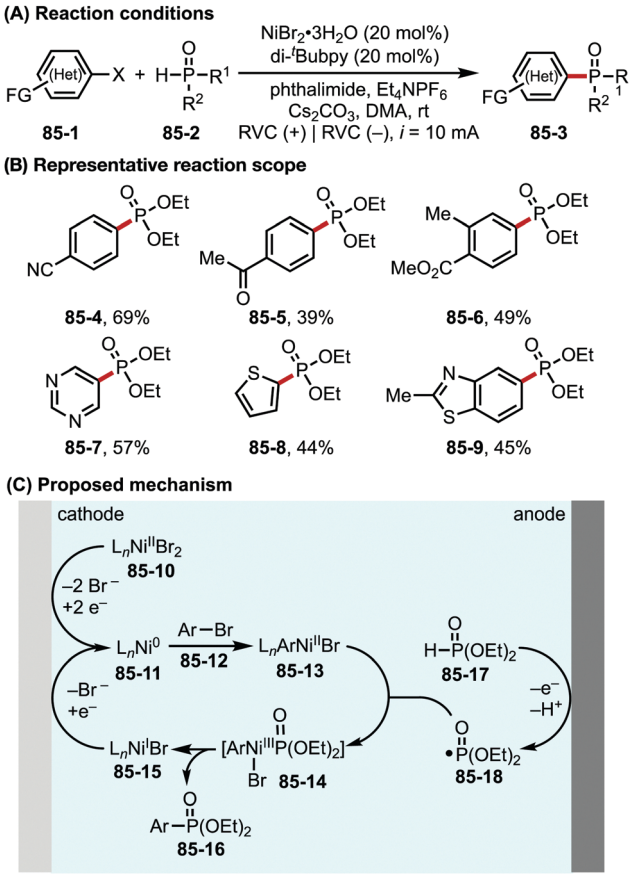


Fig. 85 (A–C) Electrochemical nickel-catalyzed carbon–phosphine bond formation.

3.1.7. C–H functionalization. In 2019, the Zeng group developed an electrochemically enabled, nickel-catalyzed reductive decarboxylative coupling reaction between *N*-hydroxyphthalimide (NHP) esters (**86-2**) and quinoxalinones (**86-1**) (Fig. 86A).[244] The proposed mechanism starts with reduction of Ni^{II} catalyst **86-2** to Ni^{I} species **86-1** at the cathode, followed by a single-electron transfer from Ni^{I} to NHP ester **86-2** and subsequent decarboxylation to give cyclohexyl radical **86-6** (Fig. 86B). The authors also proposed that direct reduction of **86-2** at the cathode can provide the same radical species **86-6.** The cyclohexyl radical then adds to substrate **86-1** in a Minisci-type pathway to generate radical cation **86-8**, and this process is proposed to be facilitated by Ni coordination to (**86-7**). A series of follow-up events ultimately lead to the formation of product **86-3.** Meanwhile, sacrificial reductant Et_3N is oxidized at the anode to give a triethylamine radical cation.

In 2020, the Ackermann group reported a nickel-catalyzed electrochemical C–H activation using primary and secondary alkyl halides *via* a directing group strategy[245] (Fig. 87). This reaction mechanism is analogous to similar C–H activation reactions reported by the same group using other transition

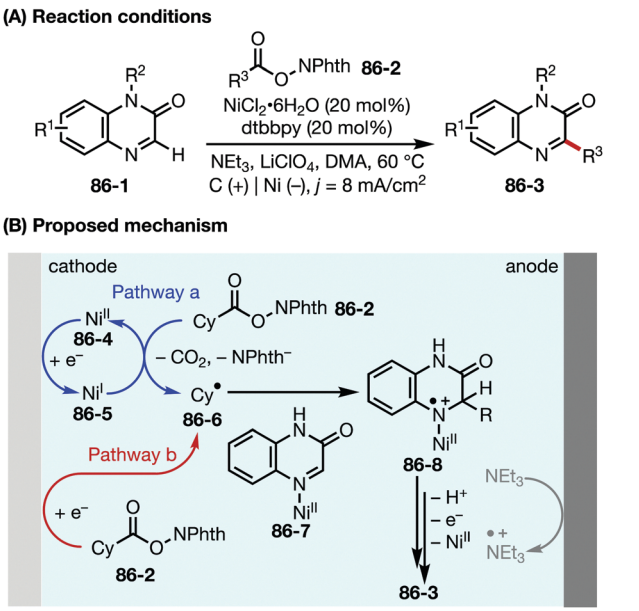


Fig. 86 (A and B) Electrochemically enabled, $NiCl_2$-catalyzed reductive decarboxylative coupling of *N*-hydroxyphthalimide (NHP) esters with quinoxalinones.

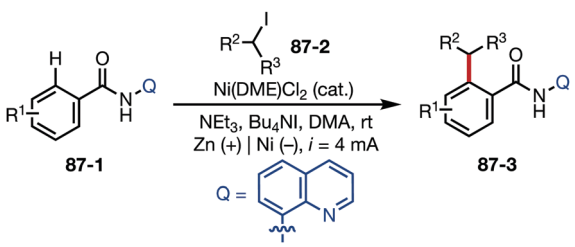


Fig. 87 Electrochemical C–H activation of benzamides.

Published on 01 June 2021. Downloaded by University of Cambridge on 12/3/2022 1:39:05 PM.

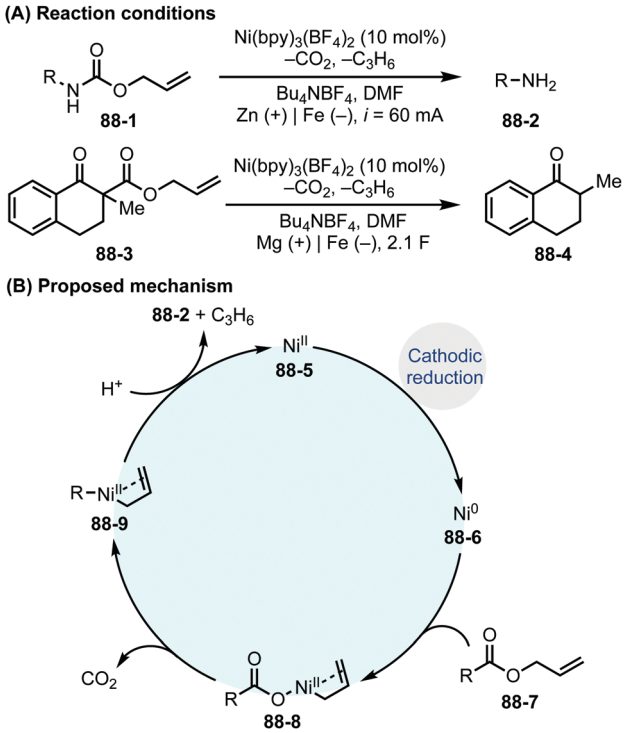


Fig. 88 (A and B) Nickel-catalyzed reductive electrochemical decarboxylation.

metals (see Section 2.14) but relies on the cathodic reduction of Ni to generate the active catalyst and maintain the catalytic cycle.

3.1.8. Miscellaneous transformations. Nickel-catalyzed reductive electrochemical decarboxylation was first reported by the Dunach group in 2000.[246] In a later work by the same group, this strategy was extended to deprotect carbamates and allyl β-keto esters (Fig. 88A).[247] Mechanistically, the reaction proceeds through the electrochemical generation of **88-6**, which inerts to the C–O bond of **88-7** to form a π-allyl Ni^{II} complex **88-8** (Fig. 88B). After decarboxylation and deallylation, **88-2** is formed.[248]

3.2. Cobalt

3.2.1. XEC. In the early 2000s, Gosmini, Nedélec, and co-workers demonstrated a series of cobalt-catalyzed electroreductive XEC of aryl halides (Fig. 89).[249,250] In these reactions, a Co^{I} species is proposed to be the active catalyst, which is generated *via* electroreduction of Co^{II} chloride and reacts with aryl halides (**89-1**, **89-2**, **89-4**) to initiate the reaction. Several functionalities, such as esters, trifluoromethyl, and ether groups, have been explored in this scheme and exhibit good reactivity. These early studies have paved the way for a variety of new developments in the area of Co electroreductive chemistry.

3.2.2. Alkene hydroalkylation. Nedélec and co-worker also reported a Co^{II}(salen) mediated electroreductive coupling of alkyl bromides with methyl vinyl ketone. In this reaction, the reduced Co^{I} intermediate (**90-4**) is transformed to Co^{II} (**90-5**) or Co^{III} (**90-6**) *via* oxidative addition, which mediates the alkyl addition to alkene **90-2** in either radical-polar crossover (Fig. 90, pathway a) or anionic pathways (Fig. 90, pathway b).[251]

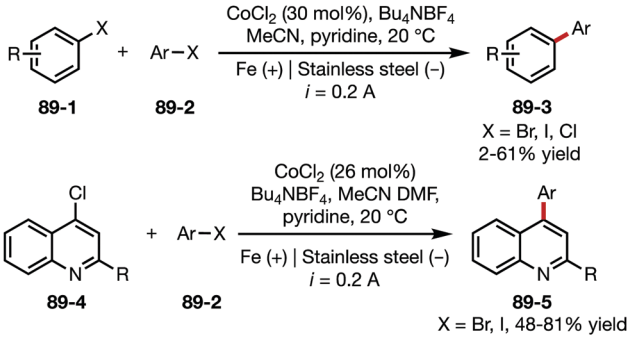


Fig. 89 Cobalt-catalyzed aryl halides coupling: early contributions from Gosmini, Nedélec and co-workers.

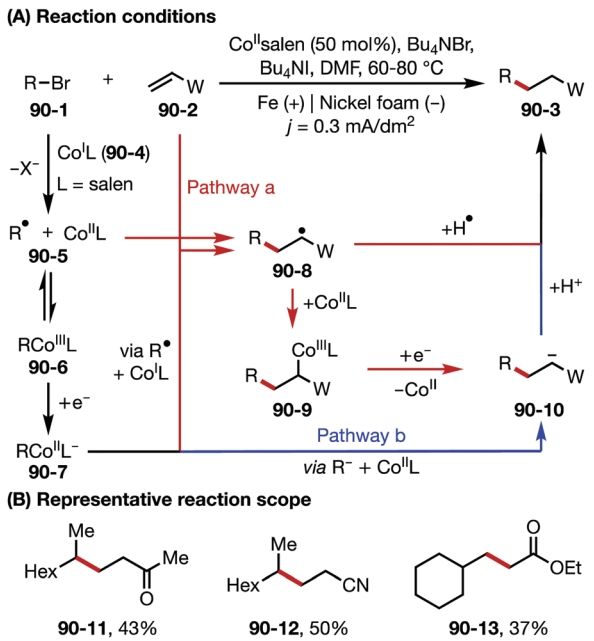


Fig. 90 (A and B) Co(salen)-catalyzed alkylation. W = electron-withdrawing group (EWG).

Bedioui and co-workers further studied this system, expanding the scope to several alkyl bromides and activated olefins, including acrylate and acrylonitriles.[252]

3.2.3. Reductive dehalogenation. Cobalt and its organometallic complexes have recently emerged as versatile redox mediators in electrocatalysis.[253] In 2013, the Atobe group reported a reductive debromination of open-chain and cyclic dibromoalkanes with a Co^{II}(salen) electrocatalyst (Fig. 91).[254] In this context, Co^{II}(salen) is reduced to Co^{I}(salen) and abstracts a bromine atom from substrate **91-3** to generate carbon-centred radical **91-4**. Upon reduction with a second equivalent of Co^{I}(salen), carbanion **91-5** undergoes protonation to complete the debromination to form **91-6**. This series of events is repeated to provide fully debrominated product **91-7**. In the case with a vicinal dibromide substrate, β-elimination takes place from intermediate **91-5** to yield an alkene product (*e.g.*, **91-10**; Fig. 91C).

 This journal is © The Royal Society of Chemistry 2021

Published on 01 June 2021. Downloaded by University of Cambridge on 12/3/2022 1:39:05 PM.

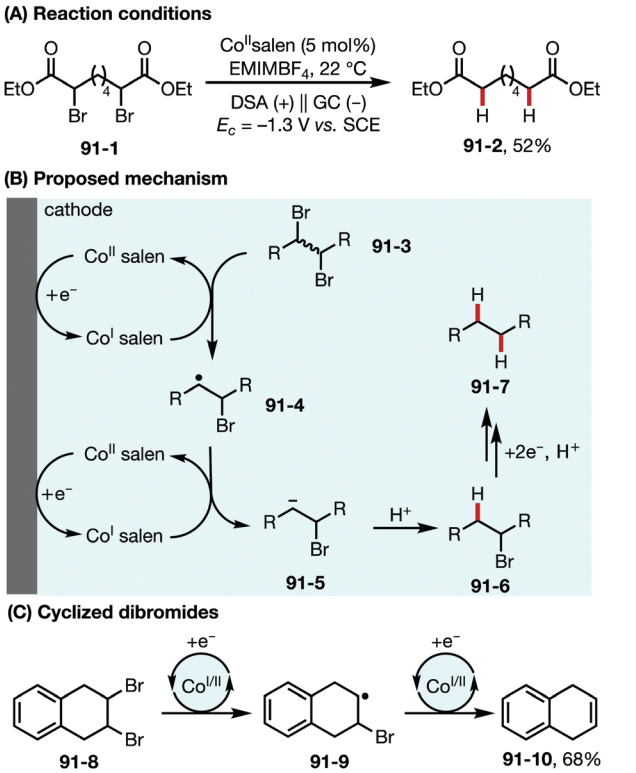


Fig. 91 (A–C) Co(salen)-catalyzed debromination. GC = glassy carbon. DSA = Dimensionally Stable Anodes, titanium mesh with metal oxides (RuO_2, IrO_2 or PtO_2). The anodic reaction was not discussed.

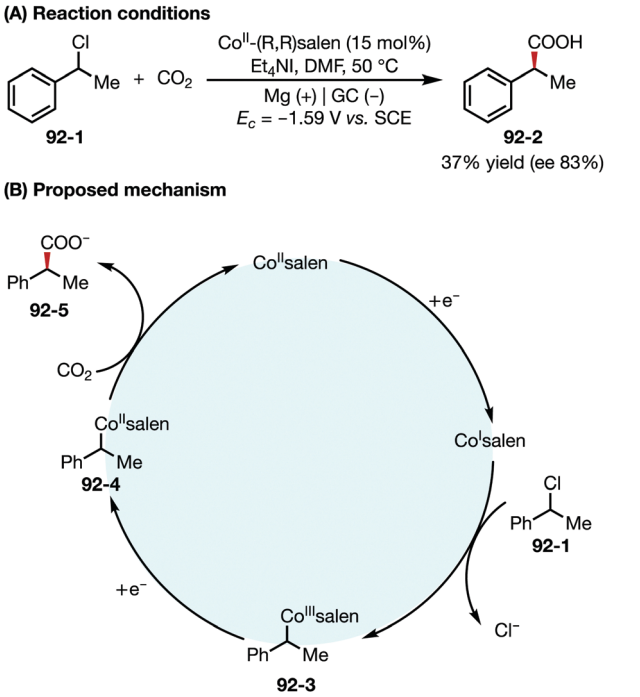


Fig. 92 (A and B) Co(salen)-catalyzed enantioselective carboxylation.

3.2.4. Reductive carboxylation. Lu and co-workers reported an asymmetric electrocarboxylation of 1-phenylethyl chloride with a chiral Co(salen) catalyst (Fig. 92).[255] In the first step, the active Co^{I}(salen) species is generated *via* cathodic reduction of Co^{II}(salen) and reacts with benzyl chloride **92-1** *via* oxidative addition, thus forming Co^{III} intermediate **92-3.** This intermediate undergoes a second single-electron reduction to form Co^{II} species **92-4**. Upon subsequent nucleophilic addition to CO_2 directed by the chiral catalyst enantioenriched carboxylate **92-5** is formed with the regeneration of Co^{II}(salen).

In 2020, the Ackerman group demonstrated a cross-electrophile coupling of cinnamoyl chlorides and CO_2 in a Co-mediated electroreductive pathway (Fig. 93).[256] In this system, Co^{II} acetate is cathodically reduced to Co^{I} species **93-4**, which undergoes oxidative addition to cinnamoyl chloride **93-1** to form π-allyl Co^{III} complex **93-5**. This intermediate then undergoes rearrangement to give η^1-allyl Co^{III} intermediates **93-6** and **93-7**, which are then converted to Co^{I} complexes **93-8** and **93-9**, respectively, *via* two-electron reduction. These low valent Co species then react with CO_2 to deliver carboxylate products **93-10** and **93-11** and liberate the active Co^{I} catalyst. Both electron-withdrawing and electron-donating aryl substituents are well-tolerated in this system, providing a useful method for the synthesis of vinylacetic acids.

3.2.5. Other Co-mediated transformations. Cobalt-containing vitamin B_{12} has also been widely used as a mediator in electroreductive reactions.[257] In a report from Rusling and co-workers, vitamin B_{12} was employed to achieve cyclopropenation of styrene with dichloromethane. In this reaction, vitamin B_{12} is reduced to Co^{I}, which then catalyzes the generation of carbon-centered radical **94-4** (Fig. 94).[258] This radical intermediate adds to styrene to generate benzylic radical **94-5**, which is reduced to carbanion **94-6** before intramolecular cyclization to form a cyclopropane ring.

Hisaeda used a similar vitamin B_{12}-mediated protocol to synthesize esters, amides, and 1,2-dichlorostilbenes from trichlorotoluenes by means of generation of 1,1-dichlorobenzyl radicals (**95-6**; Fig. 95).[259] Here, electrogenerated Co^{I} undergoes oxidative addition to a C–Cl bond of substrate **95-1**, forming Co^{III} intermediate **95-4**. Direct homolysis of the Co^{III}–C bond in **95-4** (Fig. 95, solid arrow) or single-electron reduction followed by mesolytic cleavage of the Co^{III}–C bond in **95-5** (Fig. 95, dashed arrow) give **95-6.** Upon further reaction with oxygen to generate an acyl chloride intermediate and subsequent reaction with a nucleophile (*e.g.*, an alcohol or an amine), the desired ester **95-2** or amide **95-3** can be obtained.

Peters and co-workers designed a cobaltocene mediator to facilitate concerted proton-electron transfers (CPET) under electroreductive conditions (Fig. 96).[260] CPET enables milder conditions for redox transformations by lowering the reaction energy barrier compared with conventional stepwise electron transfer-proton transfer processes. The system developed by Peters employs an aniline-substituted cobaltocene mediator, which promotes CPET reactivity to drive pinacol coupling while suppressing the competing hydrogen evolution reaction. Mechanistic studies revealed that protonated Co^{II} catalyst **96-1** reacts with acetophenone *via* CPET to give a neutral α-radical **96-3** and Co^{III} **96-5.** Radical dimerization of **96-3** affords pinacol **96-4** as the final product in 83%. Meanwhile, **96-5** is protonated

Published on 01 June 2021. Downloaded by University of Cambridge on 12/3/2022 1:39:05 PM.

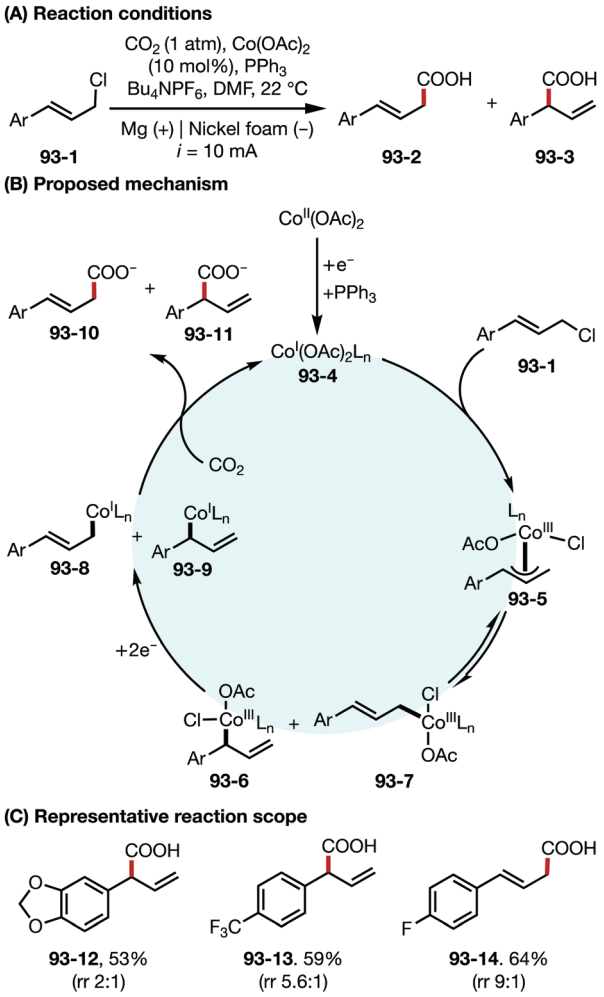


Fig. 93 (A–C) Cobalt-catalyzed allylic carboxylation.

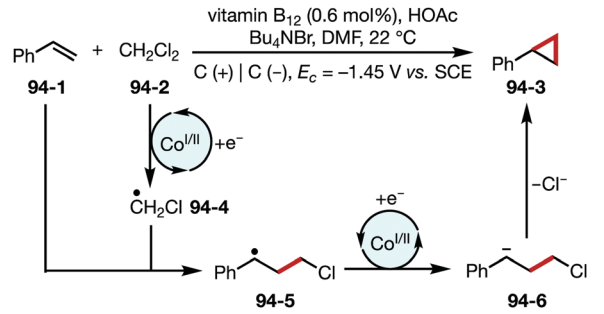


Fig. 94 Vitamin B_{12}-catalyzed cyclopropanation of styrene.

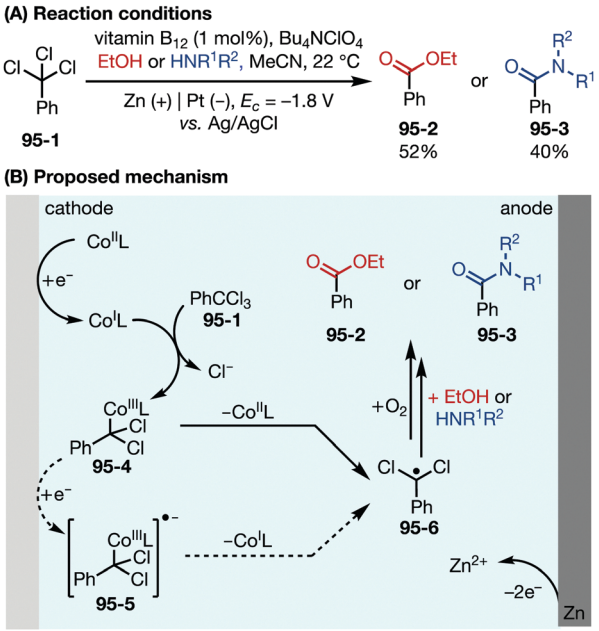


Fig. 95 (A and B) Vitamin B_{12}-catalyzed ester/amide synthesis.

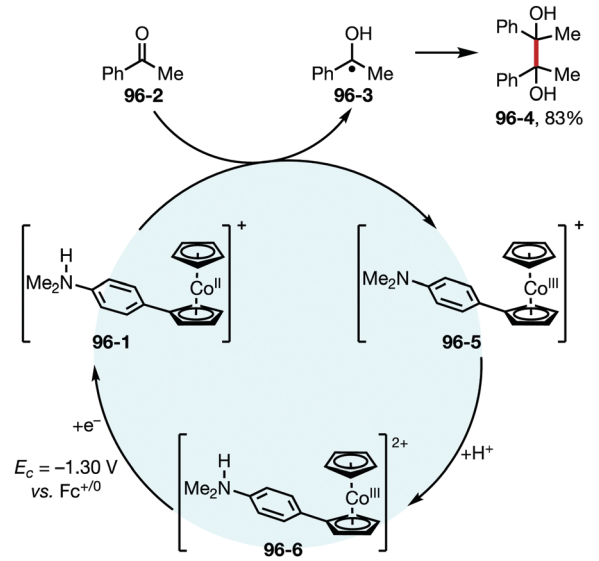


Fig. 96 Cobalt-catalyzed reductive ketone dimerization *via* CPET. Boron-doped diamond (BDD) electrode is used as cathode and glassy carbon is used as counter electrode.

to form the dimethylanilinium Brønsted acid **96-6**, which undergoes cathodic reduction at a potential of −1.30 V *vs.* Fc^{+}/Fc^{0} to regenerate Co^{II} catalyst **96-1**. This approach provides a potential solution to improving functionality tolerance for electrolysis that otherwise requires highly biased potentials.

3.3. Titanium

An early example of titanocene-catalyzed electroreductive dehalogenation of organic halides was disclosed by Magdesieva and co-workers (Fig. 97).[261] After the electroreductive generation of active Ti^{III} species **97-6**, halogen atom abstract takes place to transform the benzyl halide or pseudohalide substrate (**97-1**) to a benzyl radical prior to formation of product **97-2**. In 2011, this reactivity was extended to an electroreductive epoxide ring opening reaction by the same group using a 30% loading of titanocene dichloride as the mediator (Fig. 97).[262] In this context, Ti^{III} catalyst **97-6** induces homolytic ring opening of epoxide **97-3** to form carbon-centered radical **97-7**. Hydrogen atom transfer from 1,4-cyclohexadiene (1,4-CHD) to **97-7**

 This journal is © The Royal Society of Chemistry 2021

Published on 01 June 2021. Downloaded by University of Cambridge on 12/3/2022 1:39:05 PM.

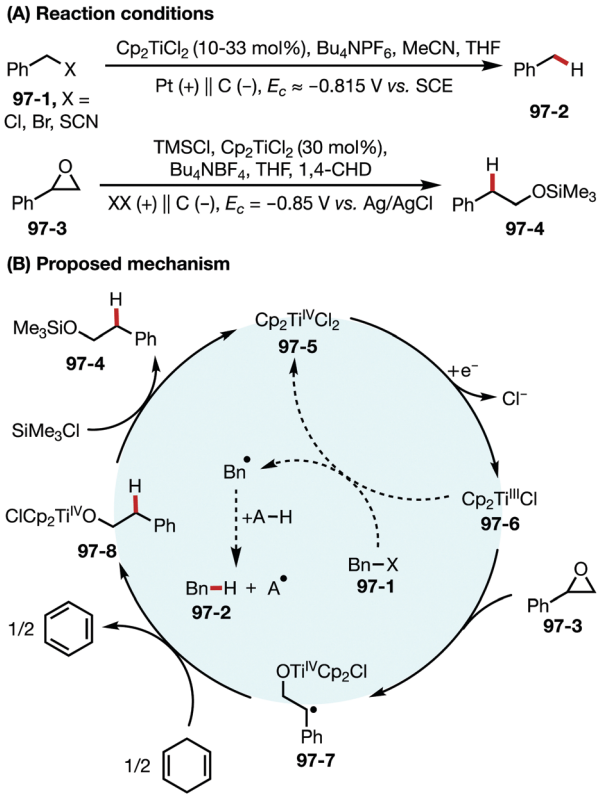


Fig. 97 (A and B) Titanocene-catalyzed dehalogenation and epoxide opening. The anode [XX(+)] in the epoxide ring-opening reaction was not disclosed.

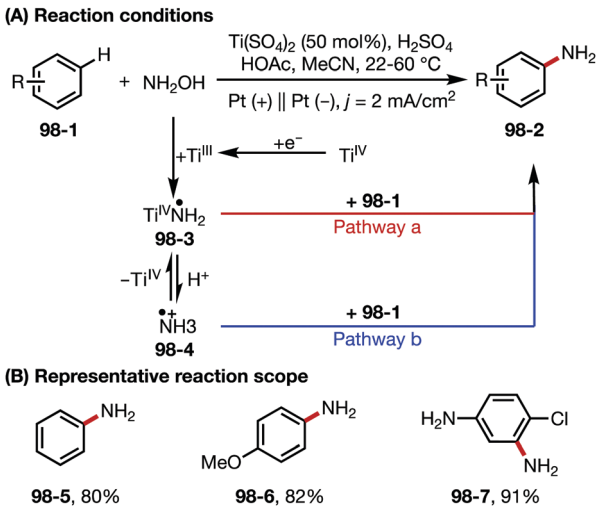


Fig. 98 (A and B) Titanium-catalyzed amination of arenes.

followed by transmetallation of the resultant **97-8** with trimethylsilyl chloride affords the product **97-4**.

In addition, Lisitsyn and co-workers achieved amination of arenes *via* electrochemical reduction of hydroxylamine using a Ti^{IV} mediator (Fig. 98).[263] Mechanistic investigation of this transformation revealed that the initial cathodic reduction of Ti^{IV} sulfate generates active Ti^{III}, which reacts with hydroxylamine to form Ti^{IV}-bound aminyl radical **98-3**. **98-3** is in equilibrium with ammonia radical cation (**98-4**). The authors proposed that either of these intermediates can react with an arene substrate (**98-1**), giving rise to the aniline product (**98-2**). Anisole,[264] benzene,[265] and chloroaniline[266] were shown to be suitable substrates for this method.

In 2018, Gansäuer and co-workers achieved the radical arylation of epoxides using a pre-generated Ti^{III} catalyst *via* electrochemistry. This approach avoids the use of heterogenous metal reductant and generates indoline products in high efficiency (Fig. 99).[267] Thiourea is found to facilitate halide abstraction from reduced titanocene to generate the active Cp_2TiCl catalyst.

3.4. Zinc

Zinc salts are frequently used as Lewis acids, but if these salts are reduced to Zn^0, they can be used to mediate reductive transformations. For example, Huang and co-workers have demonstrated a series of electrochemical allylation reactions of carbonyl species in aqueous solution *via* a Zn-mediated approach (Fig. 100).[268] The sacrificial zinc anode is oxidized

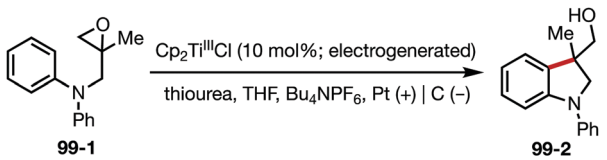


Fig. 99 Titanium-catalyzed epoxide ring-opening arylation.

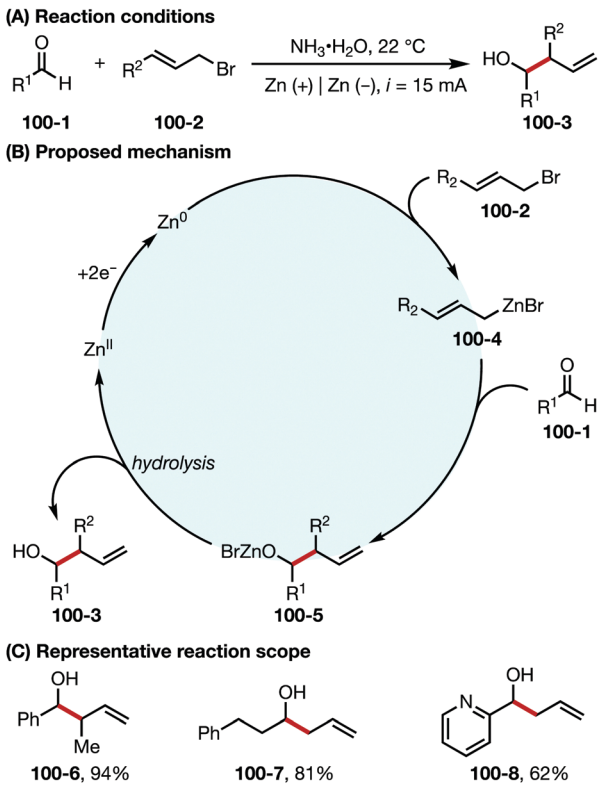


Fig. 100 (A–C) Zinc-mediated allylation of aldehydes.

Published on 01 June 2021. Downloaded by University of Cambridge on 12/3/2022 1:39:05 PM.

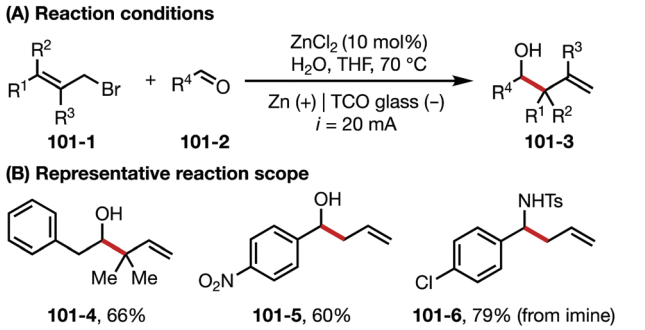


Fig. 101 (A and B) Zinc catalyzed allylation of aldehydes and sulfonimines. TCO glass = transparent conductive oxide glass, indium tin oxide.

and releases Zn^{2+} into the reaction medium. Upon forming a complex with ammonia, Zn^{II} is reduced on the cathode to give active Zn^0 particles, which react with allyl bromides (**100-2**) to afford allyl zinc reagent **100-4**. **100-4** then undergoes nucleophilic addition to aldehyde **100-1** to generate **100-5**, followed by hydrolysis to give the products **100-3**. Subsequent studies improved the atom efficiency of this reaction by introducing Pt as the anode in a divided cell to avoid consumption of stoichiometric amounts of Zn on a sacrificial anode.[269] The authors propose that in this case, oxidation of water happens on the Pt anode, which results in the formation of protons that can diffuse to the cathode chamber to participate in the reaction.

In 2014, Chakraborty, Roy and co-workers demonstrated the same transformation using a transparent conductive oxide (TCO) glass cathode and a Zn anode with additional catalytic Zn^{2+} in the solution (Fig. 101).[270] It was found that Zn^{II} was reduced to Zn^0 on the cathode surface as nanowires, which promote the reaction. In addition to aldehydes, *N*-tosylimines can also undergo allylation in good yields.

3.5. Palladium

In 1985, Torii and co-workers reported an early example of an electroreductive Pd-catalyzed homocoupling of aryl halides (Fig. 102A).[271] In 2005, the Moeller group developed a Heck-type reaction assisted by Pd and electrochemistry (Fig. 102B).[272] Both reactions are proposed to be promoted by cathodically generated Pd^0. These early developments demonstrated the possibility of reductive Pd electrocatalysis.

In 2017, Huang and co-workers reported an electrochemical Pd-mediated allylic alkylation reaction in an undivided cell system (Fig. 103).[273] A variety of alkyl iodides and benzyl bromides were converted to the desired product in high yields. Aryl halide, ester, carboxylic acid and alcohol functionalities were well tolerated.

In 2018, Mei and co-workers reported a Pd-catalyzed electroreductive carboxylation of allyl ethers (Fig. 104).[274] The oxidative addition of electrogenerated Pd^0 (**104-3**) to the allyl electrophile **104-1** generates a cationic π-allyl Pd^{II} complex (**104-4**). Complex **104-4** is in equilibrium with a terminal η^1-allyl Pd^{II} species, and this energetically favorable isomer is further reduced to Pd^0 complex **104-6**. This species reacts with

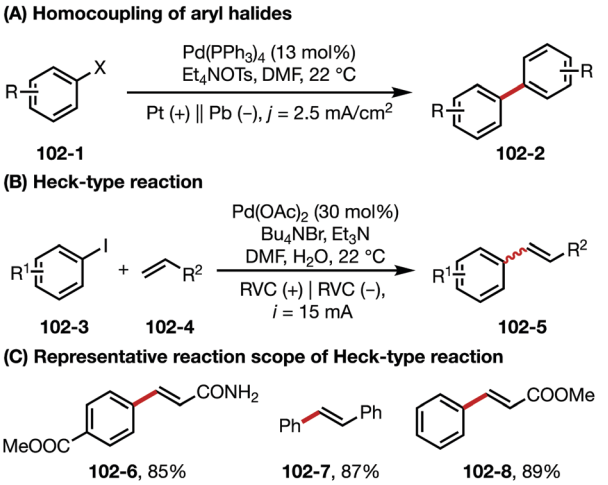


Fig. 102 (A) Palladium catalysed homocoupling of aryl halides; (B and C) palladium catalysed Heck type reaction.

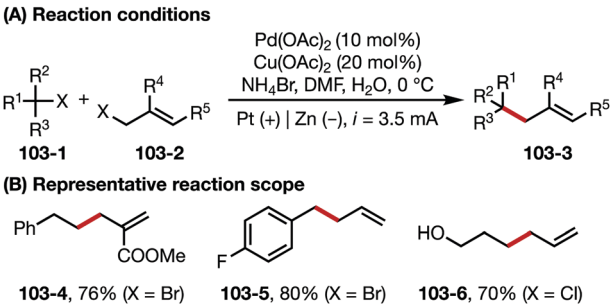


Fig. 103 (A and B) Palladium-catalyzed allylic halide coupling.

electrophilic CO_2 to deliver the product **104-7** and regenerate Pd^0. Notably, enantioselective carboxylation was also achieved when a chiral phosphine ligand, (*R*)-MeO-BIPHEP, is used.

3.6. Samarium

SmI_2, also known as Kagan's reagent, has been shown to be an outstanding single electron reductant in synthetic organic chemistry.[275] However, SmI_2 is a potent reductant that is air sensitive and can be difficult handle or store. Thus, *in situ* generation of SmI_2 *via* electroreduction constitutes an attractive approach to achieve the same types of transformations.[276–278] For example, Mellah and co-workers introduced Sm as the sacrificial anode to electrochemically generate Sm^{2+} *in situ* (Fig. 105A),[279] which reacts with iodide in the medium to form Kagan's reagent. This system was shown to promote the pinacol coupling of carbonyl compounds. This approach can also be applied to allylation, benzylideneaniline coupling, and Reformatsky-type reactions.[280] In these systems, the authors showed that catalytic Sm^{II} can be regenerated *via* cathodic reduction of Sm^{III} on a Sm cathode (Fig. 105B–D).

In 2017, the same group reported a Sm-mediated electroreduction of nitroarenes to azoarenes (Fig. 106).[281] In the first step, a pre-electrolysis is performed (Fig. 106, red conditions) to oxidize a Sm anode, releasing Sm^{II} into solution until a

 This journal is © The Royal Society of Chemistry 2021

Published on 01 June 2021. Downloaded by University of Cambridge on 12/3/2022 1:39:05 PM.

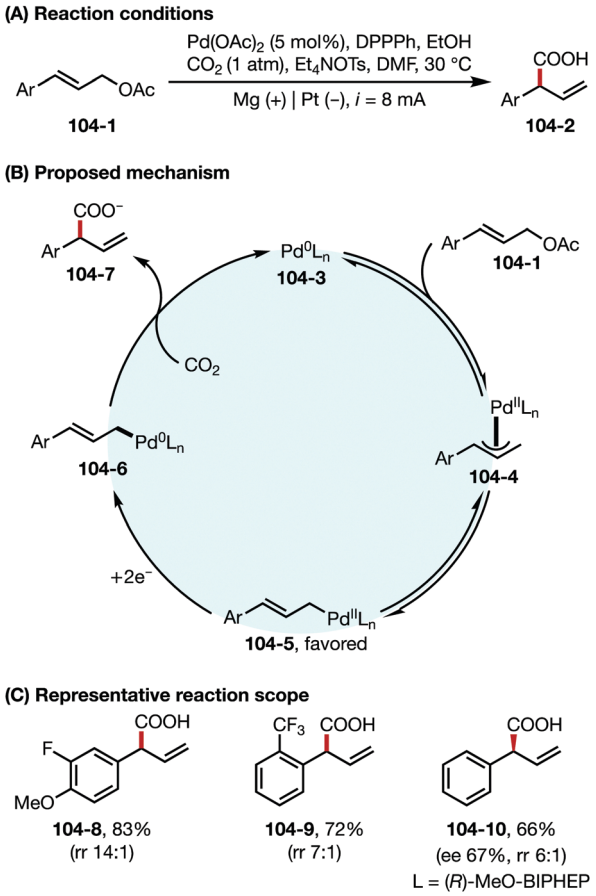


Fig. 104 (A–C) Palladium-catalyzed carboxylation of allyl ethers. DPPPH = 1,2-bis(diphenylphosphino)benzene; (*R*)-MeO-BIPHEP = (*R*)-(+)-2,2″-bis(diphenylphosphino)-6,6″-dimethoxy-1,1″-biphenyl.

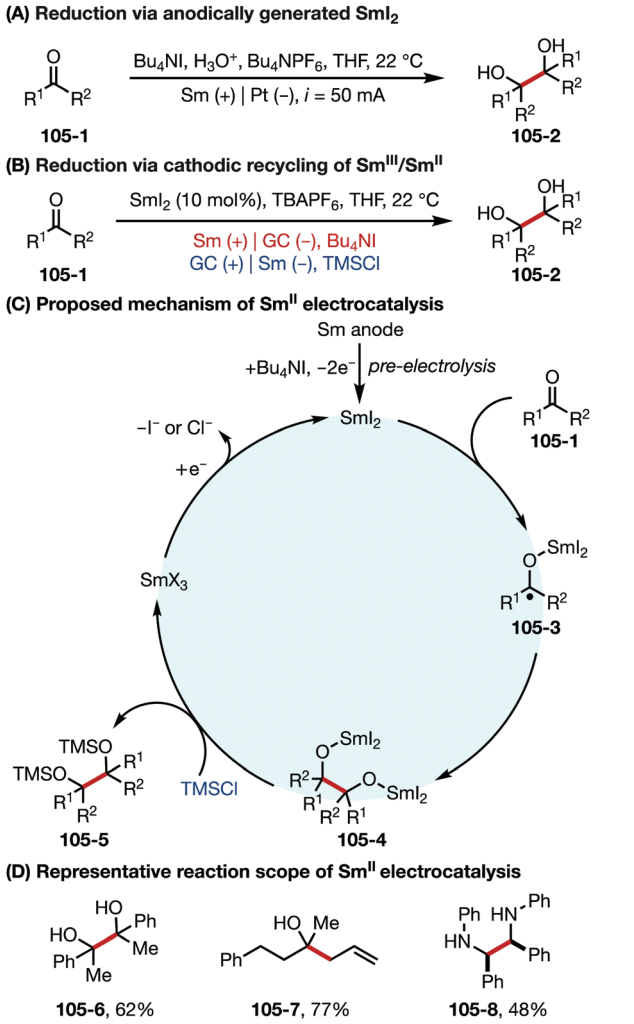


Fig. 105 (A–D) Samarium-mediated coupling reactions.

20 mol% loading with respect to the organic substrate is attained. Thereafter, the polarity of the electrolysis is reversed (Fig. 106, blue conditions), and Sm now acts as the cathode. Nitrobenzene (**106-1**) is then reduced by Sm^{II} to generate nitrosobenzene **106-3**. **106-3** then undergoes a one-electron reduction by Sm^{II} to form nitroxyl radical anions which quickly dimerize to intermediate **106-4**. Upon reduction of **106-4** with Sm^{II}, azobenzene product (**106-2**) was formed in high yields. The reaction has also been used to achieve cross coupling of two different nitroarenes by adjusting the relative stoichiometry of the substrates. Thus, when a 1 : 3 molar ratio of two nitrobenzenes are used, over 99% selectivity can be achieved.

3.7. Tin

Since 1980s, tin has been enlisted in the electroreductive allylation of carbonyl compounds. The reaction was performed by the Torii group in a divided cell with two Pt electrodes and catalyzed by a 10 mol% loading of tin (Fig. 107).[282] It is proposed that low valent tin species **107-4** reacts with two equivalents of allyl bromide to generate active diallyltin dibromide intermediate **107-5** which reacts with a ketone or aldehyde (**107-1**) to form the product **107-3**. Upon ligand exchange with methanol,

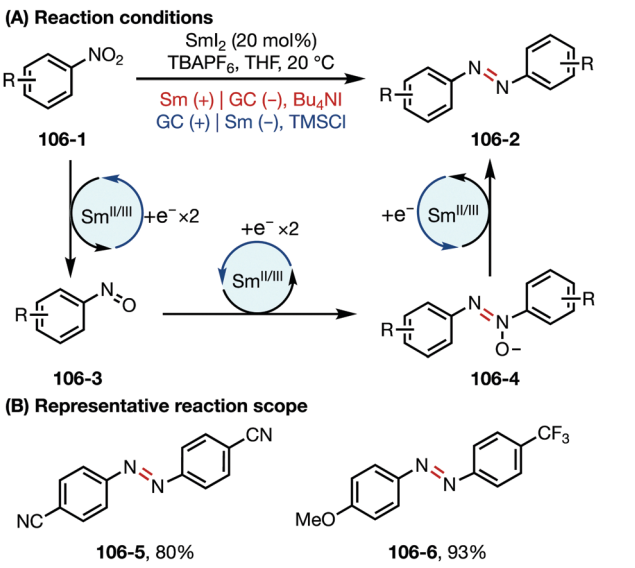


Fig. 106 (A and B) Samarium-catalyzed reductive coupling of nitroarenes.

Published on 01 June 2021. Downloaded by University of Cambridge on 12/3/2022 1:39:05 PM.

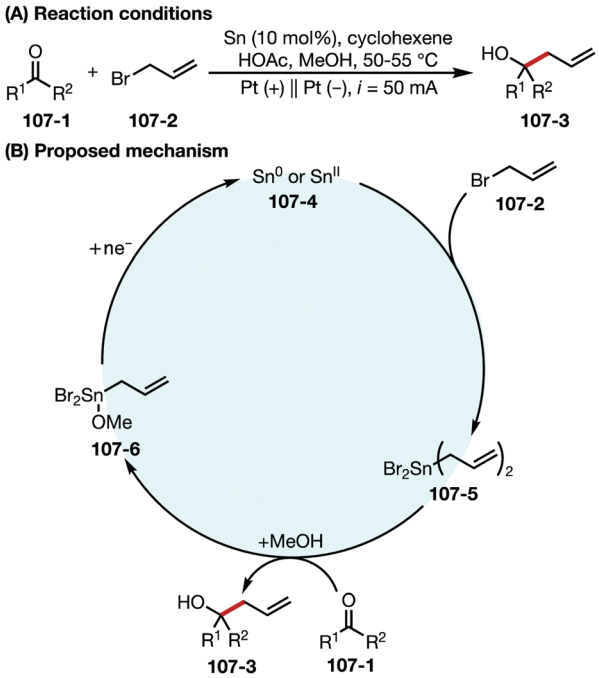


Fig. 107 (A and B) Tin-catalyzed allylation of ketones/aldehydes.

monomethoxide tin intermediate **107-6** is formed and reduced cathodically to **107-4**, completing the cycle.

Subsequently, Wang, Zhang, and co-workers demonstrated a Sn-mediated aldehyde allylation in aqueous media with two graphite electrodes.[283] The tin catalyst can be recycled by extraction and show little decrease of reactivity even after five cycles of reuse. This reaction has also been merged with anodic alcohol oxidation in a divided cell system to achieve parallel paired electrolysis.[284]

In a follow-up development, the same group developed a paired electrolysis system to synthesize secondary homoallylic alcohols.[285,286] In this case, alcohol substrate (**108-1**) is anodically oxidized to the aldehydes or ketones (**108-4**), which diffuse to the cathode to undergo Sn^0-mediated allylation with allyl bromide (Fig. 108). Both benzyl and unactivated alcohols are suitable substrates and a variety of functionalities are tolerated.

In addition to these allylation reactions, the Zhang group also demonstrated the synthesis of oximes from alcohols and KNO_3 through paired electrolysis (Fig. 109).[287] Here, alcohol substrate **109-1** was oxidized to an aldehyde or ketone (**109-3**) on the anode, which then combined with the hydroxylamine generated *via* cathodic reduction of KNO_3 to form the desired product **109-2**.

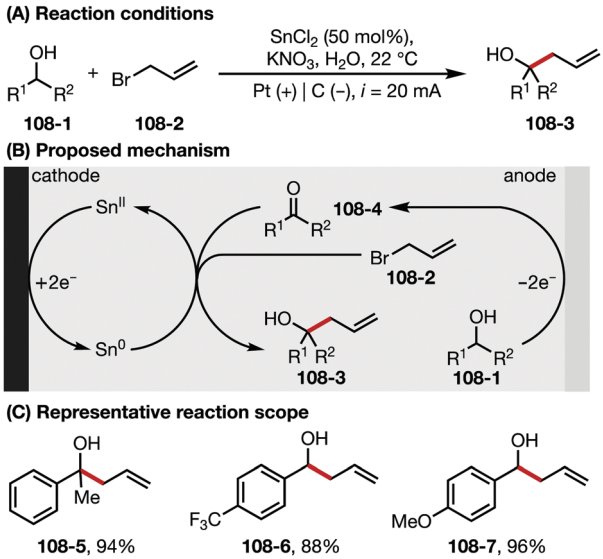


Fig. 108 (A–C) Tin-catalyzed ketone allylation in one pot.

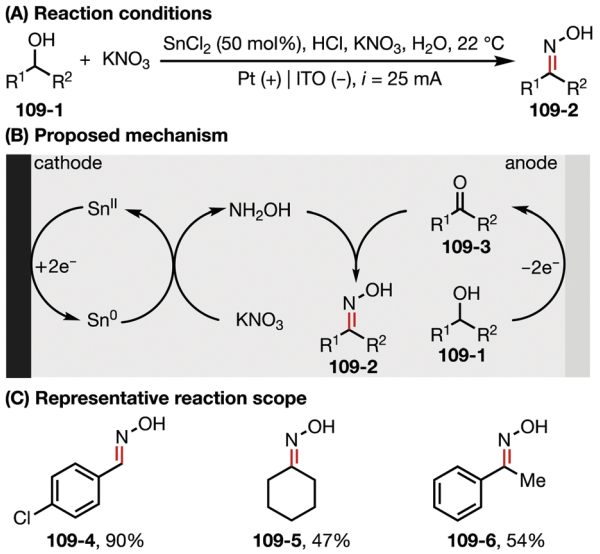


Fig. 109 (A–C) Tin-catalyzed synthesis of oximes.

Organic mediators

3.8. Arenes

Arenes are well-known for their ability to stabilize radical and charged species. This feature renders arenes suitable as mediators in electrocatalytic transformations. An early example was reported by Ban and co-workers, wherein anthracene mediates the reductive removal of arenesulfonyl groups of sulfonamides.[288] Here, anthracene serves as a redox shuttle to transfer electrons to the sulfonamide substrate. In 2010, the Senboku group further optimized this reaction system by using a Mg anode/Pt cathode system to eliminate the use of hazardous mercury electrodes in the original system (Fig. 110).[289] A variety of arene mediators were screened, and the targeted detosylation was achieved in high yields with good functional group tolerance when naphthalene was used.

Another example of arene-mediated electroreduction is the dehalogenative functionalization of aryl halides *via* aryl radical formation. In early contributions by Tokuda and Kurono, phenanthrene was employed to promote the reduction of aryl halides.[290,291] In 2013, Suga and co-workers introduced fluorene derivatives as mediators and achieved the reduction of aryl

 This journal is © The Royal Society of Chemistry 2021

Published on 01 June 2021. Downloaded by University of Cambridge on 12/3/2022 1:39:05 PM.

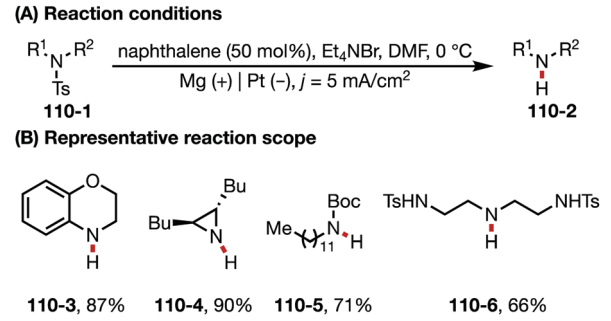


Fig. 110 (A and B) Naphthalene-mediated detosylation.

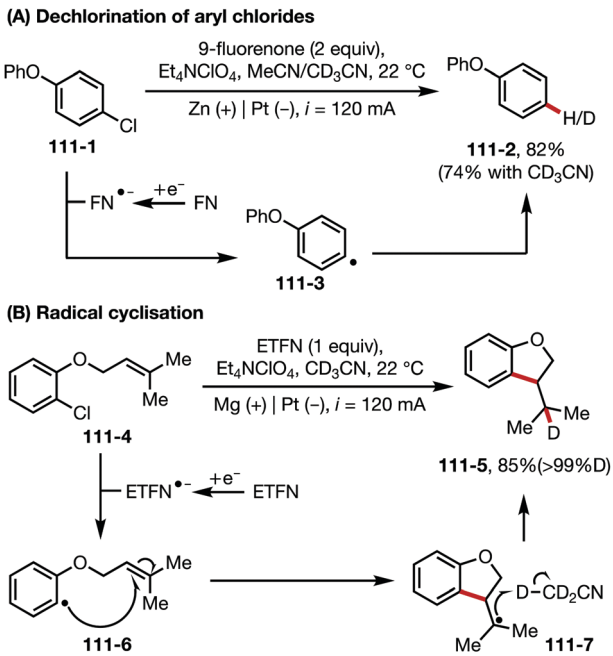


Fig. 111 Fluorene mediated: (A) dechlorination, FN = 9-fluorenone; (B) radical cyclization of aryl halides, ETFN = 9,9-diethyl-9*H*-fluorene.

chlorides (**111-1**) in high efficiency (Fig. 111A).[292] This protocol can also be incorporated in radical cyclization reactions (Fig. 111B).[293]

Perylene diimide derivatives (PDIs) are an intriguing class of organic dyes which have been widely used as semiconductors and photocatalysts.[294] In 2016, Wan and co-workers reported an electroreductive arylation of pyrroles through a PDI-catalyzed pathway (Fig. 112).[295] Several aryl halides (Cl, Br, I) with electron-withdrawing substituents and protected or unprotected pyrroles were converted to the coupled products in good yields. Mechanistic insights suggest that the PDI radical anion **112-4** acts as the key mediator of this reaction. Similar to previous examples of arene mediated reduction, PDI accepts one electron from the cathode to form **112-4**, which then reduces aryl halide **112-1** to the corresponding aryl radical. Subsequent addition of this radical intermediate to pyrrole **112-2** constructs the biaryl C–C bond and eventually led to the formation the desired product **112-3** (the mechanism after radical addition to **112-2** is not discussed).

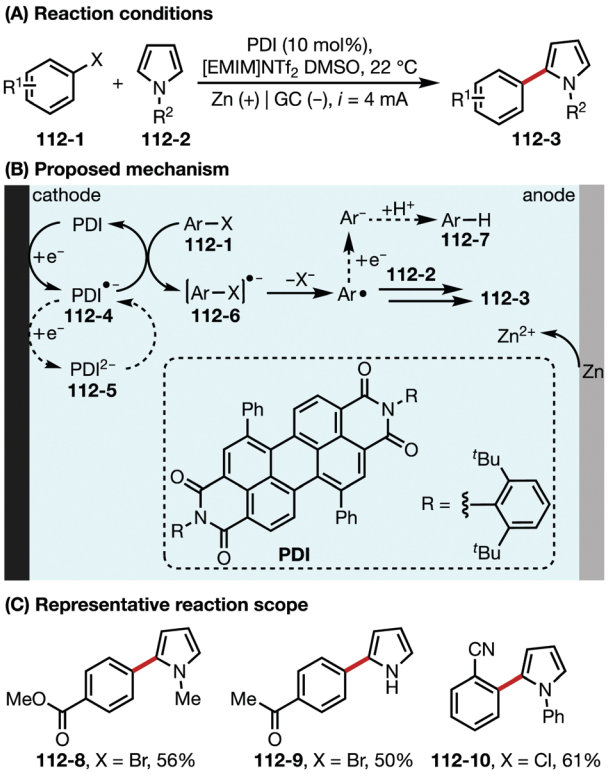


Fig. 112 (A and B) PDI-catalyzed C–H arylation of pyrroles.

3.9. Benzoate-catalyzed carboxylation

A benzoate-mediated electrochemical reaction was developed by Senboku and co-workers to achieve reductive radical cyclization of aryl halides with alkenes followed by tandem carboxylation (Fig. 113).[296] Cyclic voltammetry studies revealed a reversible peak of 4-*tert*-butylbenzoate at –2.9 V *vs.* Ag/Ag^+, which is higher than that of the aryl bromide substrate (−3.2 V), thus supporting the benzoate-mediated pathway for substrate reduction. It is proposed that 4-*tert*-butylbenzoate (**113-4**) undergoes a one-electron reduction to radical anion **113-3** which reduces aryl bromide **113-1** to aryl radical **113-5**. Following an intramolecular radical addition to the pendant alkene moiety of the substrate, the resultant carbon-centered radical **113-6** was reduced to carbanion **113-7** and then captured by CO_2 to complete the reaction. When an alkyne was used as the substrate, dicarboxylic acid was formed (*e.g.*, **113-9**).[297] This protocol can also be applied to vinyl bromide substrates (*e.g.*, **113-10**)[298] and grants access to a variety of value-added heterocyclic carboxylic acids.

3.10. Carborane/fullerene-catalyzed debromination

Fullerenes and carboranes are valuable materials in the fields of polymer synthesis,[299] supramolecular chemistry,[300] and solar cells.[301] In the context of organic synthesis, fullerene compounds can undergo a variety of transformations such as the Bingel[302] and Prato[303] reactions, and carboranes have also been engaged in interesting reactions such as borylation and metal coordination.[304] In 2011, Fuchigami and co-workers

Published on 01 June 2021. Downloaded by University of Cambridge on 12/3/2022 1:39:05 PM.

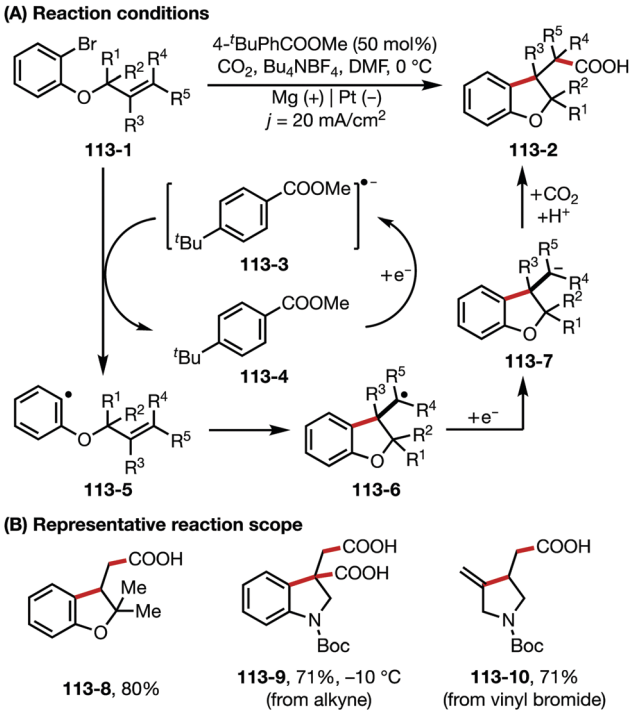


Fig. 113 (A and B) Benzoate-catalyzed radical cyclization carboxylation.

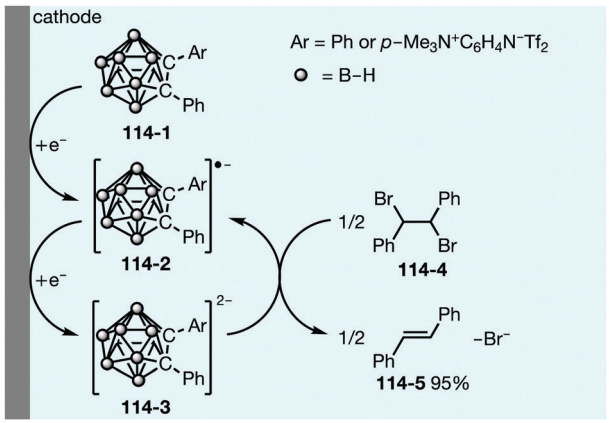


Fig. 114 Carborane-catalyzed debromination. The anodic reaction was not discussed.

demonstrated the reduction of 1,2-dibromo-1,2-diphenylethane in a divided cell system *via* an *o*-carborane mediated pathway (Fig. 114).[305] Here, *o*-carborane **114-1** underwent consecutive cathodic reduction to generate first radical anion **114-2** and then dianion species **114-3**. Electron transfer between **114-3** and vicinal dibromide substrate **114-4** proceeds rapidly, generating trans-stilbene **114-5** and catalyst **114-2**. The stilbene product can be easily separated from reaction mixture by hexanes extraction in 95% yield with only 1 mol% catalyst loading. A similar system was also reported by the same group, which used C_{60} as a mediator to cathodically reduce *vic*-dihalides to the corresponding alkenes following a similar mechanism.[306]

3.11. Viologen/Pd-catalyzed dimerization of aryl halides

Viologens are well-suited for applications in electrocatalysis. Not only do viologens exhibit high electrochemical reversibility, but they can be modification at the pyridyl groups to achieve tunable redox potentials.[307] The Tanaka group used viologens as catalytic reductants to promote a Pd-catalyzed homocoupling of aryl halides (Fig. 115).[308,309] Importantly, mechanistic studies revealed that dicationic salt (V^{2+}) is initially reduced to neutral V^0 which reduces Pd^{II} precursor to Pd^0 (**115-3**). V^0 could be regenerated *via* cathodic reduction of the resultant V^+, and a sacrificial Zn anode is used to circumvent unwanted Pd oxidation. Using this dual catalytic system, a variety of aryl halides with electron-withdrawing and neutral substituents can be efficiently converted to biaryls, whereas diminished reactivity is observed for electron-donating substituents. Pyridinium and diquat derivatives are also proven to be effective mediators for this reaction.[310]

4. Paired electrolysis

Paired electrolysis has attracted substantial attention in recent years for its ability to couple two desirable electrochemical

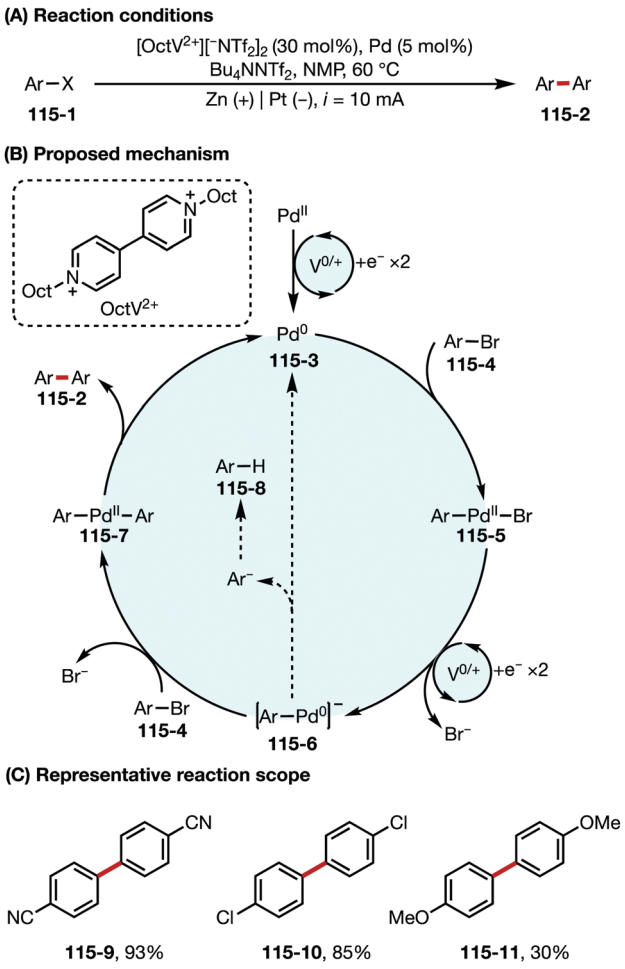


Fig. 115 (A–C) Palladium/viologen catalyzed aryl halides coupling.

This journal is © The Royal Society of Chemistry 2021

Published on 01 June 2021. Downloaded by University of Cambridge on 12/3/2022 1:39:05 PM.

reactions simultaneously within the same reaction system. This efficient and atom-economical technique has been applied to industrial synthesis[311] and energy conversion processes.[312] Despite recent advances, the strategic application of paired electrolysis remains relatively rare in the context of organic synthesis. Sequential and convergent paired electrolysis, wherein both cathode and anode are employed to promote the same transformation, can often lead to ingenious reaction design and new solutions to synthetic problems. However, challenges can arise from the competition between interelectrode mass transport of electrogenerated reactive intermediates and their undesired degradation pathways. Moreover, in many cases balancing the rates of cathodic and anodic events can be crucial to the reaction selectivity. In light of these challenges, recent developments in paired electrolysis have made use of electrochemical mediators to enhance the reaction efficiency and selectivity. In previously sections, we have discussed several examples wherein a paired electrolysis scenario is proposed to contribute to the overall transformation. In this section, we will primarily focus on recently developments in which paired electrolysis is strategically implemented to solve synthetic problems.

4.1. Nickel catalysis

In 2020, the Hu group reported a combination of 4,4′-dimethoxy-2-2′-bipyridine (L1) and (DME)$NiBr_2$ catalyst, THF/CH_3CN co-solvent, fluorine-doped tin oxide (FTO) coated glass anode and carbon fibre cathode to achieve the direct arylation of benzylic C–H bonds.[313] The reaction tolerates a variety of functional groups including ketones, esters, sulfones, and amides. The reaction is initiated by the oxidation of a toluene derivative **116-1** at the anode to form the benzylic radical **116-7** (Fig. 116). Meanwhile, catalytic precursor $LNi^{I}Br$ (**116-10**) undergoes cathodic reduction and oxidative addition with ArBr **116-2** to generate Ni^{II} species **116-8**. This intermediate is then intercepted by radical **116-7** to form Ni^{III} complex **116-9**. The subsequent reductive elimination gives the desired product **116-3**.

In the same year, Buchwald, Jensen, and co-workers designed a microfluidic redox-neutral electrochemical cell and developed a series of reactions including α-amino C–H arylation, deboronative arylation, allylic C–H arylation, Minisci-type radical addition to heteroarenes, and Ni-catalyzed C–O coupling (Fig. 117).[314] The authors strategically implemented a flow cell with very narrow and variable interelectrode distance, which allowed them to overcome the intrinsic challenge of mass transport of reactive intermediates in convergent paired electrolysis.

In 2021, Liu and co-workers reported the use of paired electrolysis to achieve redox-neutral cross coupling reaction *via* nickel catalysis (Fig. 118).[315] The combination of anodic oxidation of potassium benzyl trifluoroborate and cathodic reduction of organonickel intermediates enables this transformation to proceed with a 93% yield for the model substrates. Control experiments also suggest that electricity is essential to the reactivity despite the redox-neutral nature of the transformation. The proposed mechanism differs from Hu's system in terms of the activation of Ni catalyst by the cathode (Fig. 118). The reaction is initiated by cathodic reduction of Ni^{II} precursor

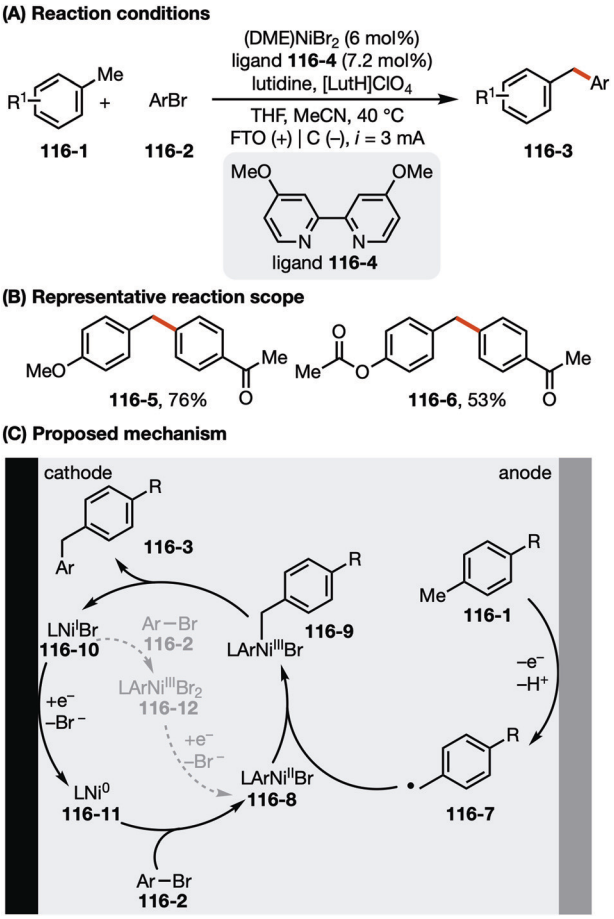


Fig. 116 (A–C) Electrochemical nickel-catalyzed direct arylation of benzylic C–H bonds.

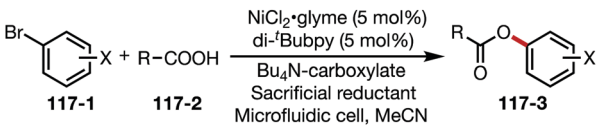


Fig. 117 Ni-Catalyzed C–O cross coupling *via* microfluidic cell.

to Ni^{I} complex **118-9**, which is followed by oxidative addition of **118-9** to **118-2** to form Ni^{III} complex **118-10**. This intermediate undergoes a second cathodic reduction to form **118-7**. At this point, anodically generated alkyl radical **118-6** adds to **118-7** followed by reductive elimination to furnish desired product **118-4** and turn over the Ni^{I} catalyst **118-9**. This transformation is also compatible with esters, nitriles, aldehydes, alkenes, amides, and N-heteroarenes.

In 2021, the Jiao group reported nickel-catalyzed oxygenation of sulfides and phosphines using water as the oxygen source.[316] The authors proposed that anodically generated O_2 and cathodically generated Ni^{0} react to form Ni^{II}-peroxo species, which delivers an oxygen atom to the substrate such as sulfides or triaryl phosphines. Notably, this transformation tolerates several other oxidatively sensitive functional groups such as aldehydes and pyridines (Fig. 119).

Published on 01 June 2021. Downloaded by University of Cambridge on 12/3/2022 1:39:05 PM.

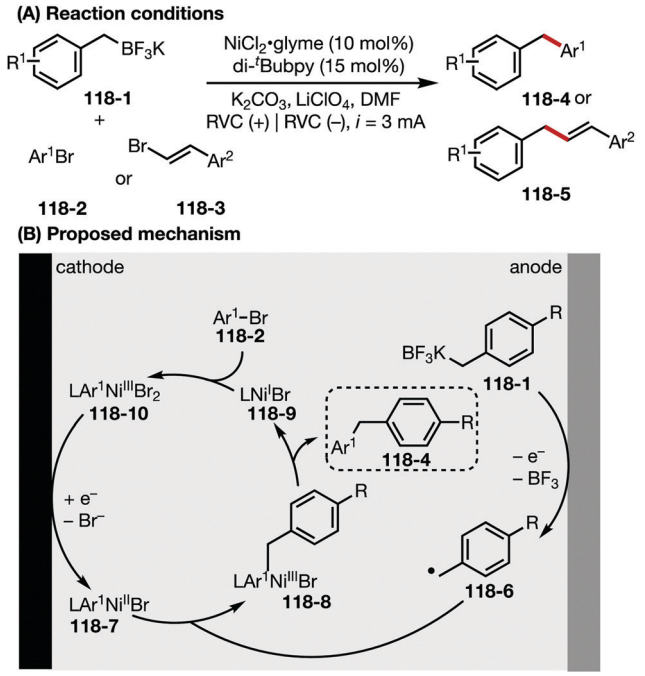


Fig. 118 (A and B) Nickel-catalyzed electrochemical cross-coupling reactions of benzyl trifluoroborate and organic halides.

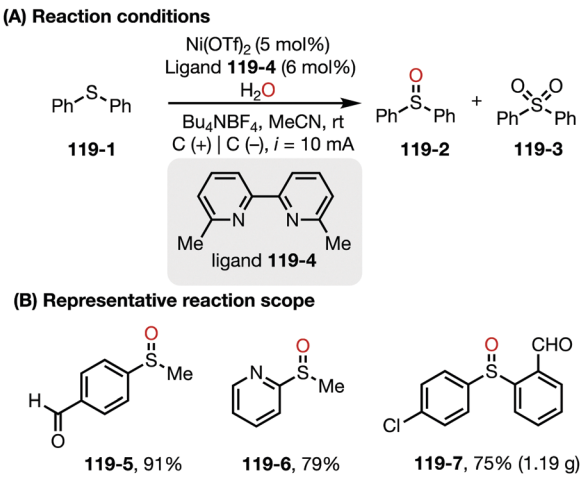


Fig. 119 (A and B) Electrochemically induced nickel catalysis for oxygenation reactions with water.

4.2. Other transformations

The Nonaka group demonstrated an early work on paired electrolytic synthesis of epoxides and dibromides in parallel (Fig. 120).[317] In this system, a divided cell is used with a dimensionally stable anode (DSA) and graphite cathode. In the anodic chamber, bromide anions were oxidized to form bromine which then reacts with alkenes to form dibromides; in the cathodic chamber, oxygen gas undergoes reduction to peroxides which then oxidize vanadyl(IV) acetylacetonate (**120-1**) to vanadyl(V) (**120-2**), which catalyzes alkene epoxidation. Several electron deficient olefins were demonstrated to be

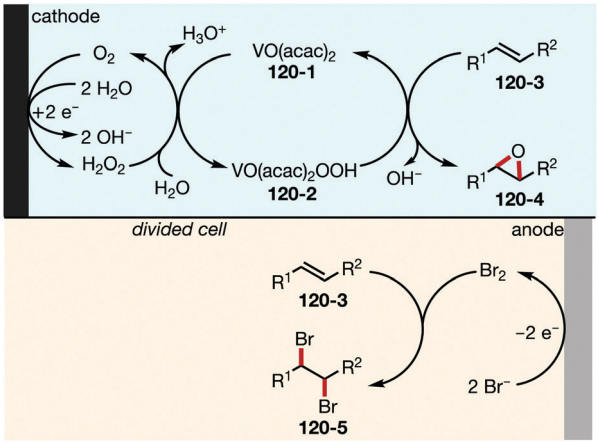


Fig. 120 Paired electrolysis of epoxide and dibromide synthesis.

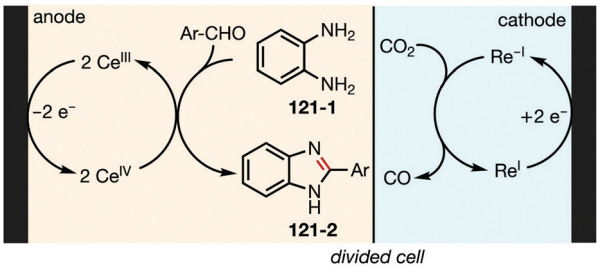


Fig. 121 Paired electrolysis of aldehyde condensation and carbon dioxide reduction.

suitable substrates and the current efficiency of the reaction could reach 132%.

In the recent years, the Moeller group also employed a divided cell design to pair anodic cerium-catalyzed condensation reaction and cathodic rhenium-catalyzed carbon dioxide reduction (Fig. 121).[318] Synthetically useful benzimidazole (**121-2**) and carbon monoxide were generated in the anodic and cathodic chambers respectively with high faradaic efficiency and in good yields.

Berlinguette and co-workers paired alcohol oxidation and Pd-catalyzed alkyne hydrogenation in a three-compartment cell system (Fig. 122).[319] Notably, the use of a Pd foam electrode enabled the two electrochemical process to be performed under two distinct conditions (aqueous and organic solvents) and high selectivity was achieved for both transformations. This protocol has also been used in the deuteration of unsaturated bonds.[320]

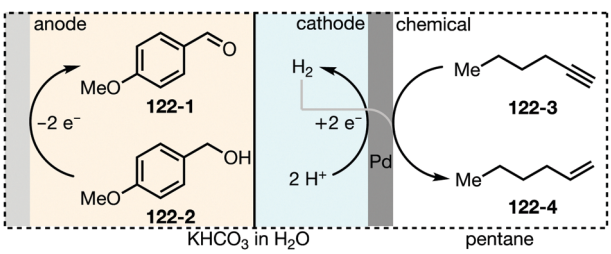


Fig. 122 Paired electrolysis of alcohol oxidation with Pd-mediated hydrogenation of alkynes.

This journal is © The Royal Society of Chemistry 2021

Published on 01 June 2021. Downloaded by University of Cambridge on 12/3/2022 1:39:05 PM.

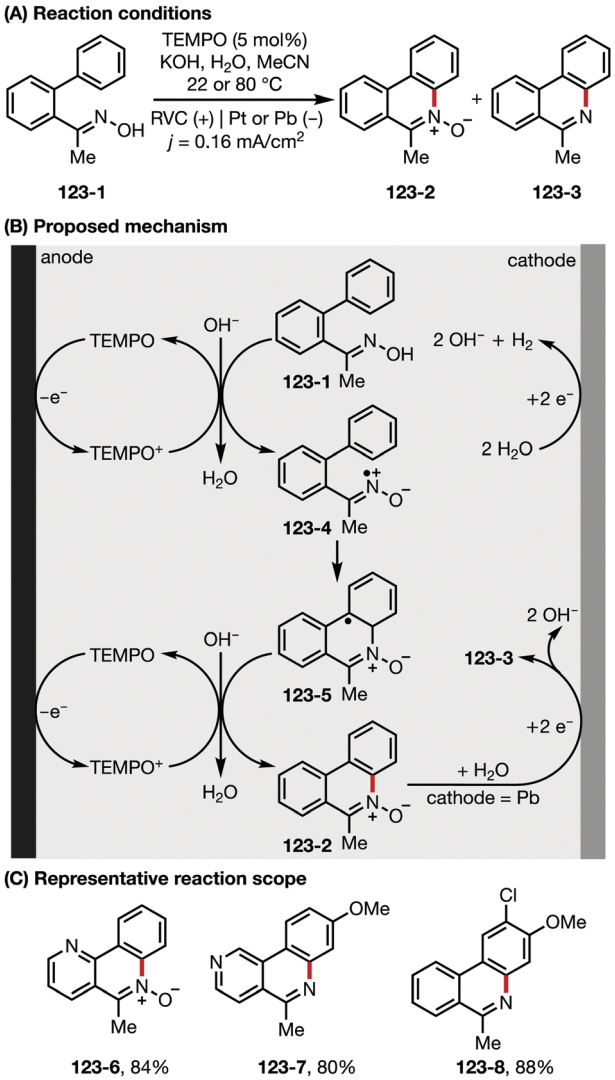


Fig. 123 (A–C) TEMPO-catalyzed aryl C-N bond construction.

In 2018, Xu and co-workers reported a TEMPO-catalyzed electrochemical C–N bond formation to synthesize polycyclic N-heteroarenes (Fig. 123).[321] In the first step, TEMPO was oxidized anodically to give TEMPO$^+$ which reacts with the oxime substrate (**123-1**) to afford iminoxyl radical intermediate (**123-4**). Upon radical cyclization to **123-5** and aromatization by one electron oxidation with TMEPO$^+$, *N*-oxide intermediate (**123-2**) was attained. Interestingly, the selectivity can be controlled by using different counter electrodes. When Pt is used as the cathode, hydrogenation become predominant and **123-2** is the final product. By introducing Pb cathode, which is known to suppress hydrogenation, cathodic cleavage of N–O bond is favored and give N-heteroarenes (**123-3**) as desired product.

5. Heterogeneous electrocatalysis

Electrodes are capable of intimately interacting with substrates during electron transfer events and can even exhibit catalytic properties themselves. Since the surface of an electrode does not fall under the same classification as the small-molecule mediators discussed in the previous sections, the role of the electrode in facilitating a specific transformation can be challenging to determine. When an electrode is used as a heterogenous catalyst, the catalytic nature of the electrode encompasses interactions of substrates and intermediates with the surface of electrode (adsorption and desorption), such as electrostatic forces, π-interactions, and chemical bonds.[322]

Such catalytic properties of electrodes have been considerably less explored in organic synthesis. In 2020, the editorial team of *ACS Catalysis* defined several features which define electrode as an electrocatalyst, such as improved TOF or product selectivity relative to alternative electrodes.[10] Some of the examples discussed in this section compare the different properties of carbon and platinum electrodes, while other examples highlight the use of electrodes modified with nanoparticles. This section does not intend to provide an exhaustive summary of developments in heterogenous electrocatalysis, but rather aims to bring attention of the community to this emerging area in the context of synthetic organic chemistry.

5.1. Carbon *versus* platinum electrodes

The differences between carbon and platinum anodes have been explored for oxidation of carboxylates (Fig. 124).[323,324] The initial step in this transformation is a single electron oxidation followed by decarboxylation. When platinum was used as anode, the resulting radical can desorb from the surface of the electrode and engage in a dimerization reaction. However, when carbon was used as anode, the intermediate radical is more strongly adsorbed, putatively through interaction with paramagnetic centers in the electrode, and a second electron can be removed generating a carbocation, which desorbs and reacts with nucleophiles present in the reaction.

These characteristics were employed by Moeller and co-workers during an anodic intramolecular cyclization of an enol-ether with an allyl-silane (Fig. 125).[325] When platinum

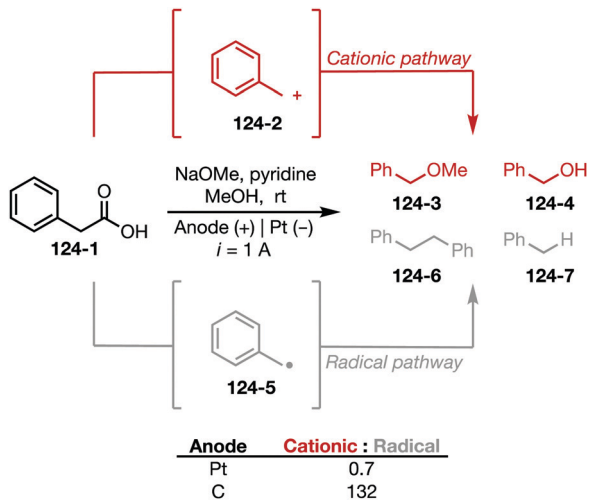


Fig. 124 Electrochemical decarboxylation of phenylacetic acid with different anode materials.

Published on 01 June 2021. Downloaded by University of Cambridge on 12/3/2022 1:39:05 PM.

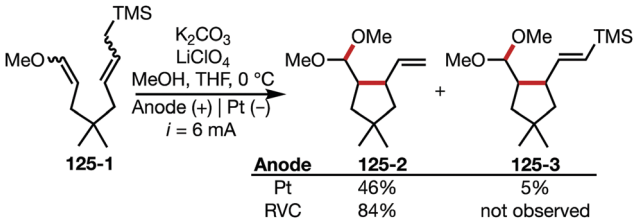


Fig. 125 Electrochemical cyclization with different anode materials.

was used as anode, a small amount of a vinyl-silane was identified, which indicated the intermediacy of a β-silyl radical. Changing the anode to RVC (reticulated vitreous carbon) allowed for this radical intermediate to be oxidized to a carbocation before desorption from the electrode surface, improving the yield of the desired product.

In 2021, Waldvogel and co-workers discussed how different carbon-based anodes can provide surprisingly disparate outcomes for the same reaction.[326] This arises from differences in morphology, the sp^2/sp^3 ratio of carbon, and manufacturing process for these materials. A remarkable recent example highlights the efficacy of different carbon anodes to promote radical or cationic mechanisms.[327] Han and co-workers demonstrated that upon anodic oxidation of hydroxamic acids, the resultant oxygen-centered radical can add to a styrene double bond, resulting in the formation of a benzylic radical (Fig. 126). If RVC is used as anode, this benzylic radical is oxidized to a carbocation, which engages in a Friedel–Crafts reaction. However, if carbon felt is used as anode the benzylic radical supposedly can desorb from the surface of the electrode and react with an *N*-oxyl radical, generating a bis-oxygenated product.

5.2. Modified electrodes

In 2019, Manthiram and co-workers explored the use of a carbon electrode coated with manganese oxide nanoparticles to promote epoxidation of alkenes (Fig. 127).[328] The authors propose the presence of a Mn^{IV}–oxo species as the epoxidation promoter. After the oxygen transfer step, the resulting Mn^{II} species would be converted back to Mn^{IV} after two anodic oxidation events. Remarkably, the oxygen transferred to the epoxide comes only from water, which is also responsible for providing protons for hydrogen evolution reaction occurring at the cathode.

On the reductive side of modified catalytic electrodes, Sun, Williard, Yu, and co-workers reported a cross-electrophile coupling promoted by a cathode coated with copper and palladium nanoparticles (CuPd NP; Fig. 128).[329] The systems containing these nanoparticles proved to be more selective than a Pd foil cathode or purely Pd nanoparticles. On the other hand, nanoparticles with a large excess of copper proved ineffective for the target transformation, highlighting the importance of the Pd/Cu ratio on the surface of electrode. The optimal CuPd NP could be recycled up to 5 times without loss in yield, and the morphology of the catalyst did not change. Although the mechanism of this transformation is not fully elucidated at this time, the authors propose an initial reduction of alkyl

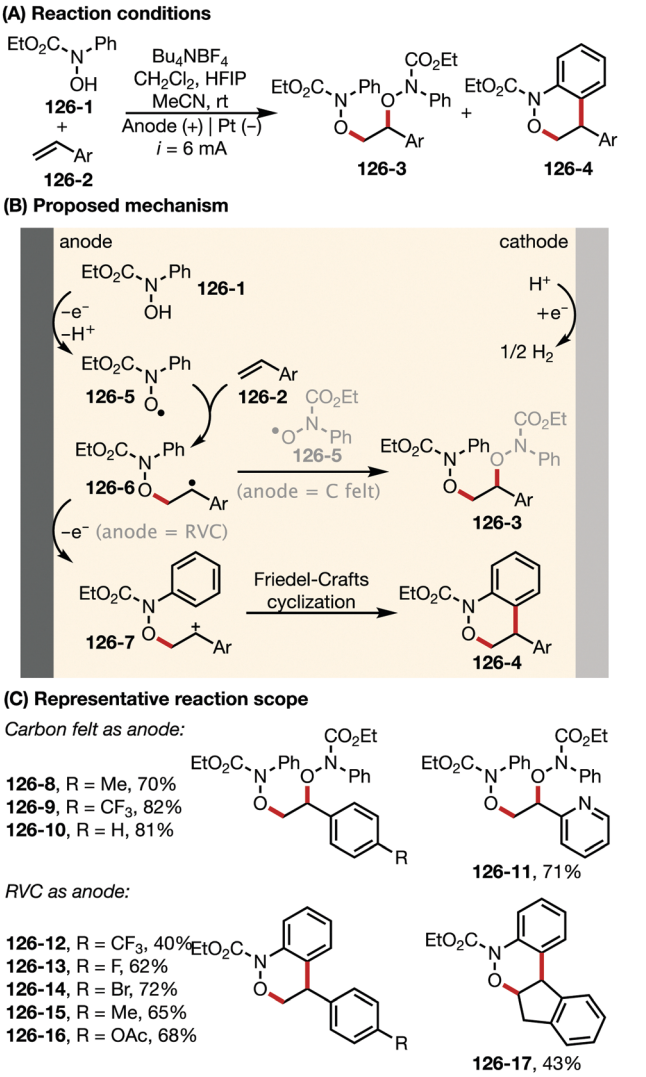


Fig. 126 (A–C) Electrochemical difunctionalization of alkenes with hydroxamic acid using different anode materials.

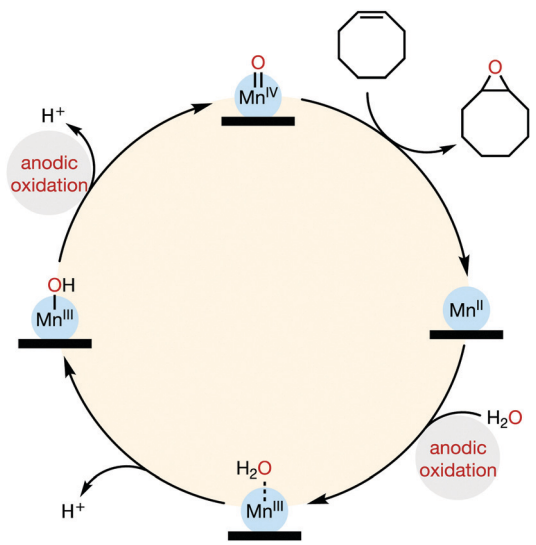


Fig. 127 Electrochemical epoxidation of alkenes with nanoparticles coated anode.

This journal is © The Royal Society of Chemistry 2021

Published on 01 June 2021. Downloaded by University of Cambridge on 12/3/2022 1:39:05 PM.

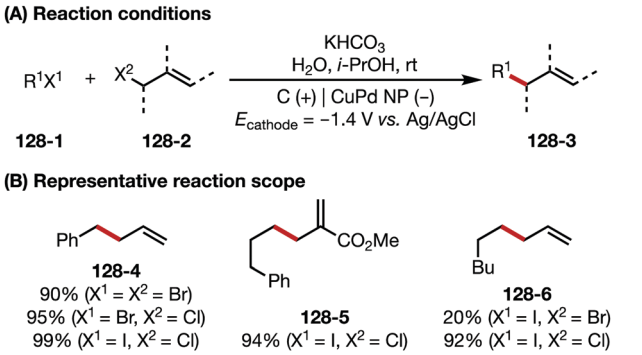


Fig. 128 (A and B) Electrochemical cross-electrophile coupling with nanoparticles coated cathode.

iodide, which is partially supported by the observation of dimer formation.

The possibility of recycling the catalyst with a simple washing procedure is an outstanding property of heterogeneous catalysts. The mechanism understanding usually requires investigation of the catalyst surface, employing a range of techniques, such as transmission electron microscopy (TEM), X-ray powder diffraction (XRD) and X-ray photoelectron spectroscopy (XPS). The field will certainly benefit from the more frequently collaborative interactions between materials scientists and organic chemists, and we foresee the development of new heterogeneous electrocatalysts for the construction of functional organic molecules as a growing area of research.

6. Bioelectrochemistry

Bioelectrocatalysis is an interdisciplinary field that aims to combine the merits of both biocatalysis and electrocatalysis for chemical synthesis. Bioelectrocatalytic methods utilize redox-active enzymes or electroactive microbial cells as catalysts to enable redox reactions. The advantages of bioelectrocatalysis include high activity, high selectivity, high atom efficiency, and mild reaction conditions. The past few years have seen an increasing number of applications of bioelectrocatalysis in the production of clean biofuels, degradable materials, and value-added chemicals.[330a]

Common bioelectrocatalysts include isolated oxidoreductases and electroactive microbial cells. Isolated oxidoreductases are frequently used in biosynthesis, and rapid advancements in protein engineering strategies such as directed evolution have allowed chemists to further optimize the reactivity of enzymes towards the desired organic transformations. Living electroactive microbials can also perform electron transfer and are used in bioelectrochemical systems. For microbial cell-based biocatalysis, diverse metabolic pathways enable microbial cells to catalyze many chemical reactions and produce a variety of products.

There are two general operating mechanisms of electron transfer between electrodes and bioelectrocatalysts: direct electron transfer (DET) and mediated electron transfer (MET). The following discussion of bioelectrocatalysis will focus on the applications of bioelectrocatalysis in the synthesis of fine chemicals and chiral organic products. More extensive reviews of bioelectrocatalysis are published recently.[330]

6.1. Direct electron transfer

DET processes involve the direct transfer of electrons from the electrode to the enzyme active site.[330a] For most oxidoreductases, these active sites are buried deep within the protein structures, thereby leading to slow electron transfer rate.[331] Additional challenges arise due to the difficulties associates with maintaining stability of the enzymes when they are within close proximity to the electrode surface. In light of these considerations, research efforts have focused on developing docking motifs to modify enzymes to promote efficient electron transfer. Some examples of docking motifs include nanoparticles that act as electron relay agents,[332] His-tag on the C or N-terminus of the enzyme to increase its binding affinity to the modified electrode surface,[333] and pyrene-modified linear poly(ethylenimine) (LPEI) that can immobilize oxidoreductases by cross-linking the enzyme and the multiwalled carbon nanotubes at the carbon electrode.[334] For example, in 2003, Willner and co-workers developed a strategy to enhance DET by reconstitution of apo-glucose oxidase with gold nanocrystals functionalized with a FAD coenzyme (Fig. 129).[332] The bioelectrocatalysis rate of the resulting "artificial" protein was enhanced significantly, as the gold nanoparticles served to efficiently wire the enzyme redox centers to the electrode.

6.2. Mediated electron transfer

6.2.1. Mediated electron transfer of free enzymes. Mediated electron transfer processes make use of small, diffusive redox mediators or redox polymers to serve as electron shuttles between the enzyme active site and the electrode surface. Some commonly used redox mediators include viologens, quinones, dyes, tetrathiafulvalene, and metal complexes such as ferrocenes.[330a] These mediators have been coupled with a variety of oxidoreductases to synthesize fine chemicals.

Electricity can be utilized to regenerate expensive cofactor NADH in enzyme-catalyzed reactions. In 2019, the Minteer group developed a bioelectrocatalytic N_2 fixation system using methyl viologen as the redox mediator (Fig. 130).[335] The N_2 fixation step is catalyzed by nitrogenase, and the resultant

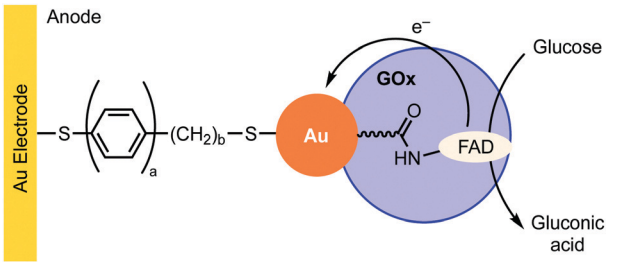


Fig. 129 Nanowiring of redox enzymes by a gold nanoparticle. a = 1 or 2, b = 0 or 1. FAD = flavin adenine dinucleotide, GOx = glucose oxidase. The author did not specify the role of the glassy carbon cathode.

Published on 01 June 2021. Downloaded by University of Cambridge on 12/3/2022 1:39:05 PM.

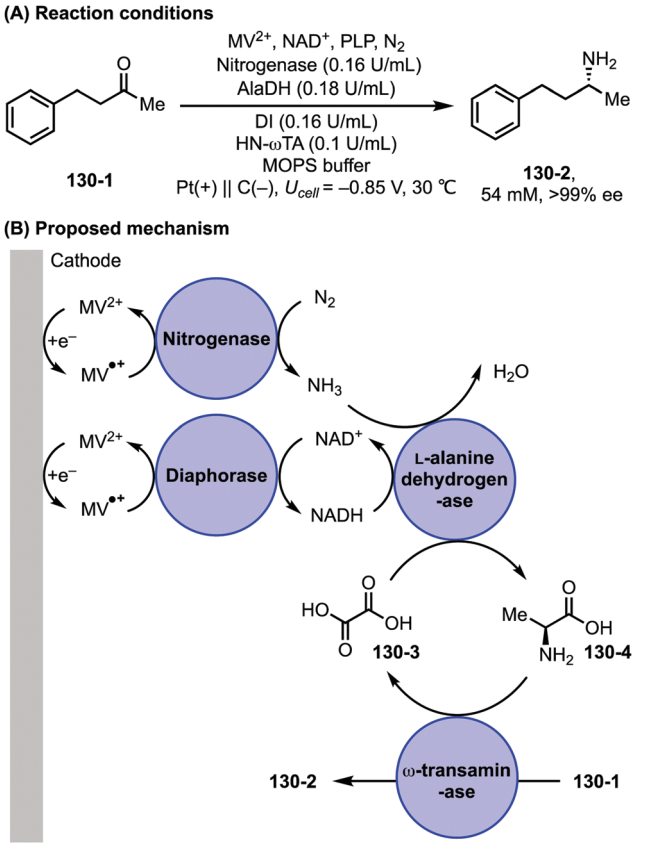


Fig. 130 (A and B) Bioelectrocatalytic N_2 fixation: from N_2 to chiral amine intermediates. The platinum anode generates protons and O_2 from water.

ammonia is further transformed into alanine (**130-4**) by L-alanine dehydrogenase with the consumption of oxalic acid (**130-3**) and NADH. Methyl viologen also facilitates the regeneration of cofactor NADH catalyzed by diaphorase. The alanine intermediate is utilized by ω-transaminase as amino-group donor to catalyze the amination of ketone substrate **130-1** to produce chiral amines **130-2** with up to 99% ee.

Neutral red is another common mediator and has been applied in the reduction of CO_2 to formic acid.[336] This reduction was catalyzed by formate dehydrogenase (FDH) which was immobilized on a graphite-based cathode.

Redox polymers can also be used to facilitate efficient electron transfer. In 2019, the Minteer group demonstrated that diaphorase immobilized in the three-dimensional network of cobaltocene-modified poly(allylamine) redox polymers (DH/Cc-PAA) can efficiently regenerate NADH, which is used by alcohol dehydrognenase to reduce aldehydes into alcohols (Fig. 131).[337] The polymer immobilization strategy allows the enzyme and redox mediators to be retained on the electrode surface after a reaction is completed, enabling these catalysts to be recycled and reused. The high efficiency, catalytic stability, and recyclability (91% of the maximum activity after five experimental cycles) renders this system among the most promising means of NADH regeneration developed heretofore.

On the basis of this pioneering work, in 2020, the Minteer group reported a biphasic bioelectrocatalytic system to synthesize

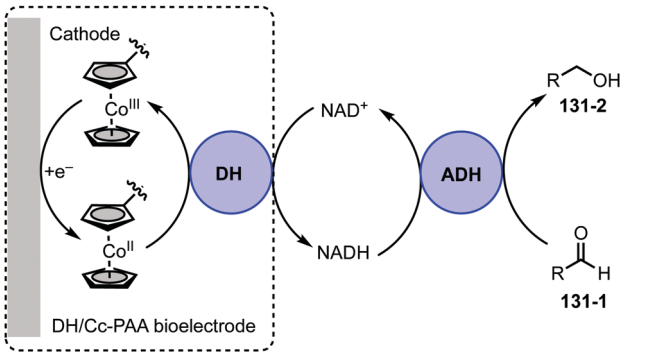


Fig. 131 NADH regeneration by a redox polymer-immobilized enzymatic system. DH = diaphorase, ADH = alcohol dehydrogenase. The platinum-wire anode generates O2 from water.

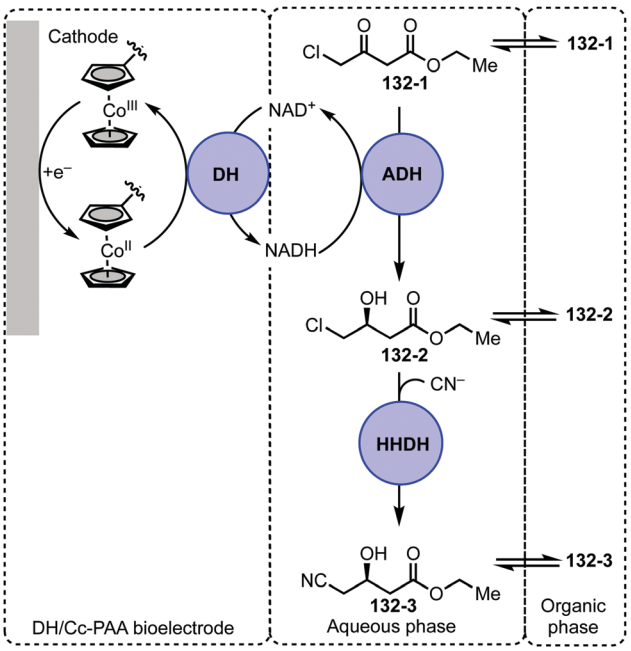


Fig. 132 Biphasic bioelectrocatalytic synthesis of chiral β-hydroxy nitriles. DH = diaphorase, ADH = alcohol dehydrogenase HHDH = halohydrin dehalogenase. A platinum mesh serves as the anode. The authors do not specify the anodic reaction.

chiral β-hydroxy nitriles from ethyl 4-chloroacetate using the DH/Cc-PAA bioelectrode (Fig. 132).[338] Powered by electrogenerated NADH, ADH catalyzed the asymmetric reduction of **132-1** to generate ethyl (S)-4-chloro-3-hydroxy-butanoate **132-2** in high enantioselectivity. Next, **132-2** was converted to **132-3** through nucleophilic substitution catalyzed by HHDH. The biphasic system ensures that the ester substrate, intermediate and product predominantly reside in the organic phase, thus suppressing their hydrolysis in the aqueous phase. At the same time, the biphasic system minimizes the inhibition of HHDH activity by the substrate **132-1**, enabling the two-step enzymatic synthesis to proceed smoothly.

With advancements in protein engineering technologies, the catalytic properties of oxidoreductases can be tuned and

 This journal is © The Royal Society of Chemistry 2021

Published on 01 June 2021. Downloaded by University of Cambridge on 12/3/2022 1:39:05 PM.

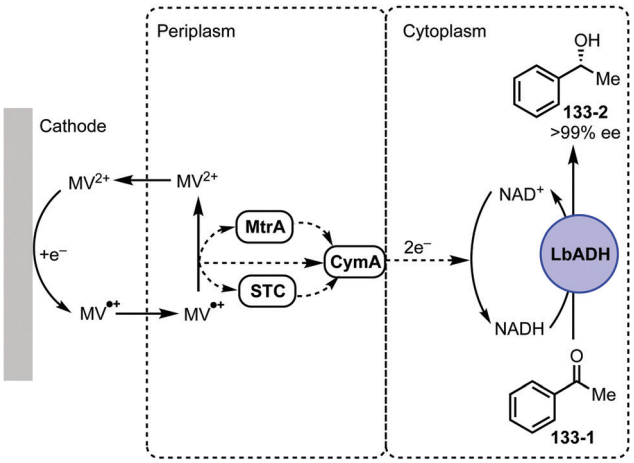


Fig. 133 Resting *E. coli* as a chassis for microbial electrosynthesis: production of chiral alcohols. MtrA, STC and CymA: proteins of the electron transfer pathway in *Shewanella oneidensis*. MR-1, LbADH: An alcohol dehydrogenase from *Lactobacillus brevis*. The graphite anode generates O_2 from water.

enhanced to meet the requirements of synthetic transformations. Directed evolution, for example, has been used to modify the redox potentials of certain enzymes to increase the power output of biofuel cells.[339]

6.2.2. Mediated electron transfer of electroactive microbial cells. Electroactive microbial cells can also act as bioelectrocatalysts. However, because the cell membrane layers of microbes are typically not conductive, extracellular electron transfer rates are slow. Recent research efforts have been directed towards overcoming this challenge using membrane-transmissible mediators.[340] Another strategy to overcome this challenge involves the combination of electrochemical technology with metabolic engineering of cells. A creative strategy to construct an engineered strain is the introduction of an electron pathway to establish electrochemical communication between the bacterial cells and electrode. Sturm-Richter and co-workers developed a protocol to heterologously express c-type cytochromes CymA, MtrA and STC from *S. oneidensis* in an *E. coli* cell to construct an electron transport chain (Fig. 133).[341] The presence of an electron transport chain accelerates the electron transfer efficiency by 183%. Based on this work, Mayr and co-workers integrated an NADPH-dependent alcohol dehydrogenase from *L. brevis* into this engineered *E. coli* platform to perform the asymmetric reduction of acetophenone to (*R*)-1-phenylethanol **133-2**.[342] Methyl viologen acts as the redox mediator that facilitates the electron transfer in the periplasm.

7. Electrophotocatalysis

Electrophotochemistry is a strategy that combines electrochemistry's ability to generate reactive intermediates with photochemistry's ability to access excited state intermediates. The synergistic combination has been applied to creatively solve challenging problems in organic synthesis. In 1970, Moutet and Reverdy first proposed electrophotochemistry as a concept in the context of photoexcitation of electrochemically generated phenothiazine radical cations.[343] In a similar pioneering work in 1985, Rusling demonstrated that the reduction of 4-chlorobiphenyl could be promoted by a super reductant in the form of photoexcited, electrochemically generated anthracene radical anion.[344] In the following section, we discuss recent developments in electrophotocatalysis wherein redox-active catalytic species participate in both electrochemical and photochemical activation events to achieve desired transformations. These examples are grouped into two major categories depending on whether the electrochemical steps are coupled to or decoupled from photochemical steps. For additional information outside of what is discussed in this section, we refer the reader to recent reviews or primary research articles on electrophotocatalysis.[345,346]

7.1. Replacing external oxidant or reductant

Electrophotocatalysis is an excellent strategy for accessing highly reactive intermediates in a selective and controlled fashion. A typical electrophotocatalytic process entails photochemical and electrochemical steps that function in tandem to activate a single catalytic species, thus giving rise to a highly reactive photoexcited catalyst or radical species without using a terminal oxidant or reductant.

In 2019, Lin *et al.* employed electophotocatalysis for the oxidation of alcohols using riboflavin tetraacetate (RFT) and thiourea catalysts (Fig. 134).[347] In the catalytic cycle, the RFT catalyst is first photoexcited to RFT* and subsequently reacts with thiourea **134-3** to generate semiquinone form RFT$^{\bullet}$-H and thiyl radical **134-4**. This thiyl radical then undergoes hydrogen atom transfer (HAT) with the alcohol substrate (**134-1**) followed by reaction of resultant intermediate **134-5** with RFT$^{\bullet}$-H to complete both catalytic cycles and yield the carbonyl product (**134-2**). Finally, RFT-H_2 is turned over at the anode, completing the catalytic cycle. Notably, the need for a sacrificial oxidant (*i.e.*, O_2) is replaced by anodic oxidation, which avoids the oxidant-induced degradation of thiourea cocatalyst and lead to critical expansion of the scope of flavin-catalyzed alcohol oxidation to include challenging unactivated aliphatic alcohols.

The generation of alkyl radicals from alkanes is challenging due to the high BDE of unactivated C(sp^3)–H bonds (98.5 kcal mol^{-1} for methylene groups).[96] In 2020, Xu and co-workers addressed this challenge *via* the electrophotochemical generation of chlorine radicals,[348] which can abstract unactivated hydrogen atoms and generate HCl (BDE = 102 kcal mol^{-1}). The resultant alkyl radicals then engage in a Minisci-type reaction to construct C2- and C4-alkylated quinolines and pyridines (Fig. 135). This method also used chlorine radicals to perform HAT of activated C–H bonds at benzylic positions and positions α to heteroatoms. In separate works, the Xu group has also explored Minisci-type reactivity through electrophotochemically generated radicals from carboxylic acids[349] and potassium trifluoroborate salts.[350]

In 2021, Ackermann group used an acridinium-based photocatalyst Mes-Acr$^+$ to achieve the electrophotocatalytic C–H trifluoromethylation of arenes (Fig. 136).[351] Anodic oxidation and subsequent irradiation of the Mes-Acr$^+$ generates its oxidized

Published on 01 June 2021. Downloaded by University of Cambridge on 12/3/2022 1:39:05 PM.

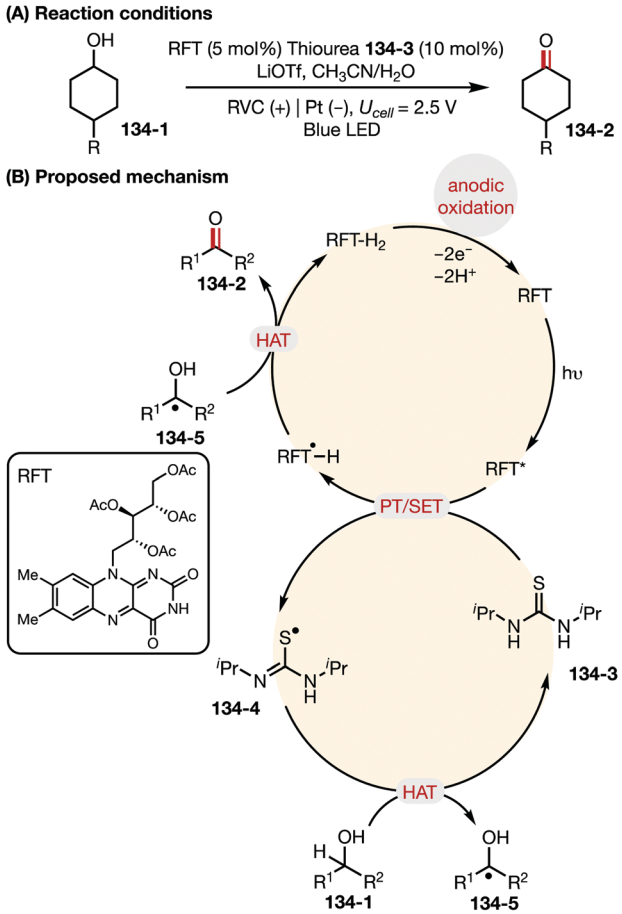


Fig. 134 (A–C) Electrophotochemical oxidation of alcohols mediated by riboflavin tetraacetate.

excited state Mes-Acr^{+}*. Single electron transfer between Mes-Acr^{+}* and the sulfinate anion generates acridinyl radical and $CF_3^{\bullet}$, the latter of which is trapped by the arene substrate, leading to final product **136-2**. The reduced form of photocatalyst Mes-Acr$^{\bullet}$ is turned over anodically without the use of a chemical oxidant.

In 2021, Ravelli group adopted an electrophotocatalytic approach to achieve dehydrogenative functionalization of benzothiazoles with simple alkanes.[352] Electrochemistry is utilized to turnover photocatalyst tetra-*n*-butylammonium decatungstate (TBADT), which undergoes photo-induced HAT with simple alkanes (*e.g.*, **137-2**) to generate alkyl radical intermediates (TBADT is designated as W in Fig. 137).

7.2. Accessing extremely oxidizing or reducing potentials

Another prominent application of electrophotocatalysis is the generation of super oxidants and reductants by means of tandem electro- and photochemical activation.

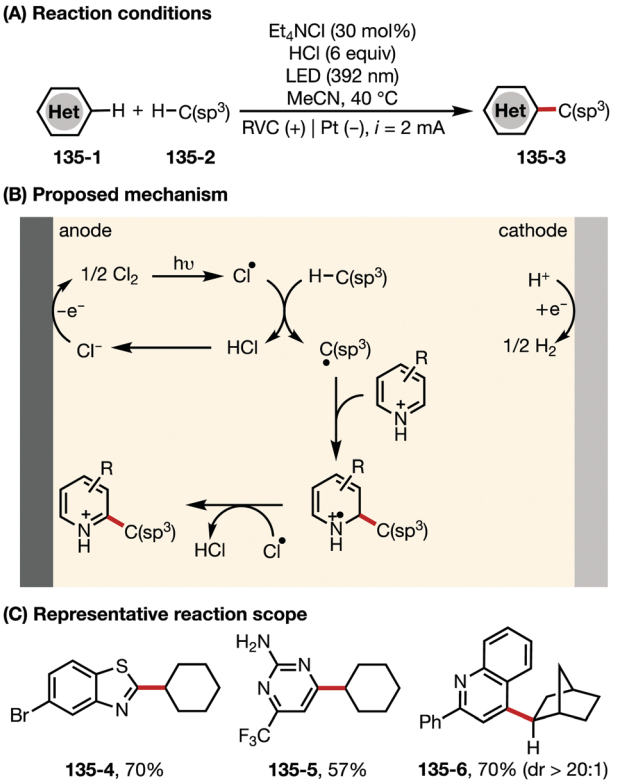


Fig. 135 (A–C) Electrophotochemical alkylation of heteroarenes mediated by chloride.

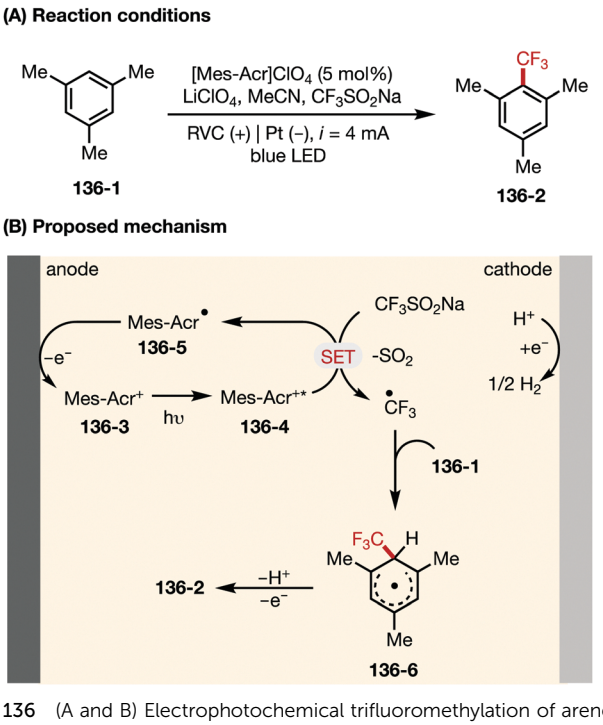


Fig. 136 (A and B) Electrophotochemical trifluoromethylation of arenes.

In 2019, Lambert and co-workers employed a trisaminocyclopropenium cation (TAC^{+}) as an electrophotocatalyst to

 This journal is © The Royal Society of Chemistry 2021

Published on 01 June 2021. Downloaded by University of Cambridge on 12/3/2022 1:39:05 PM.

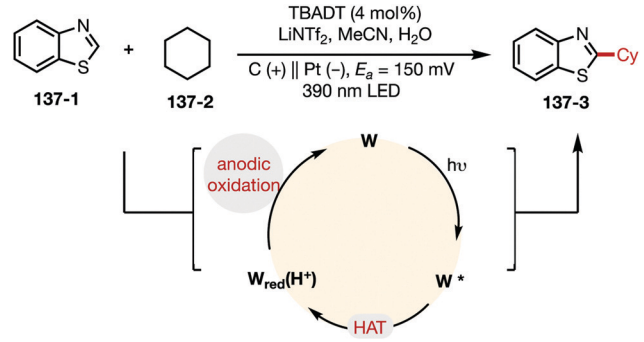


Fig. 137 Electrophotochemical alkylation of benzothiazole.

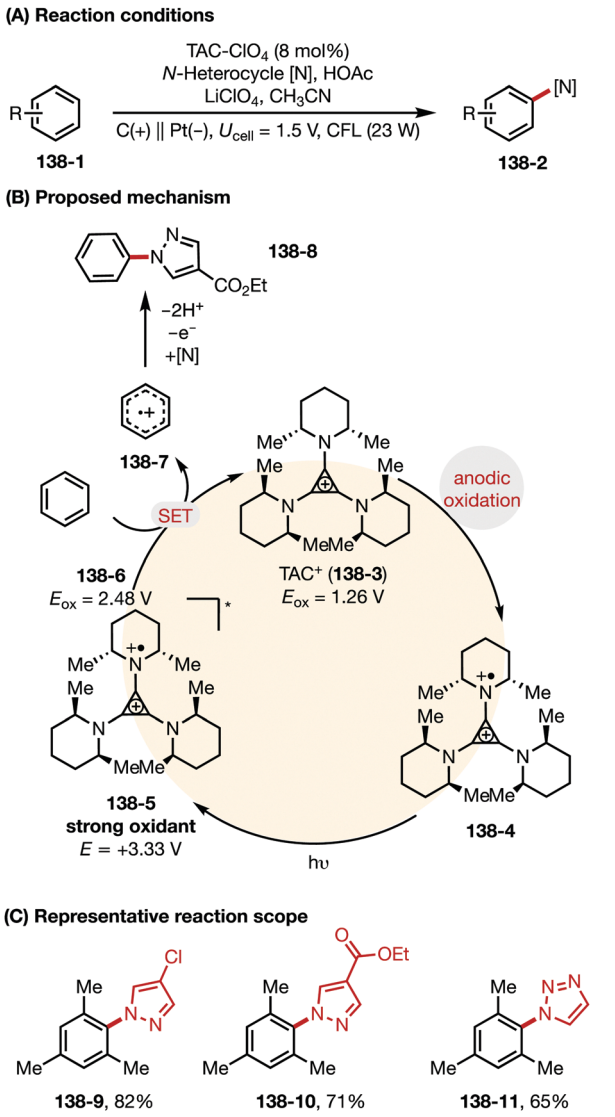


Fig. 138 (A–C) Electrophotochemical coupling of arenes with azoles mediated by trisaminocyclopropenium cation.

oxidize benzene toward C–H amination with azoles (Fig. 138).[353] In this work, TAC^{+} is first oxidized on the electrode to the radical dication TAC^{2+}. This oxidation is then followed by visible light photoexcitation to generate the highly oxidizing species $TAC^{2+}*$ ($E \approx 3.3$ V). $TAC^{2+}*$ is capable of oxidizing simple arenes to their corresponding radical cations, which are then trapped by an azole to deliver the coupled product. In 2020, this strategy was also applied to the TAC^{+}-catalyzed oxidative C–H functionalization of ethers and DDQ-catalyzed nucleophilic aromatic substitution.[354,355]

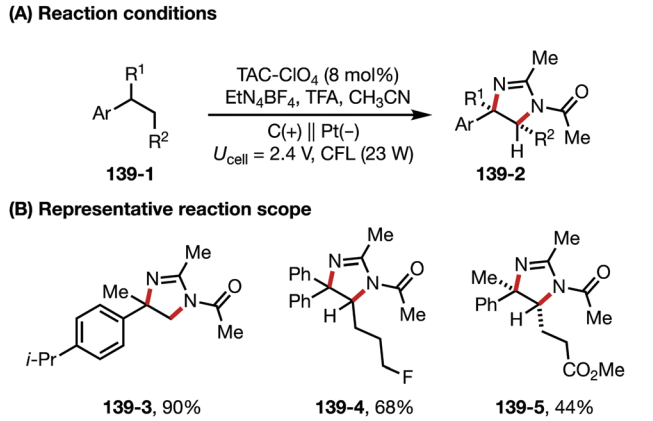


Fig. 139 Electrophotocatalytic deamination of vicinal C–H bonds.

In 2021, Lambert's group reported the diamination of alkanes using the same electrophotocatalytic strategy (Fig. 139).[356] Alkane substrates with a benzylic C–H bond (**139-1**) can be converted into 3,4-dihydroimidazoles (**139-2**), which can then be transformed to valuable vicinal diamines in a subsequent chemical reaction without purification of the intermediates. The author proposed that a key step involves the oxidation of substrates by the highly oxidizing radical dication TAC^{2+}.

In the same year, Barham and co-workers demonstrated that electrophotocatalyst (trisbiaryl)aminium radical cation (*e.g.*, TdCBPA radical cation) can oxidatively activate C–H bonds of arenes (Fig. 140).[357] The authors proposed that the pre-complexation between the catalyst and the arene substrate *via* π-stacking is key to achieving this challenging transformation.

In 2020, Lambert and Lin extended this strategy to access highly reducing electrophotocatalysts.[358] Specifically, dicyanoanthracene (DCA) was used as an electrophotocatalyst to achieve the functionalization of aryl halides (Fig. 141). DCA is first reduced on the cathode prior to photoexcitation to furnish

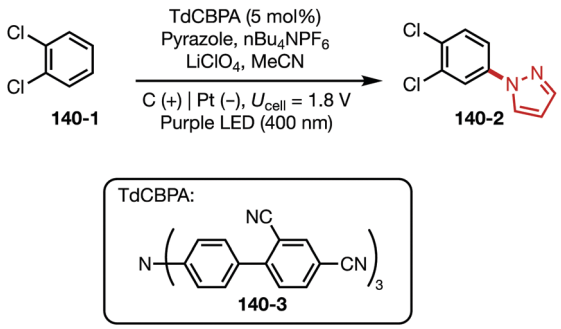


Fig. 140 Electrophotocatalytic azolation of arenes. TdCBPA = tris(2′,4;-dicyano-[1,1′-biphenyl]-4-yl)amine.

Published on 01 June 2021. Downloaded by University of Cambridge on 12/3/2022 1:39:05 PM.

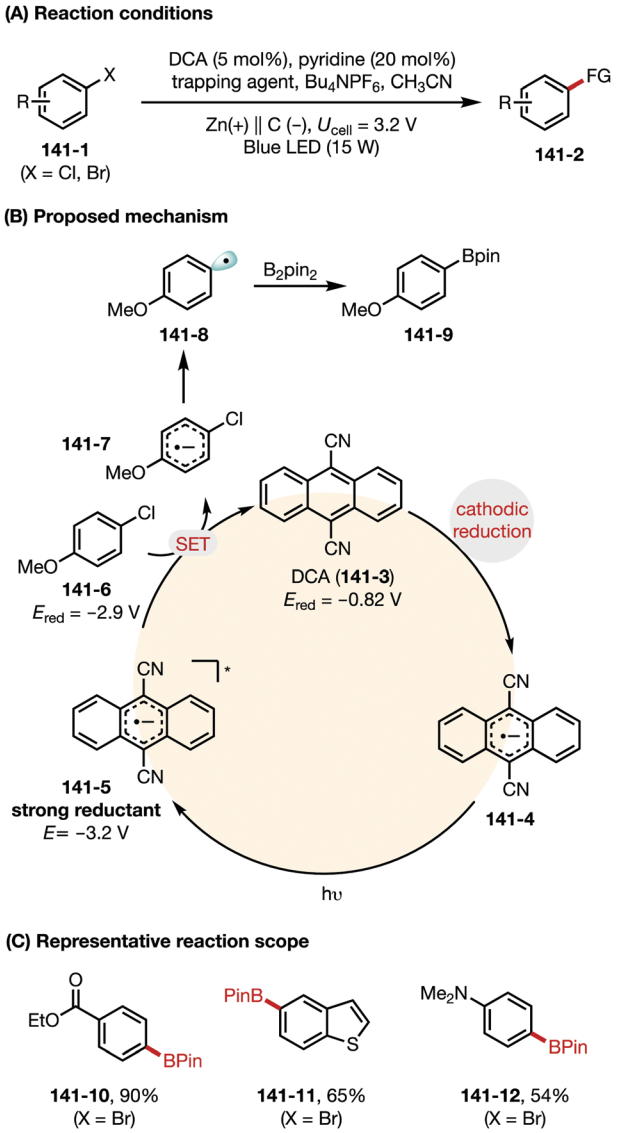


Fig. 141 (A–C) Electrophotochemical reduction of aryl halides mediated by dicyanoanthracene.

a highly reducing excited-state radical anion **141-5** ($E_{red} \approx -3.2$ V *vs.* SCE) with a sufficient lifetime to undergo subsequent electron transfer (~13.5 ns).[359] This species is potent enough to reduce electron-rich aromatic substrates such as 1-chloro-4-methoxybenzene ($E_{red} = -2.9$ V *vs.* SCE)[360] to the corresponding radical anion, which further proceeds to deliver the product **141-9** in good yields.

Concurrently, Wickens reported a similar electrophotocatalytic strategy employing naphthalene-based imide (NpMI) to promote reduction of aryl halides (Fig. 142).[361] The photoexcited radical anion of NpMI was estimated to have a reducing potential similar to Na (−2.9 V *vs.* SCE) and Li (−3.3 V *vs.* SCE). Cathodic reduction of the substrate and subsequent fragmentation of the incipient radical anion generates an aryl radical, which can undergo phosphorylation and heteroarylation upon radical trapping.

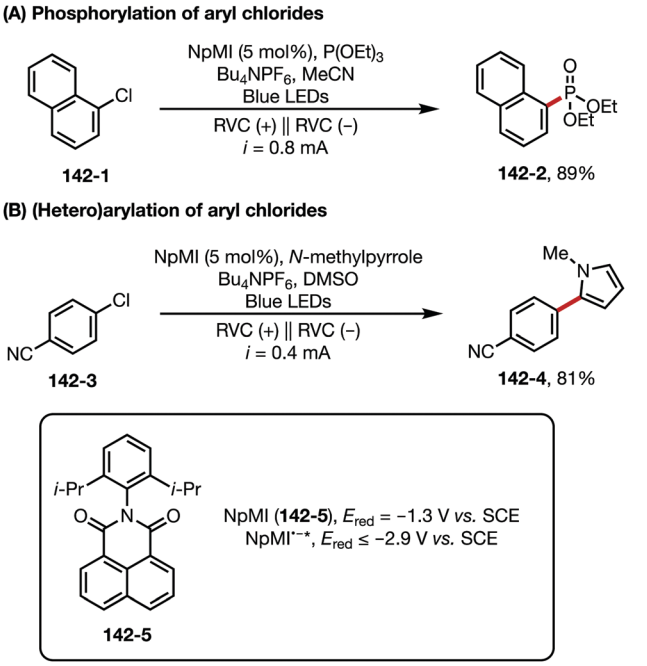


Fig. 142 (A and B) Electrophotochemical reduction of aryl halides mediated by naphthalene-based imide.

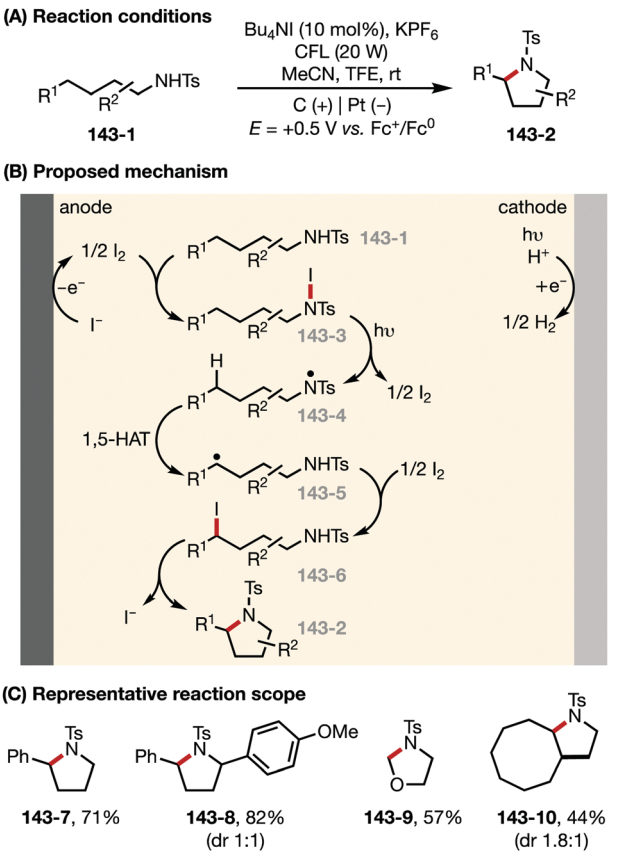


Fig. 143 (A–C) Electrophotochemical synthesis of pyrrolidines mediated by iodide. CFL = compact fluorescent lamp.

This journal is © The Royal Society of Chemistry 2021

Published on 01 June 2021. Downloaded by University of Cambridge on 12/3/2022 1:39:05 PM.

These examples showcase the highly biased redox potentials enabled by electrophotocatalysis. Recent developments in this area continue to illustrate the capacity of electrophotocatalysis to enable organic transformations at these extreme potentials, thereby expanding the toolbox of synthetic chemists.

7.3. Decoupled electrophotocatalysis

Unlike typical electrophotocatalytic systems described in this section, electrochemistry and photoexcitation can also be simultaneously harnessed to activate two discrete reactive species in nonconsecutive steps of the same reaction pathway toward the desired transformation. This type of systems is referred as decoupled electrophotocatalysis.[362]

In 2019, Stahl and co-workers demonstrated the use of anodically generated iodine for the intramolecular C–H amination (Fig. 143).[363] The proposed mechanism involves the generation of a nitrogen-centered radical from visible light promoted homolytic cleavage of a weak N–I bond in key intermediate **143-3**, which is formed from substrate **143-1** and electrogenerated I_2. A 1,5-hydrogen atom transfer process leads to the activation of an inert C–H bond in a regioselective fashion, which is followed by capture of the resultant C-centered radical **143-5** with I_2 to form a C–I bond (**143-6**). Subsequently, an intramolecular S_N2 reaction constructs a C–N bond to furnish cyclized *N*-tosyl amine **143-2**. This overall sequence was employed for the preparation of substituted pyrrolidines, oxazolines, and vicinal amino alcohols.

8. Concluding remarks and future directions

The past ten years have brought significant growth and attention towards applications of electrocatalysis in organic synthesis. Such advancements have been prompted by increased recognition of electrochemistry's ability to harness electrical current as an "imaginary" reagent to facilitate a range of single-electron oxidation and reduction events. The developments highlighted in this review demonstrate how this ability is further augmented by the introduction of electrocatalysts which serve to increase the selectivity and efficiency of electrochemically powered methodologies. Electrocatalysis has proven to be a viable pathway for accessing highly reactive radical intermediates from abundant starting materials, as well as for regulating their downstream reactivity to enable complex transformations in a single step. To date, electrocatalysis has expanded the scope of many staple reactivities such as C–C and C–X bond formation, alkene functionalization, and C–H activation, often under mild conditions.

Even with these advancements, we expect that electrocatalysis will continue to expand into new chemical spaces to address pressing challenges of efficiency and sustainability encountered in synthesis. From the perspective of this review, we see several emerging research directions amidst the renaissance of synthetic electrocatalysis, listed as follows:

(a) Application of electrocatalytic methods for the late-stage modification of complex bioactive molecules and bioorthogonal functionalization of biomacromolecules.

(b) Exploration of electroreductive strategies which allow access to deeply reducing potentials needed for challenging reductive transformations.

(c) Development of paired electrolysis systems enabling highly efficient transformations through simultaneous and synergistic use of anodic and cathodic redox events.

(d) Expansion of electrocatalysis into interdisciplinary areas such as electrophotocatalysis and bioelectrocatalysis to leverage the unique abilities of these systems.

(e) Application of heterogenous electrocatalysis and employment of modern characterization techniques to understand and rationally design catalytic electrodes.

Altogether, electrocatalysis has developed into a powerful enabling technology in the field of organic synthesis. The diversity of new synthetic transformations enabled by electrochemistry can be attributed to the myriad optimization parameters of electrochemical systems (applied potential, current, electrode material, electrolyte, cell type, *etc.*), all of which can be used to intimately and selectively influence chemical reactivity. We anticipate that future developments in the field of electrocatalysis will power the discovery of new reaction strategies needed to solve key challenges in contemporary organic synthesis.

Author contributions

All authors contributed to writing and editing the manuscript. L. F. T. N., J. L., Y. S., and L. L. contributed equally and are listed in the order of the sections that they wrote.

Conflicts of interest

There are no conflicts to declare.

Acknowledgements

Financial support was provided by NIGMS (R01GM130928). S. L. thank the Research Corporation of Science Advancements for a Cottrell Scholar Award. L. F. T. N. thank The Brazilian National Council for Scientific and Technological Development for a CNPq Postdoctoral Fellowship.

Notes and references

1 H. Lund, *J. Electrochem. Soc.*, 2002, **149**, S21–S33.
2 S. R. Waldvogel and B. Janza, *Angew. Chem., Int. Ed.*, 2014, **53**, 7122–7123.
3 K. S. McClymont, F.-Y. Wang, A. Minakar and P. S. Baran, *J. Am. Chem. Soc.*, 2020, **142**, 8608–8613.
4 D. H. Evans, *Chem. Rev.*, 2008, **108**, 2113–2144.
5 K. D. Moeller, *Chem. Rev.*, 2018, **118**, 4817–4833.
6 R. Franckle and R. D. Little, *Chem. Soc. Rev.*, 2014, **43**, 2492–2521.
7 K. Lee, N. Elgrishi, B. Kandemir and J. L. Dempsey., *Nat. Rev. Chem.*, 2017, **1**, 0039.

Published on 01 June 2021. Downloaded by University of Cambridge on 12/3/2022 1:39:05 PM.

8 M. N. Jackson and Y. Surendranath, *Acc. Chem. Res.*, 2019, **52**, 3432–3441.
9 J. M. Saveant, *Chem. Rev.*, 2008, **108**, 2348–2378.
10 A. Dey, T. Brent Gunnoe and V. R. Stamenkovic, *ACS Catal.*, 2020, **10**, 13156–13158.
11 We note that the IUPAC definition of ''electrocatalysis'' states that ''[e]lectrocatalysis is an electrochemical reaction that takes advantage of a catalyst.'' We interpret this as inclusive of both molecular and surface catalysts, which is consistent with the definition of electrocatalysis used in this review. See: https://iupac.org/materialschemistryedu/energy/photocatalysis/.
12 M. D. Kärkäs, O. Verho, E. V. Johnston and B. Åkermark, *Chem. Rev.*, 2014, **114**, 11863–12001.
13 M. Shao, Q. Chang, J.-P. Dodelet and R. Chenitz, *Chem. Rev.*, 2016, **116**, 3594–3657.
14 A. M. Appel, J. E. Bercaw, A. B. Bocarsly, H. Dobbek, D. L. Dubois, M. Dupuis, J. G. Ferry, E. Fujita, R. Hille, P. J. A. Kenis, C. A. Kerfeld, R. H. Morris, C. H. F. Peden, A. R. Portis, S. W. Ragsdale, T. B. Rauchfuss, J. N. H. Reek, L. C. Seefeldt, R. K. Thauer and G. L. Waldrop, *Chem. Rev.*, 2013, **113**, 6621–6658.
15 E. J. Horn, B. R. Rosen and P. S. Baran, *ACS Cent. Sci.*, 2016, **2**, 302–308.
16 J. C. Siu, N. Fu and S. Lin, *Acc. Chem. Res.*, 2020, **53**, 547–560.
17 G. Hilt, *ChemElectroChem*, 2020, **7**, 395–405.
18 C. Schotten, T. P. Nicholls, R. A. Bourne, N. Kapur, B. N. Nguyen and C. E. Willans, *Green Chem.*, 2020, **22**, 3358–3375.
19 C. Kingston, M. D. Palkowitz, Y. Takahira, J. C. Vantourout, B. K. Peters, Y. Kawamata and P. S. Baran, *Acc. Chem. Res.*, 2020, **53**, 72–83.
20 J. E. Steves and S. S. Stahl, *J. Am. Chem. Soc.*, 2013, **135**, 15742–15745.
21 J. Zhao, T. Nanjo, E. C. de Lucca Jr and M. C. White, *Nat. Chem.*, 2019, **11**, 213–221.
22 M. C. Bryan, P. J. Dunn, D. Entwistle, F. Gallou, S. G. Koenig, J. D. Hayler, M. R. Hickey, S. Hughes, M. E. Kopach, G. Moine, P. Richardson, F. Roschangar, A. Steven and F. J. Weiberth, *Green Chem.*, 2018, **20**, 5082–5103.
23 A. Medici, P. Pedrini, A. Battisti, G. Fantin, M. Fogagnolo and A. Guerrini, *Steroids*, 2001, **66**, 63–69.
24 T. Maki, S. Iikawa, G. Mogami, H. Harasawa, Y. Matsumura and O. Onomura, *Chem. – Eur. J.*, 2009, **15**, 5364–5370.
25 S. Liang, C.-C. Zeng, X.-G. Luo, F.-Z. Ren, H.-Y. Tian, B.-G. Sun and R. D. Little, *Green Chem.*, 2016, **18**, 2222–2230.
26 S. Doobary, A. T. Sedikides, H. P. Caldora, D. L. Poole and A. J. J. Lennox, *Angew. Chem., Int. Ed.*, 2020, **59**, 1155–1160.
27 A. N. Vereshchagin, M. N. Elinson, E. O. Dorofeeva, D. V. Demchuk, I. S. Bushmarinov, A. S. Goloveshkin and G. I. Nikishin, *Tetrahedron*, 2013, **69**, 5234–5241.
28 A. N. Vereshchagin, M. N. Elinson, E. O. Dorofeeva, R. F. Nasybullin, I. S. Bushmarinovb, A. S. Goloveshkinb and M. P. Egorov, *Electrochim. Acta*, 2015, **165**, 116–121.
29 M. Okimoto, H. Yamamori, K. Ohashi, M. Hoshi and T. Yoshida, *Synlett*, 2013, 1568–1572.
30 M. N. Elinson, E. O. Dorofeeva, A. N. Vereshchagin, R. F. Nasybullin and M. P. Egorov, *Catal. Sci. Technol.*, 2015, **5**, 2384–2387.
31 L. Chen, L. M. Barton, J. C. Vantourout, Y. Xu, C. Chu, E. C. Johnson, J. J. Sabatini and P. S. Baran, *Org. Process Res. Dev.*, DOI: 10.1021/acs.oprd.0c00270.
32 M. Okimoto, H. Yamamori, K. Ohashi, S. Nishikawa, M. Hoshi and T. Yoshida, *Synlett*, 2012, 2544–2548.
33 D. Minato, S. Mizuta, M. Kuriyama, Y. Matsumura and O. Onomura, *Tetrahedron*, 2009, **65**, 9742–9748.
34 C. Yao, Y. Wang, T. Li, C. Yu, L. Li and C. Wang, *Tetrahedron*, 2013, **69**, 10593–10597.
35 M. N. Elinson, A. S. Dorofeev, S. K. Feducovich, P. A. Belyakov and G. I. Nikishin, *Eur. J. Org. Chem.*, 2007, 3023–3027.
36 H. Gao, Z. Zha, Z. Zhang, H. Ma and Z. Wang, *Chem. Commun.*, 2014, **50**, 5034–5036.
37 S. Liang, C.-C. Zeng, H.-Y. Tian, B.-G. Sun, X.-G. Luo and F.-Z. Ren, *J. Org. Chem.*, 2016, **81**, 11565–11573.
38 X.-J. Pan, J. Gao and G.-Q. Yuan, *Tetrahedron*, 2015, **71**, 5525–5530.
39 L.-S. Kang, M.-H. Luo, C. M. Lam, L.-M. Hu, R. D. Little and C.-C. Zeng, *Green Chem.*, 2016, **18**, 3767–3774.
40 Z. Zhang, J. Su, Z. Zha and Z. Wang, *Chem. – Eur. J.*, 2013, **19**, 17711–17714.
41 Z. Zhang, J. Su, Z. Zha and Z. Wang, *Chem. Commun.*, 2013, **49**, 8982–8984.
42 K. Xu, Z. Zhang, P. Qian, Z. Zha and Z. Wang, *Chem. Commun.*, 2015, **51**, 11108–11111.
43 P. Qian, J.-H. Su, Y. Wang, M. Bi, Z. Zha and Z. Wang, *J. Org. Lett.*, 2017, **82**, 6434–6440.
44 M. N. Elinson, S. K. Feducovich, A. S. Dorofeev, A. N. Vereshchagin and G. I. Nikishin, *Tetrahedron*, 2000, **56**, 9999–10003.
45 M. N. Elinson, S. K. Feducovich, D. E. Dmitriev, A. S. Dorofeev, A. N. Vereshchagin and G. I. Nikishin, *Tetrahedron Lett.*, 2001, **42**, 5557–5559.
46 M. N. Elinson, A. S. Dorofeev, S. K. Feducovich, R. F. Nasybullin, E. F. Litvin, Mi. V. Kopyshev and G. I. Nikishin, *Tetrahedron*, 2006, **62**, 8021–8028.
47 W.-J. Gao, C. M. Lam, B.-G. Sun, R. D. Little and C.-C. Zeng, *Tetrahedron*, 2017, **73**, 2447–2454.
48 F. N. Khan, R. Jayakumar and C. N. Pillai, *J. Mol. Catal. A: Chem.*, 2003, **195**, 139–145.
49 U.-St. Bäumer and H. J. Schäfer, *Electrochim. Acta*, 2003, **48**, 489–495.
50 S. Arndt, D. Weis, K. Donsbach and S. R. Waldvogel, *Angew. Chem., Int. Ed.*, 2020, **59**, 8036–8041.
51 E. Honjo, N. Kutsumura, Y. Ishikawa and Sh. Nishiyama, *Tetrahedron*, 2008, **64**, 9495–9506.
52 S. Kitada, M. Takahashi, Y. Yamaguchi, Y. Okada and K. Chiba, *Org. Lett.*, 2012, **14**, 5960–5963.
53 J. Wen, W. Shi, F. Zhang, D. Liu, S. Tang, H. Wang, X.-M. Lin and A. Lei, *Org. Lett.*, 2017, **19**, 3131–3134.
54 Y.-Y. Jiang, S. Liang, C.-C. Zeng, L.-M. Hu and B.-G. Sun, *Green Chem.*, 2016, **18**, 6311–6319.

 This journal is © The Royal Society of Chemistry 2021

Published on 01 June 2021. Downloaded by University of Cambridge on 12/3/2022 1:39:05 PM.

55 C. Zhang, Y. Chen and G. Yuan, *Chin. J. Chem.*, 2016, **34**, 1277–1282.
56 T. Sawamura, S. Kuribayashi, S. Inagi and T. Fuchigami, *Org. Lett.*, 2010, **12**, 644–646.
57 T. Sawamura, S. Kuribayashi, S. Inagi and T. Fuchigami, *Adv. Synth. Catal.*, 2010, **352**, 2757–2760.
58 W.-J. Gao, W.-C. Li, C.-C. Zeng, H.-Y. Tian, L.-M. Hu and R. D. Little, *J. Org. Chem.*, 2014, **79**, 9613–9618.
59 Q. Qu, X. Gao, J. Gao and G. Yuan, *Sci. China: Chem.*, 2015, **58**, 747–750.
60 D. Baba and T. Fuchigami, *Tetrahedron Lett.*, 2003, **44**, 3133–3136.
61 J. Chen, W.-Q. Yan, C. M. Lam, C.-C. Zeng, L.-M. Hu and R. D. Little, *Org. Lett.*, 2015, **17**, 986–989.
62 S. Tang, X. Gao and A. Lei, *Chem. Commun.*, 2017, **53**, 3354–3356.
63 R. P. Wayne, I. Barnes, P. Biggs, J. P. Burrows, C. E. Canosa-Mas, J. Hjorth, G. Le Bras, G. K. Moortgat, D. Perner, G. Poulet, G. Restelli and H. Sidebottom, *Atmos. Environ., Part A*, 1991, **25**, 1–203.
64 C. Christopher, S. Lawrence, A. J. Bosco, N. Xavier and S. Raja, *Catal. Sci. Technol.*, 2012, **2**, 824–827.
65 C. Christopher, S. Lawrence, M. A. Kulandainathan, K. Kulangiappar, M. E. Raja, N. Xavier and S. Raja, *Tetrahedron Lett.*, 2012, **53**, 2802–2804.
66 Y. Takahira, M. Chen, Y. Kawamata, P. Mykhailiuk, H. Nakamura, B. K. Peters, S. H. Reisberg, C. Li, L. Chen, T. Hoshikawa, T. Shibuguchi and P. S. Baran, *Synlett*, 2019, 1178–1182.
67 O. L. Lebedev and S. N. Kazarnovskii, *Zhur. Obshch. Khim.*, 1960, **30**, 1631–1635.
68 A. R. Forrester and R. H. Thomson, *Nature*, 1964, **203**, 74–75.
69 Preparation of ACT (originally named as tempace): D. Metodiewa, J. Skolimowski and S. Karolczak, *IUBMB Life*, 1996, **40**, 1211–1219.
70 Preparation of AZADO: M. Shibuya, M. Tomizawa, I. Suzuki and Y. Iwabuchi, *J. Am. Chem. Soc.*, 2006, **128**, 8412–8413.
71 Preparation of ABNO: M. Shibuya, M. Tomizawa, Y. Sasano and Y. Iwabuchi, *J. Org. Chem.*, 2009, **74**, 4619–4622.
72 D. P. Hickey, D. A. Schiedler, I. Matanovic, P. V. Doan, P. Atanassov, S. D. Minteer and M. S. Sigman, *J. Am. Chem. Soc.*, 2015, **137**, 16179–16186.
73 J. E. Nutting, M. Rafiee and S. S. Stahl, *Chem. Rev.*, 2018, **118**, 4834–4885.
74 M. Kuroboshi, H. Yoshihisa, M. N. Cortona, Y. Kawakami, Z. Gao and H. Tanaka, *Tetrahedron Lett.*, 2000, **41**, 8131–8135.
75 H. Tanaka, Y. Kawakami, K. Goto and M. Kuroboshi, *Tetrahedron Lett.*, 2001, **42**, 445–448.
76 J. Kubota, Y. Shimizu, K. Mitsudo and H. Tanaka, *Tetrahedron Lett.*, 2005, **46**, 8975–8979.
77 Y. Demizu, H. Shiigi, T. Oda, Y. Matsumura and O. Onomura, *Tetrahedron Lett.*, 2008, **49**, 48–52.
78 A. Palma, J. Cárdenas and B. A. Frontana-Uribe, *Green Chem.*, 2009, **11**, 283–293.
79 M. Kuroboshi, T. Yoshida, J. Oshitani, K. Goto and H. Tanaka, *Tetrahedron*, 2009, **65**, 7177–7185.
80 J. T. Hill-Cousins, J. Kuleshova, R. A. Green, P. R. Birkin, D. Pletcher, T. J. Underwood, S. G. Leach and R. C. D. Brown, *ChemSusChem*, 2012, **5**, 326–331.
81 M. Rafiee, K. C. Miles and S. S. Stahl, *J. Am. Chem. Soc.*, 2015, **137**, 14751–14757.
82 M. Rafiee, Z. M. Konz, M. D. Graaf, H. F. Koolman and S. S. Stahl, *ACS Catal.*, 2018, **8**, 6738–6744.
83 M. Rafiee, M. Alherech, S. D. Karlen and S. S. Stahl, *J. Am. Chem. Soc.*, 2019, **141**, 15266–15276.
84 S. L. Goes, M. N. Mayer, J. E. Nutting, L. E. Hoober-Burkhardt, S. S. Stahl and M. Rafiee, *J. Chem. Educ.*, 2021, **98**, 600–606.
85 A. Badalyan and S. S. Stahl, *Nature*, 2016, **535**, 406–410.
86 C. Li, C.-C. Zeng, L.-M. Hu, F.-L. Yang, S. J. Yoo and R. D. Little, *Electrochim. Acta*, 2013, **114**, 560–566.
87 Y. Kashiwagi and J.-i. Anzai, *Chem. Pharm. Bull.*, 2001, **49**, 324–326.
88 F. Wang, M. Rafiee and S. S. Stahl, *Angew. Chem., Int. Ed.*, 2018, **57**, 6686–6690.
89 F. Xu, L. Zhu, S. Zhu, X. Yan and H.-C. Xu, *Chem. – Eur. J.*, 2014, **20**, 12740–12744.
90 J. C. Siu, G. S. Sauer, A. Saha, R. L. Macey, N. Fu, T. Chauviré, K. M. Lancaster and S. Lin, *J. Am. Chem. Soc.*, 2018, **140**, 12511–12520.
91 H. M. Nelson, J. C. Siu, A. Saha, D. Cascio, S. N. MacMillan, S.-B. Wu, C. Lu, J. A. Rodríguez, K. N. Houk and S. Lin, *Org. Lett.*, 2021, **23**, 454–458.
92 J. C. Siu, J. B. Parry and S. Lin, *J. Am. Chem. Soc.*, 2019, **141**, 2825–2831.
93 E. Grochowski, T. Bolesławska and J. Jurczak, *Synthesis*, 1977, 718–720.
94 F. Recupero and C. Punta, *Chem. Rev.*, 2007, **107**, 3800–3842.
95 R. Amorati, M. Lucarini, V. Mugnaini, G. F. Pedulli, F. Minisci, F. Recupero, F. Fontana, P. Astolfi and L. Greci, *J. Org. Chem.*, 2003, **68**, 1747–1754.
96 S. J. Blanksby and G. B. Ellison, *Acc. Chem. Res.*, 2003, **36**, 255–263.
97 M. Masui, T. Ueshima and S. Ozaki, *J. Chem. Soc., Chem. Commun.*, 1983, 479–480.
98 M. Masui, S. Hara, T. Ueshima, T. Kawaguchi and S. Ozaki, *Chem. Pharm. Bull.*, 1983, **31**, 4209–4211.
99 M. Masui, T. Kawaguchi and S. Ozaki, *J. Chem. Soc., Chem. Commun.*, 1985, 1484–1485.
100 M. Masui, T. Kawaguchi, S. Yoshida and S. Ozaki, *Chem. Pharm. Bull.*, 1986, **34**, 1837–1839.
101 M. Masui, S. Hara and S. Ozaki, *Chem. Pharm. Bull.*, 1986, **34**, 975–979.
102 M. Masui, K. Hosomi, K. Tsuchida and S. Ozaki, *Chem. Pharm. Bull.*, 1985, **33**, 4798–4802.
103 C. Ueda, M. Noyama, H. Ohmori and M. Masui, *Chem. Pharm. Bull.*, 1987, **35**, 1372–1377.
104 A. Nakamura and M. Nakada, *Synthesis*, 2013, 1421–1451.
105 E. J. Horn, B. R. Rosen, Y. Chen, J. Tang, K. Chen, M. D. Eastgate and P. S. Baran, *Nature*, 2016, **533**, 77–81.

Published on 01 June 2021. Downloaded by University of Cambridge on 12/3/2022 1:39:05 PM.

106 D. P. Hruszkewycz, K. C. Miles, O. R. Thielb and S. S. Stahl, *Chem. Sci.*, 2017, **8**, 1282–1287.
107 M. Rafiee, F. Wang, D. P. Hruszkewycz and S. S. Stahl, *J. Am. Chem. Soc.*, 2018, **140**, 22–25.
108 R. Curci, L. D'Accolti and C. Fusco, *Acc. Chem. Res.*, 2006, **39**, 1–9.
109 M. S. Chen and M. C. White, *Science*, 2007, **318**, 783–787.
110 Y. Kawamata, M. Yan, Z. Liu, D.-H. Bao, J. Chen, J. T. Starr and P. S. Baran, *J. Am. Chem. Soc.*, 2017, **139**, 7448–7451.
111 L. A. Wein, K. Wurst, P. Angyal, L. Weisheit and T. Magauer, *J. Am. Chem. Soc.*, 2019, **141**, 19589–19593.
112 J. H. P. Utley and G. G. Rozenberg, *J. Appl. Electrochem.*, 2003, **33**, 525–532.
113 O. R. Luca, T. Wang, S. J. Konezny, V. S. Batista and R. H. Crabtree, *New J. Chem.*, 2011, **35**, 998–999.
114 L.-S. Kang, H.-l. Xiao, C.-C. Zeng, L.-M. Hu and R. D. Little, *J. Electroanal. Chem.*, 2016, **767**, 13–17.
115 E. T. Seo, R. F. Nelson, J. M. Fritsch, L. S. Marcoux, D. W. Leedy and R. N. Adams, *J. Am. Chem. Soc.*, 1966, **88**, 3498–3503.
116 R. F. Nelson and R. N. Adams, *J. Am. Chem. Soc.*, 1968, **90**, 3925–3930.
117 T. Fuchigami, M. Tetsu, T. Tajima and H. Ishii, *Synlett*, 2001, 1269–1271.
118 L. Drouin, R. G. Compton and A. J. Fairbanks, *J. Phys. Org. Chem.*, 2008, **21**, 516–522.
119 X. Wu, A. P. Davis and A. J. Fry, *Org. Lett.*, 2007, **9**, 5633–5636.
120 Y. S. Park, S. C. Wang, D. J. Tantillo and R. D. Little, *J. Org. Chem.*, 2007, **72**, 4351–4357.
121 Y. S. Park and R. D. Little, *J. Org. Chem.*, 2008, **73**, 6807–6815.
122 S. J. Yoo, L.-J. Li, C.-C. Zeng and R. D. Little, *Angew. Chem., Int. Ed.*, 2015, **54**, 3744–3747.
123 C.-c. Zeng, N.-t. Zhang, C. M. Lam and R. D. Little, *Org. Lett.*, 2012, **14**, 1314–1317.
124 N.-n. Lu, S. J. Yoo, L.-J. Li, C.-C. Zeng and R. D. Little, *Electrochim. Acta*, 2014, **142**, 254–260.
125 N.-n. Lu, N.-t. Zhang, C.-C. Zeng, L.-M. Hu, S. J. Yoo and R. D. Little, *J. Org. Chem.*, 2015, **80**, 781–789.
126 R. Francke and R. D. Little, *J. Am. Chem. Soc.*, 2014, **136**, 427–435.
127 Y. Zhu, J. Zhang, Z. Chen, A. Zhang and C. Ma, *Chinese J. Catal.*, 2016, **37**, 533–538.
128 Z.-W. Hou, Z.-Y. Mao, Y. Y. Melcamu, X. Lu and H.-C. Xu, *Angew. Chem., Int. Ed.*, 2018, **57**, 1636–1639.
129 Z.-J. Wu, S.-R. Li and H.-C. Xu, *Angew. Chem., Int. Ed.*, 2018, **57**, 14070–14074.
130 J. C. Siu, N. Fu and S. Lin, *Acc. Chem. Res.*, 2020, **53**, 547–560.
131 (*a*) C. Ma, P. Fang and T.-S. Mei, *ACS Catal.*, 2018, **8**, 7179–7189; (*b*) W. Liu and L. Ackermann, *ACS Catal.*, 2016, **6**, 3743–3752; (*c*) L. Ackermann, *Acc. Chem. Res.*, 2020, **53**(1), 84–104.
132 (*a*) W. Liu and L. Ackermann, *ACS Catal.*, 2016, **6**, 3743–3752; (*b*) M. Palucki, N. S. Finney, P. J. Pospisil, M. L. Güler, T. Ishida and E. N. Jacobsen, *J. Am. Chem. Soc.*, 1998, **120**, 948–954; (*c*) X. Huang and J. T. Groves, *Chem. Rev.*, 2018, **118**, 2491–2553.
133 B. B. Snider and H. Lin, *Synth. Commun.*, 1998, **28**, 1913–1922.
134 N. Fu, G. S. Sauer, A. Saha, A. Loo and S. Lin, *Science*, 2017, **357**, 575–579.
135 N. Fu, G. S. Sauer and S. Lin, *J. Am. Chem. Soc.*, 2017, **139**, 15548–15553.
136 K. Ye, G. Pombar, N. Fu, G. S. Sauer, I. Keresztes and S. Lin, *J. Am. Chem. Soc.*, 2018, **140**, 2438–2441.
137 L. Lu, N. Fu and S. Lin, *Synlett*, 2019, 1199–1203.
138 N. Fu, Y. Shen, A. R. Allen, L. Song, A. Ozaki and S. Lin, *ACS Catal.*, 2019, **9**, 746–754.
139 K.-Y. Ye, Z. Song, G. S. Sauer, J. H. Harenberg, N. Fu and S. Lin, *Chem. – Eur. J.*, 2018, **24**, 12274–12279.
140 Z. Zhang, L. Zhang, Y. Cao, F. Li, G. Bai, G. Liu, Y. Yang and F. Mo, *Org. Lett.*, 2019, **21**, 762–766.
141 Y. Yuan, Y. Zheng, B. Xu, J. Liao, F. Bu, S. Wang, J.-G. Hu and A. Lei, *ACS Catal.*, 2020, **10**, 6676–6681.
142 L. Niu, C. Jiang, Y. Liang, D. Liu, F. Bu, R. Shi, H. Chen, A. D. Chowdhury and A. Lei, *J. Am. Chem. Soc.*, 2020, **142**, 17693–17702.
143 T. H. Meyer, R. C. Samanta, A. Del Vecchio and L. Ackermann, *Chem. Sci.*, 2021, **12**, 2890–2897.
144 B. D. W. Allen, M. D. Hareram, A. C. Seastram, T. McBride, T. Wirth, D. L. Browne and L. C. Morrill, *Org. Lett.*, 2019, **21**, 9241–9246.
145 D. Lin, Y. Lai and J. Huang, *ChemElectroChem*, 2019, **6**, 4188–4193.
146 P. Xiong and H. C. Xu, *Acc. Chem. Res.*, 2019, **52**, 3339–3350.
147 P. Xiong, H.-H. Xu, J. Song and H.-C. Xu, *J. Am. Chem. Soc.*, 2018, **140**, 2460–2464.
148 Z.-J. Wu, S.-R. Li, H. Long and H.-C. Xu, *Chem. Commun.*, 2018, **54**, 4601–4604.
149 H. Long, J. Song and H.-C. Xu, *Org. Chem. Front.*, 2018, **5**, 3129–3132.
150 A. L. J. Beckwith and C. H. Schiesser, *Tetrahedron*, 1985, **41**, 3925–3941.
151 C. Zhu, M. Stangier, J. C. A. Oliveira, L. Massignan and L. Ackermann, *Chem. – Eur. J.*, 2019, **25**, 16382–16389.
152 L. J. Li and S. Z. Luo, *Org. Lett.*, 2018, **20**, 1324–1327.
153 D. Saha, I. M. Taily, S. Naik and P. Banerjee, *Chem. Commun.*, 2021, **57**, 631–634.
154 L. Song, N. Fu, B. G. Ernst, W. H. Lee, M. O. Frederick, R. A. DiStasio and S. Lin, *Nat. Chem.*, 2020, **12**, 747–754.
155 C. Tian, U. Dhawa, A. Scheremetjew and L. Ackermann, *ACS Catal.*, 2019, **9**, 7690–7696.
156 P. Gao, X. Weng, Z. Wang, C. Zheng, B. Sun, Z. Chen, S. You and T. Mei, *Angew. Chem.*, 2020, **132**, 15366–15371.
157 Q. L. Yang, X. Y. Wang, J. Y. Lu, L. P. Zhang, P. Fang and T. S. Mei, *J. Am. Chem. Soc.*, 2018, **140**, 11487–11494.
158 S. Kathiravan, S. Suriyanarayanan and I. A. Nicholls, *Org. Lett.*, 2019, **21**, 1968–1972.
159 X. Yi and X. Hu, *Angew. Chem., Int. Ed.*, 2019, **58**, 4700–4704.

 This journal is © The Royal Society of Chemistry 2021

Published on 01 June 2021. Downloaded by University of Cambridge on 12/3/2022 1:39:05 PM.

160 C. Amatore, C. Cammoun and A. Jutand, *Eur. J. Org. Chem.*, 2008, 4567–4570.
161 Y. B. Dudkina, D. Y. Mikhaylov, T. V. Gryaznova, A. I. Tufatullin, O. N. Kataeva, D. A. Vicic and Y. H. Budnikova, *Organometallics*, 2013, **32**, 4785–4792.
162 T. V. Grayaznova, Y. B. Dudkina, D. R. Islamov, O. N. Kataeva, O. G. Sinyashin, D. A. Vicic and Y. H. Budnikova, *J. Organomet. Chem.*, 2015, **785**, 68–71.
163 M. Konishi, K. Tsuchida, K. Sano, T. Kochi and F. Kakiuchi, *J. Org. Chem.*, 2017, **82**, 8716–8724.
164 C. Ma, C.-Q. Zhao, Y.-Q. Li, L.-P. Zhang, X.-T. Xu, K. Zhang and T.-S. Mei, *Chem. Commun.*, 2017, **53**, 12189–12192.
165 M. E. O'Reilly, R. S. Kim, S. Oh and Y. Surendranath, *ACS Cent. Sci.*, 2017, **3**, 1174–1179.
166 L. Zeng, H. Li, J. Hu, D. Zhang, J. Hu, P. Peng, S. Wang, R. Shi, J. Peng, C.-W. Pao, J.-L. Chen, J.-F. Lee, H. Zhang, Y.-H. Chen and A. Lei, *Nat. Catal.*, 2020, **3**, 438–445.
167 Q.-L. Yang, Y.-Q. Li, C. Ma, P. Fang, X.-J. Zhang and T.-S. Mei, *J. Am. Chem. Soc.*, 2017, **139**, 3293–3298.
168 A. Shrestha, M. Lee, A. L. Dunn and M. S. Sanford, *Org. Lett.*, 2018, **20**, 204–207.
169 R. Mei, J. Koeller and L. Ackermann, *Chem. Commun.*, 2018, **54**, 12879–12882.
170 Y. Qiu, C. Tian, L. Massignan, T. Rogge and L. Ackermann, *Angew. Chem., Int. Ed.*, 2018, **57**, 5818–5822.
171 X. Tan, X. Hou, T. Rogge and L. Ackermann, *Angew. Chem., Int. Ed.*, 2021, **60**, 4619–4624.
172 F. Xu, Y.-J. Li, C. Huang and H.-C. Xu, *ACS Catal.*, 2018, **8**, 3820–3824.
173 Y. Qiu, M. Stangier, T. H. Meyer, J. C. A. Oliveira and L. Ackermann, *Angew. Chem., Int. Ed.*, 2018, **57**, 14179–14183.
174 Q.-L. Yang, Y.-K. Xing, X.-Y. Wang, H.-X. Ma, X.-J. Weng, X. Yang, H.-M. Guo and T.-S. Mei, *J. Am. Chem. Soc.*, 2019, **141**, 18970–18976.
175 (*a*) C. Tian, L. Massignan, T. H. Meyer and L. Ackermann, *Angew. Chem., Int. Ed.*, 2018, **57**, 2383–2387; (*b*) R. Mei, N. Sauermann, J. C. A. Oliveira and L. Ackermann, *J. Am. Chem. Soc.*, 2018, **140**(25), 7913–7921.
176 C. Tian, L. Massignan, T. H. Meyer and L. Ackermann, *Angew. Chem., Int. Ed.*, 2018, **57**, 2383–2387.
177 U. Dhawa, C. Tian, W. Li and L. Ackermann, *ACS Catal.*, 2020, **10**, 6457–6462.
178 (*a*) S. Tang, D. Wang, Y. Liu, L. Zeng and A. Lei, *Nat. Commun.*, 2018, **9**, 1–7; (*b*) X. Gao, P. Wang, L. Zeng, S. Tang and A. Lei, *J. Am. Chem. Soc.*, 2018, **140**, 4195–4199.
179 X. Gao, P. Wang, L. Zeng, S. Tang and A. Lei, *J. Am. Chem. Soc.*, 2018, **140**, 4195–4199.
180 Y. Cao, Y. Yuan, Y. Lin, X. Jiang, Y. Weng, T. Wang, F. Bu, L. Zeng and A. Lei, *Green Chem.*, 2020, **22**, 1548–1552.
181 J. Chen, L. Jin, J. Zhou, X. Jiang and C. Yu, *Tetrahedron Lett.*, 2019, **60**, 2054–2058.
182 Y. B. Dudkina, D. Y. Mikhaylov, T. V. Gryaznova, O. G. Sinyashin, D. A. Vicic and Y. H. Budnikova, *Eur. J. Org. Chem.*, 2012, 2114–2117.
183 S. Zhang, J. Struwe, L. Hu and L. Ackermann, *Angew. Chem., Int. Ed.*, 2020, **59**, 3178–3183.
184 Y. Qiu, W.-J. Kong, J. Struwe, N. Sauermann, T. Rogge, A. Scheremetjew and L. Ackermann, *Angew. Chem., Int. Ed.*, 2018, **57**, 5828–5832.
185 Y. Qiu, A. Scheremetjew and L. Ackermann, *J. Am. Chem. Soc.*, 2019, **141**, 2731–2738.
186 Z. Wu, F. Su, W. Lin, J. Song, T. Wen, H. Zhang and H. Xu, *Angew. Chem., Int. Ed.*, 2019, **58**, 16770–16774.
187 B. K. Peters, K. X. Rodriguez, S. H. Reisberg, S. B. Beil, D. P. Hickey, Y. Kawamata, M. Collins, J. Starr, L. Chen, S. Udyavara, K. Klunder, T. J. Gorey, S. L. Anderson, M. Neurock, S. D. Minteer and P. S. Baran, *Science*, 2019, **363**, 838–845.
188 S. Manabe, C. M. Wong and C. S. Sevov, *J. Am. Chem. Soc.*, 2020, **142**, 3024–3031.
189 L. Lu, J. C. Siu, Y. Lai and S. Lin, *J. Am. Chem. Soc.*, 2020, **142**, 21272–21278.
190 W. Zhang and S. Lin, *J. Am. Chem. Soc.*, 2020, **142**, 20661–20670.
191 M. Mori, Y. Hashimoto and Y. Ban, *Tetrahedron Lett.*, 1980, **21**, 631–634.
192 G. Schiavon, G. Bontempelli and B. Corain, *J. Chem. Soc., Dalton Trans.*, 1981, 1074–1081.
193 Y. Rollin, M. Troupel, D. G. Tuck and J. Perichon, *J. Organomet. Chem.*, 1986, **303**, 131–137.
194 J. Chaussard, J.-C. Folest, J.-Y. Nedelec, J. Périchon, S. Sibille and M. Troupel, *Synthesis*, 1990, 369–381.
195 T. Yamamoto and N. Saito, *Macromol. Chem. Phys.*, 1996, **197**, 165–175.
196 J.-Y. Nédélec, J. Périchon and M. Troupel, *Top. Curr. Chem.*, 1997, **185**, 141–173.
197 T. M. Cassol, F. W. J. Demnitz, M. Navarro and E. A. De Neves, *Tetrahedron Lett.*, 2000, **41**, 8203–8206.
198 K. W. R. de França, M. Navarro, É. Léonel, M. Durandetti and J.-Y. Nédélec, *J. Org. Chem.*, 2002, **67**, 1838–1842.
199 J. L. Oliveira, M. J. Silva, T. Florencio, K. Urgin, S. Sengmany, E. Léonel, J.-Y. Nédélec and M. Navarro, *Tetrahedron*, 2012, **68**, 2383–2390.
200 J. L. Oliveira, E. Le Gall, S. Sengmany, E. Léonel, P. Dubot, P. Cénédèse and M. Navarro, *Electrochim. Acta*, 2015, **173**, 465.
201 R. Rahil, S. Sengmany, E. Le Gall and E. Léonel, *Synthesis*, 2018, 146–154.
202 H. Qiu, B. Shuai, Y.-Z. Wang, D. Liu, Y.-G. Chen, P.-S. Gao, H.-X. Ma, S. Chen and T.-S. Mei, *J. Am. Chem. Soc.*, 2020, **142**, 9872–9878.
203 C. Gosmini, S. Lasry, J.-Y. Nedelec and J. Périchon, *Tetrahedron*, 1998, **54**, 1289–1298.
204 C. Gosmini, J.-Y. Nédélec and J. Périchon, *Tetrahedron Lett.*, 2000, **41**, 201–203.
205 S. Sengmany, E. Léonel, F. Polissaint, J.-Y. Nédélec, M. Pipelier, C. Thobie-Gautier and D. Dubreuil, *J. Org. Chem.*, 2007, **72**, 5631–5636.
206 S. Sengmany, E. Le Gall and E. Léonel, *Molecules*, 2011, **16**, 5550–5560.
207 S. Sengmany, A. Vitu-Thiebaud, E. Le Gall, S. Condon, E. Léonel, C. Thobie-Gautier, M. Pipelier, J. Lebreton and D. Dubreuil, *J. Org. Chem.*, 2013, **78**, 370–379.

Published on 01 June 2021. Downloaded by University of Cambridge on 12/3/2022 1:39:05 PM.

208 K. Urgin, R. Barhdadi, S. Condon, E. Léonel, M. Pipelier, V. Blot, C. Thobie-Gautier and D. Dubreuil, *Electrochim. Acta*, 2010, **55**, 4495–4500.
209 B. R. Walker and C. S. Sevov, *ACS Catal.*, 2019, **9**, 7197–7203.
210 A. Conan, S. Sibille, E. D'Incan and J. Périchon, *J. Chem. Soc., Chem. Commun.*, 1990, **1**, 48–49.
211 M. Durandetti, S. Sibille, J.-Y. Nédélec and J. Périchon, *Synth. Commun.*, 1994, **24**, 145–151.
212 M. Durandetti, J. Y. Nédélec and J. Périchon, *J. Org. Chem.*, 1996, **61**, 1748–1755.
213 M. Durandetti, J. Périchon and J. Y. Nédélec, *J. Org. Chem.*, 1997, **62**, 7914–7915.
214 M. Durandetti and J. Périchon, *Synthesis*, 2004, 3079–3083.
215 R. J. Perkins, J. D. Pedro and E. C. Hansen, *Org. Lett.*, 2017, **19**, 3755–3758.
216 S. Biswas and D. J. Weix, *J. Am. Chem. Soc.*, 2013, **135**, 16192.
217 R. J. Perkins, J. A. Hughes, D. J. Weix and E. C. Hansen, *Org. Process Res. Dev.*, 2019, **23**, 1746–1751.
218 H. Li, C. P. Breen, H. Seo, T. F. Jamison, Y.-Q. Fang and M. M. Bio, *Org. Lett.*, 2018, **20**, 1338–1341.
219 T. Koyanagi, A. Herath, A. Chong, M. Ratnikov, A. Valiere, J. Chang, V. Molteni and J. Loren, *Org. Lett.*, 2019, **21**, 816–820.
220 G. S. Kumar, A. Peshkov, A. Brzozowska, P. Nikolaienko, C. Zhu and M. Rueping, *Angew. Chem., Int. Ed.*, 2020, **59**, 6513–6519.
221 K. J. Jiao, D. Liu, H. X. Ma, H. Qiu, P. Fang and T. S. Mei, *Angew. Chem., Int. Ed.*, 2020, **59**, 6520–6524.
222 B. L. Truesdell, T. B. Hamby and C. S. Sevov, *J. Am. Chem. Soc.*, 2020, **142**, 5884–5893.
223 T. J. DeLano and S. E. Reisman, *ACS Catal.*, 2019, **9**, 6751–6754.
224 S. Condon-Gueugnot, E. Léonel, J.-Y. Nédélec and J. Périchon, *J. Org. Chem.*, 1995, **60**, 7684–7686.
225 J. C. de Medonca Cavalcanti, M. O. F. Goulart, E. Léonel and J.-Y. Nédélec, *Tetrahedron Lett.*, 2002, **43**, 6343–6345.
226 J. Pelletier, S. Olivero and E. Dunach, *Synth. Commun.*, 2004, **34**, 3343–3348.
227 E. Dunach, A. P. Esteves, M. J. Medeiros, C. S. dos Santos Neves and S. Olivero, *C. R. Chim.*, 2009, **12**, 889–894.
228 A. P. Esteves, D. M. Goken, L. J. Klein, M. A. Lemos, M. J. Medeiros and D. G. Peters, *J. Org. Chem.*, 2003, **68**, 1024–1029.
229 M. A. Ischay, M. S. Mubarak and D. G. Peters, *J. Org. Chem.*, 2006, **71**, 623–628.
230 S. Condon, D. Dupré, G. Falgayrac and J.-Y. Nédélec, *Eur. J. Org. Chem.*, 2002, 105–111.
231 S. Condon, D. Dupré, I. Lachaise and J.-Y. Nédélec, *Synthesis*, 2002, 1752–1758.
232 D. Mikhaylov, T. Gryaznova, Y. Dudkina, M. Khrizanphorov, S. Latypov, O. Kataeva, D. A. Vicic, O. G. Sinyashina and Y. Budnikova, *Dalton Trans.*, 2012, **41**, 165–172.
233 J. A. Miranda, C. J. Wade and R. D. Little, *J. Org. Chem.*, 2005, **70**(20), 8017–8026.
234 S. Zhang, L. Li, X. Li, J. Zhang, K. Xu, G. Li and M. Findlater, *Org. Lett.*, 2020, **22**, 3570–3575.
235 C. Li, Y. Kawamata, H. Nakamura, J. C. Vantourout, Z. Liu, Q. Hou, D. Bao, J. T. Starr, J. Chen, M. Yan and P. S. Baran, *Angew. Chem., Int. Ed.*, 2017, **56**, 13088–13093.
236 Y. Kawamata, J. C. Vantourout, D. P. Hickey, P. Bai, L. Chen, Q. Hou, W. Qiao, K. Barman, M. A. Edwards, A. F. Garrido-Castro, J. N. deGruyter, H. Nakamura, K. Knouse, C. Qin, K. J. Clay, D. Bao, C. Li, J. T. Starr, C. Garcia-Irizarry, N. Sach, H. S. White, M. Neurock, S. D. Minteer and P. S. Baran, *J. Am. Chem. Soc.*, 2019, **141**, 6392–6402.
237 D. Liu, H.-X. Ma, P. Fang and T.-S. Mei, *Angew. Chem., Int. Ed.*, 2019, **58**, 5033–5037.
238 Y. Wang, L. Deng, X. Wang, Z. Wu, Y. Wang and Y. Pan, *ACS Catal.*, 2019, **9**, 1630–1634.
239 M. Zhu, M. Alami and S. Messaoudi, *Chem. Commun.*, 2020, **56**, 4464–4467.
240 S. Sengmany, A. Ollivier, E. Le Gall and E. Léonel, *Org. Biomol. Chem.*, 2018, **16**, 4495–4500.
241 Y. Bai, N. Liu, S. Wang, S. Wang, S. Ning, L. Shi, L. Cui, Z. Zhang and J. Xiang, *Org. Lett.*, 2019, **21**, 6835–6838.
242 F. Daili, A. Ouarti, M. Pinaud, I. Kribii, S. Sengmany, E. L. Gall and E. Léonel, *Eur. J. Org. Chem.*, 2020, 3452–3455.
243 C. Zhu, H. Yue, P. Nikolaienko and M. Rueping, *CCS Chem.*, 2020, **2**, 179–190.
244 F. Lian, K. Xu, W. Meng, H. Zhang, Z. Tan and C. Zeng, *Chem. Commun.*, 2019, **55**, 14685–14688.
245 R. C. Samanta, J. Struwe and L. Ackermann, *Angew. Chem., Int. Ed.*, 2020, **59**, 14154–14159.
246 D. Franco and E. Dunach, *Tetrahedron Lett.*, 2000, **41**, 7333–7336.
247 D. Franco, A. Riahi, F. Henin, J. Muzart and E. Dunach, *Eur. J. Org. Chem.*, 2002, 2257–2259.
248 T. Yamamoto, J. Ishizu and A. Yamamoto, *J. Am. Chem. Soc.*, 1981, **103**, 6863–6869.
249 P. Gomes, H. Fillon, C. Gosmini, E. Labbé and J. Périchon, *Tetrahedron*, 2002, **58**, 8417–8424.
250 E. Le Gall, C. Gosmini, J.-Y. Nédélec and J. Périchon, *Tetrahedron Lett.*, 2001, **42**, 267–269.
251 C. Cannes, F. Bedioui, S. C. Gueugnot, J. Y. Nédélec and J. Devynck, *New J. Chem.*, 1999, **23**, 489–494.
252 S. Condon, C. Céline and F. Bedioui, *J. Chem.*, 2019, 1–6.
253 P. Gandeepan, L. H. Finger, T. H. Meyer and L. Ackermann, *Chem. Soc. Rev.*, 2020, **49**, 4254–4272.
254 Y. Shen, S. Inagi, M. Atobe and T. Fuchigami, *Res. Chem. Intermed.*, 2013, **39**, 89–99.
255 B. L. Chen, H. W. Zhu, Y. Xiao, Q. L. Sun, H. Wang and J. X. Lu, *Electrochem. Commun.*, 2014, **42**, 55–59.
256 N. W. J. Ang, J. C. A. Oliveira and L. Ackermann, *Angew. Chem., Int. Ed.*, 2020, **59**, 12842–12847.
257 H. Shimakoshi and Y. Hisaeda, *Curr. Opin. Electrochem.*, 2018, **8**, 24–30.
258 C. K. Njue, B. Nuthakki, A. Vaze, J. M. Bobbitt and J. F. Rusling, *Electrochem. Commun.*, 2001, **3**, 733–736.

 This journal is © The Royal Society of Chemistry 2021

Published on 01 June 2021. Downloaded by University of Cambridge on 12/3/2022 1:39:05 PM.

259 H. Shimakoshi, Z. Luo, T. Inaba and Y. Hisaeda, *Dalton Trans.*, 2016, **45**, 10173–10180.
260 M. J. Chalkley, P. Garrido-Barros and J. C. Peters, *Science*, 2020, **369**, 850–854.
261 T. V. Magdesieva, M. Graczyk, A. Vallat, O. M. Nikitin, P. I. Demyanov, K. P. Butin and M. A. Vorotyntsev, *Electrochim. Acta*, 2006, **52**, 1265–1280.
262 O. M. Nikitin and T. V. Magdesieva, *Mendeleev Commun.*, 2011, **21**, 194–195.
263 Y. A. Lisitsyn and L. V. Grigor'eva, *Russ. J. Electrochem.*, 2009, **45**, 132–138.
264 Y. A. Lisitsyn and A. V. Sukhov, *Russ. J. Electrochem.*, 2011, **47**, 1180–1185.
265 Y. A. Lisitsyn and A. V. Sukhov, *Russ. J. Electrochem.*, 2015, **51**, 1092–1095.
266 Y. A. Lisitsyn and A. V. Sukhov, *Russ. J. Electrochem.*, 2020, **56**, 426–430.
267 T. Liedtke, P. Spannring, L. Riccardi and A. Gansäuer, *Angew. Chem., Int. Ed.*, 2018, **57**, 5006–5010.
268 J.-M. Huang and Y. Dong, *Chem. Commun.*, 2009, 3943–3945.
269 J. M. Huang and H. R. Ren, *Chem. Commun.*, 2010, **46**, 2286–2288.
270 A. K. Sinha, B. Mondal, M. Kundu, B. Chakraborty and U. K. Roy, *Org. Chem. Front.*, 2014, **1**, 1270–1275.
271 S. Torii, H. Tanaka and K. Morisaki, *Tetrahedron Lett.*, 1985, **26**, 1655–1658.
272 J. Tian and K. D. Moeller, *Org. Lett.*, 2005, **7**, 5381–5383.
273 Y.-L. Lai and J.-M. Huang, *Org. Lett.*, 2017, **19**, 2022–2025.
274 K. J. Jiao, Z. M. Li, X. T. Xu, L. P. Zhang, Y. Q. Li, K. Zhang and T. S. Mei, *Org. Chem. Front.*, 2018, **5**, 2244–2248.
275 A. Krief and A. M. Laval, *Chem. Rev.*, 1999, **99**, 745–778.
276 E. Léonard, E. Duñach and J. Périchon, *J. Chem. Soc., Chem. Commun.*, 1989, **5**, 276–277.
277 H. Hebri, E. Duñach, M. Heintz, M. Troupel and J. Périchon, *Synlett*, 1991, 901–902.
278 J. D. Parrish and R. L. Little, *Tetrahedron Lett.*, 2001, **42**, 7767–7770.
279 K. Sahloul, L. Sun, A. Requet, Y. Chahine and M. Mellah, *Chem. – Eur. J.*, 2012, **18**, 11205–11209.
280 L. Sun, K. Sahloul and M. Mellah, *ACS Catal.*, 2013, **3**, 2568–2573.
281 Y. F. Zhang and M. Mellah, *ACS Catal.*, 2017, **7**, 8480.
282 K. Uneyama, H. Matsuda and S. Torii, *Tetrahedron Lett.*, 1984, **25**, 6017–6020.
283 Z. Zha, A. Hui, Y. Zhou, Q. Miao, Z. Wang and H. Zhang, *Org. Lett.*, 2005, **7**, 1903–1905.
284 L. Zhang, Z. Zha, Z. Wang and S. Fu, *Tetrahedron Lett.*, 2010, **51**, 1426–1429.
285 L. Zhang, Z. Zha, Z. Zhang, Y. Li and Z. Wang, *Chem. Commun.*, 2010, **46**, 7196–7198.
286 L. Zhang, Z. G. Zha and Z. Y. Wang, *Synlett*, 2010, 1915–1918.
287 L. Zhang, H. Chen, Z. G. Zha and Z. Y. Wang, *Chem. Commun.*, 2012, **48**, 6574.
288 K. Oda, T. Ohnuma and Y. Ban, *J. Org. Chem.*, 1984, **49**, 953–959.
289 H. Senboku, K. Nakahara, T. Fukuhara and S. Hara, *Tetrahedron Lett.*, 2010, **51**, 435–438.
290 N. Kurono, E. Honda, F. Komatsu, K. Orito and M. Tokuda, *Chem. Lett.*, 2003, **32**, 720–721.
291 N. Kurono, E. Honda, F. Komatsu, K. Orito and M. Tokuda, *Tetrahedron*, 2004, **60**, 1791–1801.
292 K. Mitsudo, T. Okada, S. Shimohara, H. Mandai and S. Suga, *Electrochemistry*, 2013, **81**, 362–364.
293 K. Mitsudo, Y. Nakagawa, J. I. Mizukawa, H. Tanaka, R. Akaba, T. Okada and S. Suga, *Electrochim. Acta*, 2012, **82**, 444–449.
294 C. Li and H. Wonneberger, *Adv. Mater.*, 2012, **24**, 613–636.
295 G. Sun, S. Ren, X. Zhu, M. Huang and Y. Wan, *Org. Lett.*, 2016, **18**, 544–547.
296 H. Senboku, J. Y. Michinishi and S. Hara, *Synlett*, 2011, 1567–1572.
297 A. Katayama, H. Senboku and S. Hara, *Tetrahedron*, 2016, **72**, 4626–4636.
298 A. Katayama and H. Senboku, *ChemElectroChem*, 2016, **3**, 2052–2057.
299 R. N. Grimes, *Dalton Trans.*, 2015, **44**, 5939–5956.
300 F. Diederich and M. GómezLópez, *Chem. Soc. Rev.*, 1999, **28**, 263–277.
301 G. Yu, J. Gao, J. C. Hummelen, F. Wudl and A. J. Heeger, *Science*, 1995, **270**, 1789–1791.
302 K. Bingel, *Chem. Ber.*, 1993, **126**, 1957–1959.
303 M. Maggini, G. Scorrano and M. Prato, *J. Am. Chem. Soc.*, 1993, **115**, 9798–9799.
304 A. M. Spokoyny, *Pure Appl. Chem.*, 2013, **85**, 903–919.
305 K. Hosoi, S. Inagi, T. Kubo and T. Fuchigami, *Chem. Commun.*, 2011, **47**, 8632–8634.
306 T. Fuchigami, M. Kasuga and A. Konno, *J. Electroanal. Chem.*, 1996, **411**, 115–119.
307 W. W. Porter III, T. P. Vaid and A. L. Rheingold, *J. Am. Chem. Soc.*, 2005, **127**, 16559–16566.
308 M. Kuroboshi, R. Kobayashi, T. Nakagawa and H. Tanaka, *Synlett*, 2009, 85–88.
309 M. Kuroboshi, T. Shiba and H. Tanaka, *Tetrahedron Lett.*, 2013, **54**, 3666–3668.
310 H. Tanaka, M. Kuroboshi, R. Kataoka and R. Suzuki, *Electrochemistry*, 2013, **81**, 356–358.
311 E. Steckhan, T. Arns, W. R. Heineman, G. Hilt, D. Hoormann, J. Jorissen, L. Kröner, B. Lewall and H. Putter, *Chemosphere*, 2001, **43**, 63–73.
312 B. Zhang, X. Qu, J. Qu, X. Chen, H. Xie, P. Xing, D. Wang and H. Yin, *Green Chem.*, 2020, **22**, 8633–8641.
313 L. Zhang and X. Hu, *Chem. Sci.*, 2020, **11**, 10786–10791.
314 Y. Mo, Z. Lu, G. Rughoobur, P. Patil, N. Gershenfeld, A. I. Akinwande, S. L. Buchwald and K. F. Jensen, *Science*, 2020, **368**, 1352–1357.
315 J. Luo, B. Hu, W. Wu, M. Hu and T. L. Liu, *Angew. Chem., Int. Ed.*, 2021, **60**, 2–12.
316 Y. Liang, S.-H. Shi, R. Jin, X. Qiu, J. Wei, H. Tan, X. Jiang, X. Shi, S. Song and N. Jiao, *Nat. Catal.*, 2021, **4**, 116–123.
317 Y. Shen, M. Atobe, W. Li and T. Nonaka, *Electrochim. Acta*, 2003, **48**, 1041–1046.

Published on 01 June 2021. Downloaded by University of Cambridge on 12/3/2022 1:39:05 PM.

318 M. J. Llorente, B. H. Nguyen, C. P. Kubiak and K. D. Moeller, *J. Am. Chem. Soc.*, 2016, **138**, 15110–15113.
319 R. S. Sherbo, R. S. Delima, V. A. Chiykowski, B. P. MacLeod and C. P. Berlinguette, *Nat. Catal.*, 2018, **1**, 501–507.
320 A. Kurimoto, R. S. Sherbo, Y. Cao, N. W. Loo and C. P. Berlinguette, *Nat. Catal.*, 2020, **3**, 719–726.
321 H.-B. Zhao, P. Xu, J. Song and H.-C. Xu, *Angew. Chem., Int. Ed.*, 2018, **57**, 15153–15156.
322 D. M. Heard and A. J. J. Lennox, *Angew. Chem., Int. Ed.*, 2020, **59**, 18866–18884.
323 S. D. Ross and M. Finkelstein, *J. Org. Chem.*, 1969, **34**, 2923–2927.
324 M. P. J. Brennan and R. Brettle, *J. Chem. Soc., Perkin Trans. 1*, 1973, 257–261.
325 C. M. Hudson, M. R. Marzabadi, K. D. Moeller and D. G. New, *J. Am. Chem. Soc.*, 1991, **113**, 7372–7385.
326 S. Beil, D. Pollok and S. R. Waldvogel, *Angew. Chem., Int. Ed.*, DOI: 10.1002/anie.202014544.
327 B.-Y. Wei, D.-T. Xie, S.-Q. Lai, Y. Jiang, H. Fu, D. Wei and B. Han, *Angew. Chem., Int. Ed.*, 2021, **60**, 3182–3188.
328 K. Jin, J. H. Maalouf, N. Lazouski, N. Corbin, D. Yang and K. Manthiram, *J. Am. Chem. Soc.*, 2019, **141**, 6413–6418.
329 Z. Yin, H. Pang, X. Guo, H. Lin, M. Muzzio, M. Shen, K. Wei, C. Yu, P. Williard and S. Sun, *Angew. Chem., Int. Ed.*, 2020, **132**, 16067–16070.
330 For examples of reviews on bioelectrocatalysis, see: (*a*) H. Chen, O. Simoska, K. Lim, M. Grattieri, M. Yuan, F. Dong, Y. S. Lee, K. Beaver, S. Weliwatte, E. M. Gaffney and S. D. Minteer, *Chem. Rev.*, 2020, **120**, 12903–12993; (*b*) H. Chen, F. Y. Dong and S. D. Minteer, *Nat. Catal.*, 2020, **3**, 225–244; (*c*) X. Xiao, H. Xia, R. Wu, L. Bai, L. Yan, E. Magner, S. Cosnier, E. Lojou, Z. Zhu and A. Liu, *Chem. Rev.*, 2019, **119**, 9509–9558.
331 J. Masa and W. Schuhmann, *Nano Energy*, 2016, **29**, 466–475.
332 Y. Xiao, F. Patolsky, E. Katz, J. F. Hainfeld and I. Willner, *Science*, 2003, **299**, 1877–1881.
333 A. Koto, S. Taniya, H. Sakamoto, T. Satomura, H. Sakuraba, T. Ohshima and S. Suye, *Biosens. Bioelectron.*, 2014, **5**, 1.
334 D. P. Hickey, K. Lim, R. Cai, A. R. Patterson, M. Yuan, S. Sahin, S. Abdellaoui and S. D. Minteer, *Chem. Sci.*, 2018, **9**, 5172–5177.
335 H. Chen, R. Cai, J. Patel, F. Dong, H. Chen and S. D. Minteer, *J. Am. Chem. Soc.*, 2019, **141**, 4963–4971.
336 H. Seelajaroen, M. Haberbauer, C. Hemmelmair, A. Aljabour, L. M. Dumitru, A. W. Hassel and N. S. Sariciftci, *ChemBioChem*, 2019, **20**, 1196–1205.
337 M. W. Yuan, M. J. Kummer, R. D. Milton, T. Quah and S. D. Minteer, *ACS Catal.*, 2019, **9**, 5486–5495.
338 F. Dong, H. Chen, C. A. Malapit, M. B. Prater, M. Li, M. Yuan, K. Lim and S. D. Minteer, *J. Am. Chem. Soc.*, 2020, **142**, 8374–8382.
339 L. Zhang, H. Cui, Z. Zou, T. M. Garakani, C. Novoa-Henriquez, B. Jooyeh and U. Schwaneberg, *Angew. Chem.*, 2019, **131**, 4610–4613.
340 C. Liu, K. K. Sakimoto, B. C. Colon, P. A. Silver and D. G. Nocera, *Proc. Natl. Acad. Sci. U. S. A.*, 2017, **114**, 6450–6455.
341 K. Sturm-Richter, F. Golitsch, G. Sturm, E. Kipf, A. Dittrich, S. Beblawy, S. Kerzenmacher and J. Gescher, *Bioresour. Technol.*, 2015, **186**, 89–96.
342 J. C. Mayr, J. H. Grosch, L. Hartmann, L. F. M. Rosa, A. C. Spiess and F. Harnisch, *ChemSusChem*, 2019, **12**, 1631–1634.
343 J. C. Moutet and G. Reverdy, *Tetrahedron Lett.*, 1979, **20**, 2389–2392.
344 S. S. Shukla and J. F. Rusling, *J. Phys. Chem.*, 1985, **89**, 3353–3358.
345 Y. Yu, P. Guo, J. S. Zhong, Y. Yuan and K. Y. Ye, *Org. Chem. Front.*, 2019, **7**, 131–135.
346 J. P. Barham and B. König, *Angew. Chem., Int. Ed.*, 2020, **59**, 11732–11747.
347 W. Zhang, K. L. Carpenter and S. Lin, *Angew. Chem., Int. Ed.*, 2020, **59**, 409–417.
348 P. Xu, P.-Y. Chen and H.-C. Xu, *Angew. Chem., Int. Ed.*, 2020, **59**, 14275–14280.
349 X.-L. Lai, X.-M. Shu, J. Song and H.-C. Xu, *Angew. Chem., Int. Ed.*, 2020, **59**, 10626–10632.
350 H. Yan, Z.-W. Hou and H.-C. Xu, *Angew. Chem., Int. Ed.*, 2019, **58**, 4592–4595.
351 Y. Qiu, A. Scheremetjew, L. H. Finger and L. Ackermann, *Chem. – Eur. J.*, 2020, **26**, 3241–3246.
352 L. Capaldo, L. L. Quadri, D. Merli and D. Ravelli, *Chem. Commun.*, 2021, **57**, 4424–4427.
353 H. Huang, Z. M. Strater, M. Rauch, J. Shee, T. J. Sisto, C. Nuckolls and T. H. Lambert, *Angew. Chem., Int. Ed.*, 2019, **58**, 13318–13322.
354 H. Huang and T. H. Lambert, *Angew. Chem., Int. Ed.*, 2020, **59**, 658–662.
355 H. Huang and T. H. Lambert, *Angew. Chem., Int. Ed.*, 2021, **60**, 11163–11167.
356 T. Shen and T. H. Lambert, *Science*, 2021, **371**, 620–626.
357 S. Wu, J. Žurauskas, M. Domański, P. S. Hitzfeld, V. Butera, D. J. Scott, J. Rehbein, A. Kumar, E. Thyrhaug, J. Hauer and J. P. Barham, *Org. Chem. Front.*, 2021, **8**, 1132–1142.
358 H. Kim, H. Kim, T. H. Lambert and S. Lin, *J. Am. Chem. Soc.*, 2020, **142**, 2087–2092.
359 J. Eriksen, H. Lund, A. I. Nyvad, T. Yamato, R. H. Mitchell, T. W. Dingle, R. V. Williams and R. Mahedevan, *Acta Chem. Scand.*, 1983, **37**, 459–466.
360 G. J. Choi, Q. Zhu, D. C. Miller, C. J. Gu and R. R. Knowles, *Nature*, 2016, **539**, 268–271.
361 N. G. W. Cowper, C. P. Chernowsky, O. P. Williams and Z. K. Wickens, *J. Am. Chem. Soc.*, 2020, **142**, 2093–2099.
362 J. Liu, L. Lu, D. Wood and S. Lin, *ACS Cent. Sci.*, 2020, **6**, 1317–1340.
363 F. Wang and S. S. Stahl, *Angew. Chem., Int. Ed.*, 2019, **58**, 6385–6390.

 This journal is © The Royal Society of Chemistry 2021